3542
TR 3542

Structural reliability using Finite Element Analysis

An appraisal of DARS:

Directional Adaptive Response surface Sampling

P.H. WAARTS

Structural reliability using Finite Element Analysis

An appraisal of DARS:

Directional Adaptive Response surface Sampling

BIBLIOTHEEK TECHNISCHE UNIVERSITEIT
Prometheusplein 1
DELFT

Proefschrift

Ter verkrijging van de graad van doctor
aan de Technische Universiteit Delft,
op gezag van de Rector Magnificus prof. ir. K.F. Wakker,
in het openbaar te verdedigen ten overstaan van een commissie,
door het College voor Promoties aangewezen,

op dinsdag 20 juni 2000 te 16:00 uur,

door Paul Hendrik WAARTS

civiel ingenieur
Geboren te ´s-Gravenhage

Dit proefschrift is goedgekeurd door de promotor:
Prof. ir. A.C.W.M. Vrouwenvelder

Samenstelling promotiecommissie:

Rector Magnificus,	voorzitter
Prof. ir. A.C.W.M. Vrouwenvelder,	Technische Universiteit Delft, promotor
Prof. dr. ir. F.B.J. Barends	Technische Universiteit Delft
Prof. J. Beirlant	Katholieke Universiteit Leuven
Prof. dr. ir. J.G.M. Kerstens	Technische Universiteit Eindhoven
Prof. Dr. Ing. R. Rackwitz	Technische Universität München
Dr. ir. L.J. Sluys	Technische Universiteit Delft
Prof. drs. ir. J.K. Vrijling,	Technische Universiteit Delft

Published and distributed by:

Delft University Press
P.O. Box 98
2600 MG Delft
The Netherlands
Telephone: +31 15 2785121
Telefax: +31 15 2781661
E-mail: DUP@Library.TUDelft.NL

ISBN 90-407-2073-8

Copyright 2000 by P.H. Waarts

All rights reserved. No part of the material protected by this copyright notice may be reproduced or utilised in any form or by any means, electronic or mechanical, including photocopying, recording or by any information storage and retrieval system, without written permission from the publisher: Delft University Press.

Printed in The Netherlands

Acknowledgements

The research reported in this thesis was started in 1995 as a part of the Beek project "Probabilistic design" in which both the Faculty of Aerospace engineering and the Faculty of Civil Engineering, of the Delft University of Technology, were involved.

I like to express my thanks to my employer, TNO Building and Construction Research, for giving me the opportunity to perform this study. Furthermore the financial support of the Dutch Ministry of Transport, Public Works and Water Management is greatly appreciated.

I would like to express my gratitude to my supervisor and colleague Ton Vrouwenvelder for his support to make this research and thesis valuable. Acknowledgements are also directed to Ane de Boer of the Civil Engineering Division of the Dutch Ministry of Transport, Public Works and Water Management for his support and FEA applications. I wish to record special thanks to my colleagues at TNO, especially Pier Nauta and Wim Courage for their support and help with the DIANA Finite Element program. Last but last not I want to express my gratitude to my partner and dear friend Jacqueline Cieremans for her support and patience and whose help in preparing the manuscript was indispensable.

Paul Waarts
April 2000

Table of Contents

List of symbols and abbreviations

e	limit strain
$\underline{f}$	load vector
f	limit stress
$f_x(\xi)$	density function
g	limit state function
g^*	fitted response surface
h(x)	importance sampling density
k	number of limit states
m	number of standard normal variables
n	number of random variables
q	number of random variables with reduced standard deviation
u	standard normal random variable
u^*	design-point
$\underline{v}$	displacement vector
v	relaxation factor
x	random variable
α	FORM influence factor
β	reliability index
γ	safety factor
ε	strain
$\underline{\theta}$	directional vector
λ	distance from origin to limit state in u-space
μ	mean value, expectation
ν	number of truncated variables
ρ	correlation factor
σ	standard deviation
σ	stress
τ	load increment factor
χ^2	chi-squared distribution
Γ	matrix with covariances
Λ	diagonal matrix with eigenvalues
Φ	normal (Gaussian) distribution function

A	cross section
D	error in estimate
E	estimate of variable
$F_x(\xi)$	distribution function
I	moment of inertia
K	stiffness matrix
N	number of simulations
P_f	probability of failure
R	resistance
S	solicitation
V	coefficient of variation
W	matrix with eigenvectors

ADI	(u-space coordinate) Axis Directional Integration
ARS	Adaptive Response Surface
DARS	Directional Adaptive Response surface Sampling
DI	Directional Integration
DS	Directional Sampling
CPU	Computer Central Processing Unit
FA	Computer File Access
FE	Finite Element
FEA	Finite Element Analysis
FERM	Finite Element Reliability Method
FORM	First Order Reliability Method
IO	Computer Input-Output
LSF	Limit State Function
LSFE	Limit State Function Evaluation(s)
MC	Monte Carlo sampling
MCI	Monte Carlo Importance sampling
NI	Numerical Integration
SORM	Second Order Reliability Method
DS	Directional Sampling
RS	Response Surface
RSM	Response Surface Method
SLS	Serviceability Limit State
ULS	Ultimate Limit State

1. Introduction

1.1 Background

The structural behaviour of a complex structure is often calculated using a Finite Element Analysis (FEA). Stresses and deformations of the structure can be computed given the (deterministic) parameters of loads, geometry and material behaviour.

Structural codes require a certain level of structural reliability. The Dutch Building code, for example, demands a maximum probability of failure of 10^{-4} within a given reference period (lifetime of the structure). This probability of failure is ideally translated into partial safety factors by which variables like strength and load have to be divided or multiplied to find the so-called design values. These design values are to be used as input for a Finite Element Analysis. The outcome of the calculations is compared with the limit states (for example collapse or maximum deformation). The structure is supposed to have met the reliability requirements when the limit states are not exceeded.

Reality is different. First of all the method using partial safety factors makes it only plausible that the reliability requirements are met. There is, however, no certainty. A second aspect is that safety factors are often based on experience only. A link with the required reliability on a theoretical basis often does not exist. Third aspect is the system behaviour of structures. The safety factors are often derived for components of the structure like girders and columns. A structure as a whole behaves like a system of these components. As a result, depending on the system under consideration, the structure can be more or less reliable than its components. Given these problems, it would be useful to have a method to calculate an accurate (system) probability of failure of the total structure at once.

Standard reliability methods compute the probability of failure given a limit state and stochastic parameters. Limit states might be for instance exceedance of yield stress in a structural member, exceedance of maximum deformation or global collapse. Well-known methods to compute the reliability are Numerical Integration (NI) [Ouy87], Monte Carlo simulation (MC) [Rub81] and the First Order Reliability Method (FORM) [Has74].

For large and complex structures it is almost impossible to provide an explicit limit state function. Points of the limit state function can however be calculated using the Finite Element Analysis (FEA). Combining reliability methods and Finite Element

Analysis is often referred to as Finite Element Reliability Methods (FERM). Instead of computing the structural behaviour (with FEA) in terms of deformations and stresses, the behaviour is computed in terms of probability of failure and uncertainty contributions. In this way the basic demands of the codes are met, i.e. meet the required probability of failure.

The problem arising is that the mentioned standard reliability methods are traditionally used for problems with only a few random variables using little time to evaluate the limit state function. In combination with FEA, the opposite occurs as there are many random variables and evaluating the limit state function takes much computational effort. The standard reliability methods in combination with FEA lead to a computational effort that is just too much.

A probabilistic Finite Element Analysis or FERM leads to the following advantages:
- In comparison to standard FE it gives direct insight into the structural reliability and decisive parameters;
- Structures designed using FERM will either be safer or more economically built in comparison to structures designed using safety factors.

The Finite Element Reliability Method is expected to be useful for code writing especially in the areas where the component reliability is still a black box (for instance soil structures). Furthermore it is expected to be useful in areas where the component reliability is known (steel, concrete structures) but little knowledge exist on the systems reliability. Initially it may give way to the calibration of partial material safety factors and safety factors for system behaviour.

1.2 Existing procedures and their limitations

Most reliability methods are applied on and suitable for more or less simple problems with analytical limit state functions and a few random variables [Tho98]. In FERM, often extensive FE models have to be used to compute the limit state function instead of an explicit analytical limit state function. This causes a substantial increase of the required computational time, which is certainly the case with many random variables and when the physically and geometrically non-linear structural behaviour is taken into account.

For example, consider a structure modelled by an FE model consisting of 50 elements. When the description of the σ-ε diagram for each element requires four variables, the material properties amount to $50 \times 4 = 200$ random variables. When every element is loaded by two forces, an additional 100 stochastic load variables have to be taken into account. When the geometrical properties are stochastic as well, the total number of random variables will go up to 1000. If some variables are fully correlated, which is not customary, this number can be reduced.

Additionally, a real structure may have many failure paths and limit states. Therefore, the calculation of the reliability of such a structure with standard reliability analysis tools like FORM, Monte Carlo (MC) or Numerical Integration (NI) is exceedingly time consuming. Having 1000 random variables, the numerical integration methods are at any rate out of the question. The standard Monte Carlo simulation (assuming a failure probability of $P_f = 10^{-4}$) uses approximately 5 10^6 FE computations. Although this number can decrease by applying more advanced techniques like importance sampling, still an enormous amount of FE computations will remain. The standard FORM procedure is very time consuming as well. The number of FE computations needed is approximately equal to 1 10^4.

In order to reduce the number of FE calculations a Response Surface (RS) technique is often employed [Far89]. The standard option is to execute a number of FE calculations, followed by the construction of a Response Surface. Finally a reliability analysis (FORM) is performed using the response surface for the limit state function evaluations. It is questionable whether the accuracy of this method is sufficient.

In short the main burdens of existing procedures are:

- The fact that a large number of random variables leads to a large amount of limit state function evaluations;
- The large computational time per limit state function evaluation when evaluated with FE analysis;
- The questionable accuracy of faster reliability methods.

1.3 Scope of the project

Incentive

The probability of failure of a structure as a whole, modelled with an FEA, is to be computed. All reliability methods make use of Limit State Function Evaluations (LSFE). For reliability analysis in combination with FEA, every LSFE means one FEA computation. Since FE computations take considerable computational time, the number of LSFE should be minimised. Besides, the computational time per LSFE or per FEA computation should be minimised.

Accuracy

Minimising the computational effort can only be carried out meaningfully under the constraint of sufficient accuracy. Very precise answers are not required. The accuracy should be such that the discrepancy in the probability of failure is acceptable for the normal design process.

Capabilities

To create a useful probabilistic analysis, all variables in FEA should be treated as random variables, in particular:

- Material properties:
  - Yield stress, modulus of elasticity, ultimate stress and ultimate strain;
- Geometrical properties:
  - Cross-sectional dimensions, nodal co-ordinates (eccentricities);
- Loads:
  - Nodal and element forces, settlements of supports, temperature loads.

The input option for the probabilistic analysis should allow a wide variety of distribution types and correlation patterns. It is however limited to time invariant variables.

Most probabilistic methods can be speeded up by prior knowledge of the probabilistic behaviour. An example is importance sampling [Eng93]. In this thesis it is supposed that prior knowledge is not necessarily available. The probabilistic FE method should be a tool that can be used without knowledge of probabilistic methods or probabilistic behaviour. Another requirement is that the reliability method can easily be implemented in a standard FE code.

Computational time

The objective is to compute the structural reliability as fast as possible. Both the number of Limit State Function Evaluations (LSFE) and the computational time per LSFE should be minimised.

Computational time might be minimised at cost of extensive computer coding. This leads to a decrease of universality and capabilities and is therefore not the objective of this research.

Another approach worth mentioning is metacomputing [Mar98], where structural reliability computations are carried out on computers with many (more than 100) processors or on many computers. This of course reduces the elapsed computational time (but not the computational effort).

The result of this research, in practical present day terms, should be that probabilistic static analysis of a structure with physically and geometrically non-linear behaviour is carried out within 24 hours computational time on a standard UNIX computer (using one processor). Using for instance 150 parallel processors would lead to a computation within 10 minutes.

1.4 Outline of the thesis

A straightforward use of reliability methods in combination with FEA takes considerable computational effort. Research is needed to determine how numerical methods developed in standard reliability engineering, like First and Second Order Reliability Methods and the various Monte Carlo techniques, can be used in combination with Finite Element analysis.

First of all the standard reliability methods are discussed in chapter 2. Chapter 2 starts discussing the efficiency and accuracy of the level III reliability methods such as Numerical Integration (NI) and Monte Carlo (MC) simulation. Level III reliability methods are known for their accurate and direct computation of the system failure probability. Special emphasis is put on the Directional Sampling method.

Following the discussion of the level III methods, the so called level II reliability methods like First and Second Order Reliability Method (FORM/SORM) are discussed. Level II reliability methods use an approximation of the probability of failure, and are designed for component reliability studies. Methods for computing the system reliability out of (level II) component reliability are summarised.

Chapter 3 introduces two adapted reliability methods, both making use of a response surface. The response surface as such has already been used as an interface between reliability methods and FEA. In this thesis, an adaptive response surface is used in combination with FORM. Furthermore, an adapted directional sampling method is introduced. In chapter 4 the effectiveness and accuracy of both adapted methods is researched on the basis of artificial limit state functions. Comparison is made with the accuracy and efficiency of the existing reliability methods.

The best performing reliability method according to chapter 4 is further researched on the performance on structural reliability in combination with FEA. Several examples are given of FEA of complex structures. Proof is given on the effectiveness and accuracy of the method in combination with (non-linear) FEA computations in chapter 5.

Finally, remarks and conclusions are given in chapter 6 and 7.

2. Efficiency and Accuracy of standard reliability methods

2.1 Basis formulation of the reliability problem

A reliability problem is defined by a limit state function $g(\underline{x})$ and a set of n random variables $\underline{x}$. Failure is defined by the event $g(\underline{x}) \leq 0$. The equality $g(\underline{x}) = 0$ is called the limit state equation, the corresponding surface is called the failure surface.

The failure probability can be formally expressed as:

$$P_f = P[g(\underline{x}) \leq 0] = \int_{g(\underline{x})<0} f_{\underline{x}}(\underline{\xi})d\xi \tag{2.1}$$

where $f_{\underline{X}}(\underline{\xi})$ is the joint probability density function of $\underline{x}$.

The primary purpose of reliability methods is to evaluate integral (2.1). For structural reliability, the Joint Committee of Structural Safety [JCSS82] has proposed three levels of reliability analysis to evaluate equation (2.1):

- Level III methods such as Monte Carlo sampling and Numerical Integration are considered most accurate. They compute the exact probability of failure of the whole structural system, or structural elements, using the exact probability density functions of all random variables.
- Level II methods such as FORM and SORM compute the probability of failure by means of an idealisation of the limit state function where the probability density functions of all random variables are approximated by equivalent normal distribution functions.
- Level I methods verify whether or not the reliability of the structure is sufficient instead of computing the probability of failure explicitly. In practise this is often carried out by means of partial safety factors.

Some of the reliability methods solely work with standard normal independent random variables. Each set of n basic random variables (x-space) can be transformed into a set of m ($m \leq n$) independent standard normal variables (u-space). The (dependent) basic random variables are first remodelled into standard normal variables by equating the cumulative distribution functions for the basic random variable and the standard normal variable:

$$\Phi(u_i) = F_{X_i}(\xi_i) \longrightarrow u_i = \Phi^{-1}[F_{X_i}(\xi_i)] \tag{2.2}$$

where $\Phi(\,)$ is the standard normal distribution function.

Correlated variables may have to be transformed into non-correlated variables. There are several methods for the transformation of correlated variables into uncorrelated variables. The Rosenblatt transformation [Ros52] is the most used. Other methods proposed for transformation are Nataf [Nat62], Hermite [Win88] and Johnson [Joh72].

In case of the Rosenblatt transformation, a successive conditioning of the dependent variables leads to a transformation of the form:

$$\Phi(u_1) = F_{X_1}(\xi_1)$$
$$\Phi(u_2) = F_{X_2|X_1}(\xi_2|\xi_1)$$
$$\Phi(u_3) = F_{X_3|X_2,X_1}(\xi_3|\xi_2,\xi_1)$$

The transformation for normally distributed correlated variables can simply be performed by calculating the eigenvalues and eigenvector of the matrix Γ containing the covariance [Sta71].

$$\Gamma = W^T \Lambda W \tag{2.3}$$

where

Λ is the diagonal matrix with eigenvalues of the matrix Γ

W is the matrix with eigenvectors of the matrix Γ

The vector $\underline{u}^*$ with correlated variables can be transformed into a vector $\underline{u}$ with non-correlated variables using the following equation:

$$\underline{u} = W\sqrt{\Lambda}\ \underline{u}^* \tag{2.4}$$

Note that, in principle, there are n! possible different transformations, depending on the arrangement of the eigenvectors. In the case of non-normal dependent random variables, each arrangement may lead to a different estimate of the probability of failure [Dol83].

2.2 Required accuracy

The general goal in this thesis is to minimise the computational effort of FEA reliability calculations. This can only be carried out meaningful under the constraint of sufficient accuracy. In this thesis, the considerations of the Eurocode [ENV91] are joined. For the Serviceability and Ultimate Limit State (SLS and ULS) the Eurocode 1 (informal Annex A) requires a reliability index β of 1.5 and 3.8 respectively. How accurate the calculation of this reliability index should be is debatable. Eurocode 1 demands a maximum deficiency of 10 % in the structural calculations. The deficiency should of course not be caused solely by an error in the reliability index calculation. Errors in modelling may cause deficiencies as well.

Let an error of 2 % be caused by an error in the reliability index. For normally distributed variables, the partial safety factor on the mean is calculated as:

$$\gamma = 1 + |\alpha|\beta V \tag{2.5}$$

Using common parameters for the influence factor $\alpha = 0.7$, the reliability index $\beta = 3.8$ and the coefficient of variation $V = 0.15$ leads to the fact that a 2 % mismatch in the safety factor could be caused by an 8 % error in the reliability index. This 8 % error is here chosen to be the limit in the reliability analysis. Given a 95% confidence interval, this can be translated into a 0.05 coefficient of variation of the reliability index.

Another approach is to express the limit state function of a reliability study as:

$$g = \beta - u \tag{2.6}$$

where u is a standard normal distributed variable and β is the conditional reliability index.

If β is considered as uncertain, the effective reliability index β^*, for g is given by:

$$\beta^* = \mu(\beta) / \{1 + (\mu(\beta)\, V(\beta))^2\} \tag{2.7}$$

Using $\mu(\beta) = 3.8$ and $V(\beta) = 0.05$ leads to an effective reliability index β^* equal to 3.67 (a discrepancy of only 3.5 %). As a result $V(\beta) = 0.05$ is chosen as the limit for a sufficient accurate result.

The amount of samples that are needed by the standard reliability methods to meet this accuracy will be used as a measure for the efficiency.

2.3 Standard level III reliability methods

Level III reliability methods compute the probability of failure based on the exact probability density function and the exact limit state functions. Level III reliability methods are therefore considered being the most accurate. Well-known and straightforward procedures are Numerical Integration (NI) [Ouy87] and Monte Carlo sampling techniques (MC) [Rub81]. Errors can only be caused by a too large integration step size in NI and a too low number of simulations in MC. Improvements to the basic method with respect to efficiency that have been suggested (all some type of importance sampling [Eng93]) will be discussed in section 2.4.

2.3.1 Numerical integration

For the basic reliability problem where all variables are standard normal and independent, equation (2.1) can be rewritten as:

$$P_f = \sum_{i=-\infty}^{\infty} \sum_{j=-\infty}^{\infty} \cdots\cdots\cdots \sum_{k=-\infty}^{\infty} I(g(\underline{x}))f(\underline{x})\,\Delta x \tag{2.8}$$

where $I(g(x)) = 1$ if $g(\underline{x}) \leq 0$ and
$I(g(x)) = 0$ if $g(\underline{x}) > 0$

The accuracy of the numerical integration procedure will here be investigated by means of numerical experiments. A limit state function g is used where all (standard normal) variables u_i have equal importance:

$$g = \beta - \sum_{i=1}^{n} u_i/\sqrt{n} \tag{2.9}$$

The procedure is applied to limit state functions with 4, 8 and 12 variables respectively and $\beta = 4$. The probability of failure (in case of 4 variables) is calculated from:

$$P_f = \sum_{i=-\infty}^{\infty} \sum_{j=-\infty}^{\infty} \sum_{k=-\infty}^{\infty} \sum_{l=-\infty}^{\infty} I(g(\underline{u}))f(u_1,u_2,u_3,u_4)\Delta u_1 \Delta u_2 \Delta u_3 \Delta u_4 \quad (2.10)$$

Figure 2.1 shows the relative error in reliability index D defined as:

$$D = | \beta_{NI}-\beta_{exact} | / \beta_{exact} \quad (2.11)$$

For 8 and 12 variables, no results are presented for $\Delta u < 1$ and $\Delta u < 1.5$ respectively. This is due to the tremendous computational effort to perform these operations.

A straight line through the origin is fitted to the error data in order to investigate the error as a function of the integration step size. A global increase of discrepancy with increasing integration step size Δu can be observed. A maximum error D in the reliability index of 8 % is acceptable (as discussed in section 2.2). According to Figure 2.1, this globally means that a step size $\Delta u = 1.7$ is sufficient. There seems to be no influence of the number of variables n on the error D (at least not for the range of the investigated number of variables).

Figure 2.1: Relative error D as a function of step size.

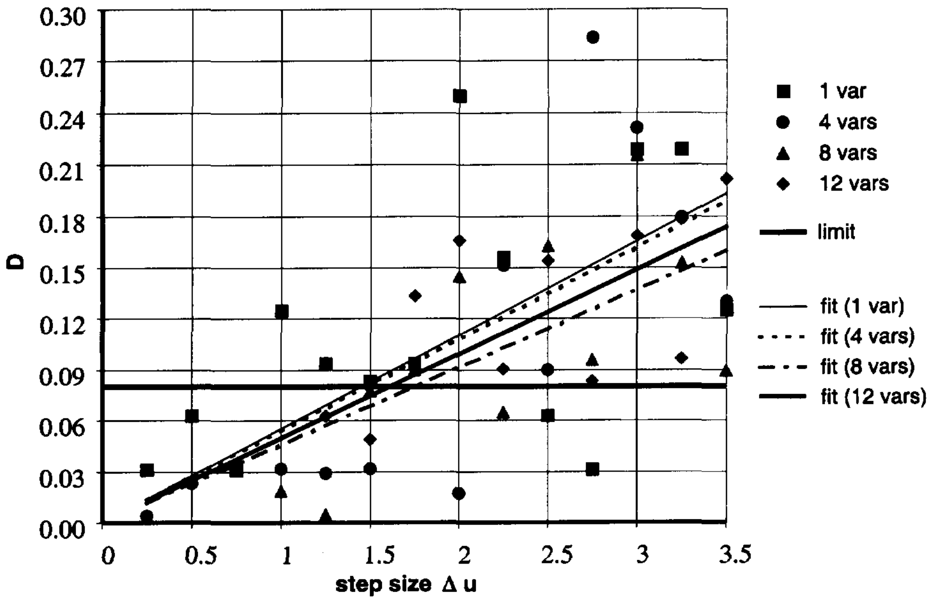

The error D depends on the number of steps compared to the distance β. In this example the step size $\Delta u = 1.7$ can be seen as $\Delta u \approx \beta/3$. Simulations with $n = 12$ and $\beta = 4$ show that this is sufficient accurate to perform the numerical integration from –4 to 4 instead of from $-\infty$ to ∞. Given this information, the number of samples N can now be calculated from: $N = 7^n$.

This shows a significant increase of the number of samples with increasing number of variables. For high dimensional problems ($n > 10$) an exceedingly computational time would be needed. Therefore in most structural applications, numerical integration is applied only for validation of other methods while using a low number of variables.

2.3.2 Crude Monte Carlo simulation

The Monte Carlo technique consists of sampling random x-values from their distributions f(x) and calculating the relative number of simulations for which $g(\underline{x}) < 0$:

$$P_f = \frac{N_f}{N} \text{ or } P_f = \frac{\sum_i^N I(g(\underline{x}))}{N} \tag{2.12}$$

where N is the total number of simulations and N_f the number of simulations in the failed state ($g(\underline{x}) \leq 0$).

The minimum required number of samples in Monte Carlo sampling, given a target for $V(P_f)$, can be calculated from [Vro84]:

$$N > \frac{1}{V(P_f)^2}\left(\frac{1}{P_f} - 1\right) \tag{2.13}$$

In section 2.2 a $V(\beta) = 0.05$ was chosen to be acceptable. For $\beta = 4$, the coefficient of variation of the reliability index $V(\beta) = 0.05$ can be translated into the coefficient of variation of the probability of failure estimate $V(P_f) = 0.57$. Equation (2.13) can then be simplified to

$$N > 3 / P_f. \tag{2.14}$$

The number of samples for the case where $\beta = 4$ is therefore: $N > 10^5$. The number of samples depends on the probability of failure and is independent of the number of random variables. The lower the probability of failure, the more samples have to be used.

2.3.3 Directional integration

Deák [Dea80] first suggested the method of transforming the normal coordinates (u-space) into polar coordinates. The basic idea is to remodel the basic variables $\underline{u}$ into polar co-ordinates (λ, $\underline{\theta}$). The unit vector $\underline{\theta}$ defines the direction and a scalar quantity λ defines the length of the vector in u-space. Equation (2.1) is altered into:

$$P_f = \int_{g(\underline{x})\leq 0} dF(x) = \int P(g(\lambda\underline{\theta}) \leq 0) f(\underline{\theta}) d\underline{\theta} \tag{2.15}$$

where $f(\underline{\theta})$ is the (constant) density on the unit sphere.
For each direction $\underline{\theta}_i$ the value of λ_i is determined for which the limit state function equals zero:

$$g_i = g(\lambda_i \, \underline{\theta}_i) = 0 \tag{2.16}$$

In other words λ_i is a measure of the distance to the limit state in the direction defined by the vector $\underline{\theta}_i$. The factor λ_i is found via an iteration procedure and requires several Limit State Function Evaluations (LSFE). Annex A.1 shows the iteration procedure. Examples in this thesis show that on average, approximately 3 LSFE are required. The derivation of the method for two variables is given in Annex A.2.

The directional integration method integrates over the directions $\underline{\theta}$:

$$P_f = \int \left(1 - \chi_n^2(\lambda^2(\underline{\theta})\right) d\underline{\theta} \tag{2.17}$$

Examples of directional integration can be found in [Kat98] and [Yon98]. The accuracy and efficiency will be discussed in section 2.3.5.

2.3.4 Crude Directional sampling

Instead of performing a Directional Integration, an estimate of the probability of failure P_f can be obtained by performing N directional Monte Carlo simulations of the $\underline{\theta}$-vector. Every simulation results in a sample value P_i:

$$P_i = P(g(\lambda_i \; \underline{\theta}_i) < 0\} = 1 - \chi_n^2(\lambda_i^2) \tag{2.18}$$

$\chi^2(..)$ is the chi-squared distribution function;
n is the number of random variables in the limit state function.

An estimate for the probability of failure is calculated as the mean value of the sample values P_i:

$$E(P_f) = \frac{1}{N}\sum_{i=1}^{N} P_i \tag{2.19}$$

An estimate of the standard deviation is given by [Dit88]:

$$\sigma^2(P_f) = \frac{1}{N(N-1)}\sum_{i=1}^{N}\{P_i - E(P_f)\}^2 \tag{2.20}$$

When the number of samples N is sufficiently large, the estimator for P_f is assumed to be normally distributed. The confidence intervals of the probability of failure are calculated from:

$$E(P_f) + k\,\sigma(P_f) < P_f < E(P_f) - k\,\sigma(P_f) \tag{2.21}$$

The probability of failure lies between the confidence limits with a probability approximately equal to 1-2Φ(k) [Dit88]. The number of samples required to make it plausible that the estimator is normally distributed is analysed by means of experiments.

Figure 2.2: Required number of samples N before the estimator is normally distributed.

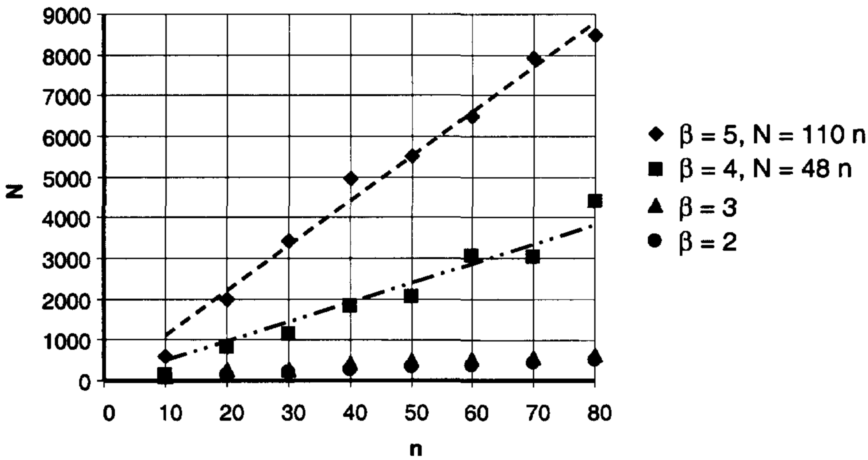

The required number of samples N is given in Figure 2.2 as a function of n and β. The number of samples is calculated using equation (2.9) such that there is a 95% confidence that the hypothesis of a normal distribution can not be rejected (according to the test on normality [Soe79]). For $\beta = 4$, Figure 2.2 shows that approximately $N > 48$ n samples are required before reaching normality. For $\beta = 5$, $N > 110$ n samples are required.

Figure 2.3 shows, as an example, the results of directional simulation for a limit state function where all variables have equal importance (eq. (2.9) with $\beta = 4$, n=10). Besides the mean value (bold line), the lower and upper confidence interval are given (solid lines)

In section 2.2 a $V(\beta) = 0.05$ was chosen to be acceptable for the needs of structural reliability. Figure 2.5 shows the required number of samples N for a coefficient of variation $V(\beta) = 0.05$, for reliability indices $\beta = 2$, 3 and 4. This required number of samples is calculated as the mean of 50 numerical experiments. A linear limit state function g is used where all (standard normal) variables u_i have equal importance, see equation (2.9). The number of necessary samples N increases with the number of variables n in the limit state function. The amount of samples increases also with increasing β. For high n and $\beta = 4$, the mean number of required samples approximately converges to 160 n. For example: with $\beta = 4$ using 100 variables, the mean needed number of samples N equals 16000. The number of 160 n is always higher than 48 n (normality). Reaching a sufficiently low coefficient of variation V(β) ensures the estimator to be normally distributed.

Figure 2.3 : Example of the crude directional sampling estimate of the reliability index β, as a function of the number of samples, inclusive confidence limits (eq. 2.9, n = 10, $\beta = 4$).

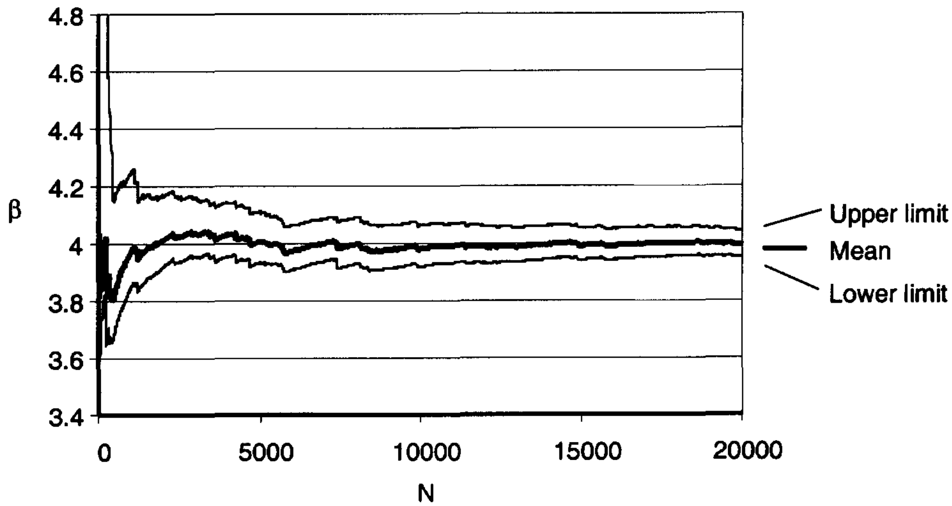

Figure 2.4: Difference between directional sampling and integration.

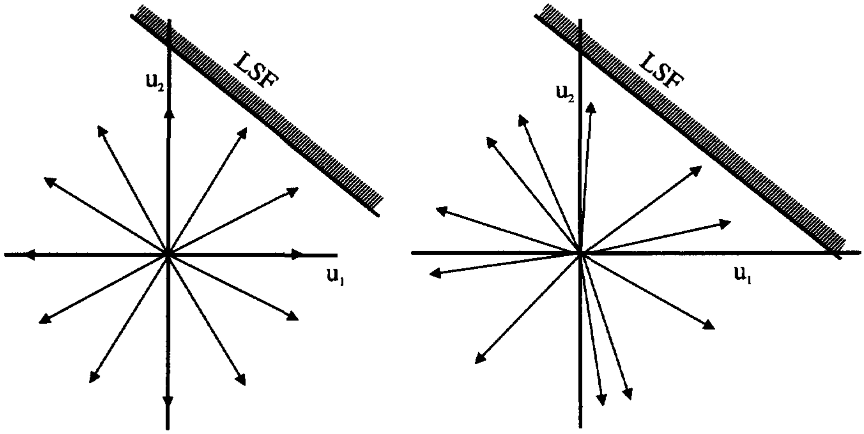

Directional Integration Directional Sampling

The difference between Directional Integration (DI) and Directional Sampling (DS) lies in the fact that the space is equally divided using DI and randomly divided using DS (see Figure 2.4). The accuracy of DI and DS will be equal for large N. The accuracy of directional sampling is therefore supposed to be the same as for directional integration. For low N there will be a difference, depending on the shape of the limit state function. This difference is not discussed here.

2.3.5 Comparison of the efficiency of the four standard level III methods

In the previous sections, the procedure and required number of samples have been dealt with. This section compares the required number of samples as a function of the number of random variables under the constraint $V(\beta) < 0.05$. Figure 2.5 shows the required number of samples for the level III standard reliability methods. The number of samples is shown for a reliability index $\beta = 2$, 3 and 4 and $V(\beta) = 0.05$. As discussed in the previous section, directional sampling and directional integration procedures are supposed to perform the same. The numerical integration procedure results in a constant increase of the number of samples. The directional sampling procedures converges into increase of samples linear to the number of variables. For $\beta = 4$, the required number of samples for directional sampling approximates N = 160 n.

For $\beta = 4$ and 100 random variables Monte Carlo simulation requires 10^5 samples, where directional sampling requires 1.6 10^4 samples. Bear in mind that Monte Carlo simulation uses one LSFE per sample, where directional sampling uses approximately 3 to

4 LSFE per sample. The difference is therefore approximately a factor 2 in the number of LSFE. The profit of directional sampling grows the less random variables are applied. Monte Carlo sampling becomes faster than directional sampling when more than about 100 random variables are involved. It is furthermore shown that numerical integration is only to be performed for low dimensional problems (n < 5).

It is concluded that for most structures, with less than 100 random variables, directional sampling performs best. Monte Carlo simulation becomes appropriate only for high (n > 100) dimensional problems.

Figure 2.5: Required numbers of samples, all variables have equal importance in the limit state function (eq. 2.9).

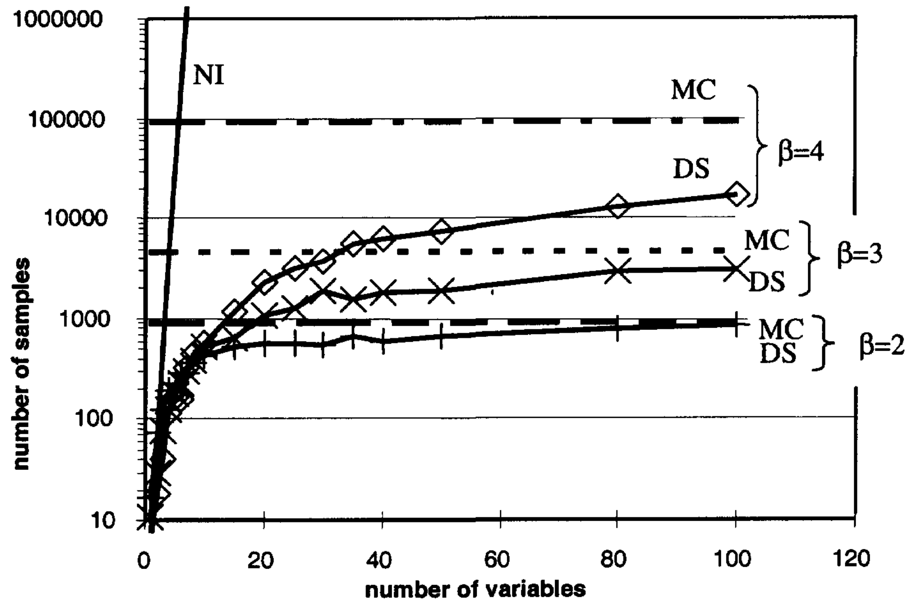

NI = Numerical Integration, MC = Monte Carlo sampling, DS = Directional sampling

2.4 Level III, Monte Carlo Importance sampling

The Monte Carlo procedures can be speeded up by means of importance sampling. A sampling density h(x) is used instead of the actual probability density function f(x). For Monte Carlo simulation the probability of failure is calculated by:

$$P_f = \frac{\sum_i^N I(g(\underline{x}))\frac{f(\underline{x})}{h(\underline{x})}}{N} \tag{2.22}$$

In practice, importance sampling usually means that the sampling is concentrated in the area with a high likelihood of failure (see left part of Figure 2.6). The problem is that prior knowledge is needed of the failure area, which in most cases is not available. A reliable procedure, for cases where no prior knowledge exist on the influence of variables on the limit state function, is to increase the variance of all variables (see right part of Figure 2.6). The limit state function (2.9), where all (standard normally distributed) variables have equal influence on the limit state function is researched. A normal distribution with $\sigma_h > 1$ is used in the importance sampling density $h(\underline{x})$.

Figure 2.6 : Importance sampling.

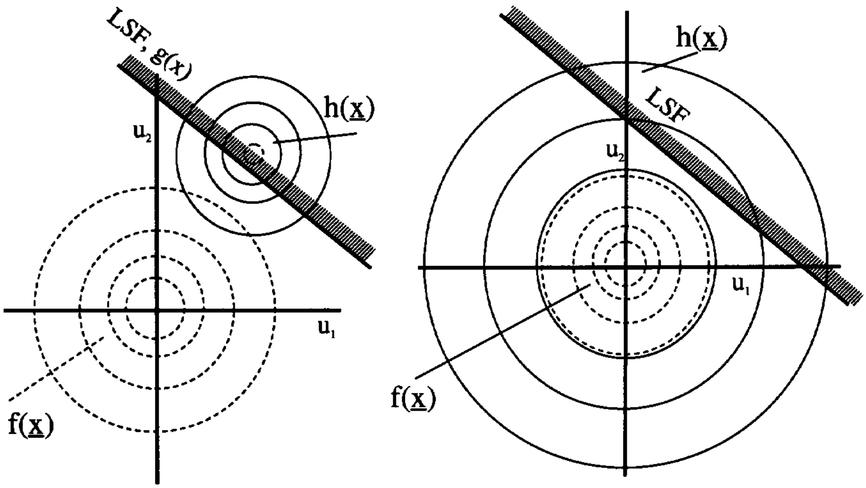

Standard importance sampling — Increased variance sampling

The number of samples is calculated, by means of numerical experiments, to find a coefficient of variation of P_f conform section 2.2 and 2.3.2. For $\beta = 4$ this means a coefficient of variation $V(P_f) < 0.57$.

Figure 2.7 shows the required number of samples as a function of the number of variables n and the importance sampling standard deviation σ_h. The situation with $\sigma = 1$ is equal to crude directional sampling (without importance sampling). The required number of samples for this case is in line with equation (2.23). Figure 2.7 shows that a small increase of σ results in a considerable decrease of the required number of samples. It shows furthermore that the required number of samples increases with the number of variables.

Figure 2.7: required number of samples by Monte Carlo importance sampling, all variables have equal importance to the limit state function (eq. 2.9, $\beta = 4$).

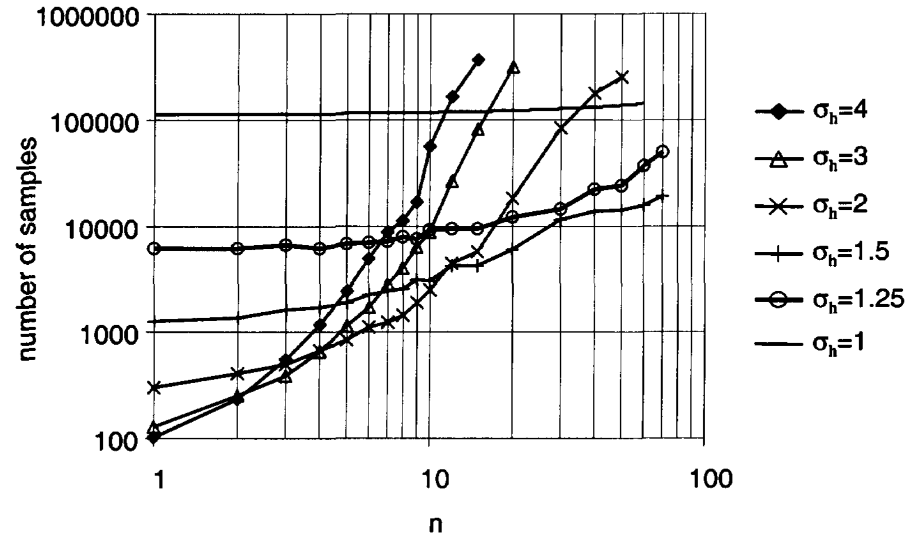

The optimal importance sampling strategy (σ_h) depends on the number of variables. On the basis of the simulation results, an empirical relation has been derived. The optimal σ_h is approximately equal to:

$$\sigma_h = \beta n^{-0.4} \tag{2.24}$$

Figure 2.7 shows that for an optimal σ_h in relation with the number of variables n, the number of samples equals approximately N = 300 n. This means that the proposed Monte Carlo importance sampling, requires more samples than crude directional sampling (Figure 2.5: N=160 n). Directional sampling uses approximately 3 LSFE per sample, where Monte Carlo simulation uses only one LSFE per sample. Consequently Monte Carlo importance sampling requires LSFE = 300 n and crude Directional sampling requires LSFE = 3 160 n = 480 n. This means that Monte Carlo importance sampling is to be slightly preferred above crude directional sampling. A disadvantage, however, is that the reliability index β has to be known on forehand in order to choose an optimal σ_h. The amount of samples can be higher than without importance sampling when a non-optimal σ_h is chosen.

Since the outcome of the computations can not be known on forehand, the ideal σ_h will never be reached in practise. Maybe an adaptive technique can be used here.

It can be observed from Figure 2.7 that a slight deviation in σ_h easily leads to a factor 2 increase of the required number of samples N. It is therefore expected that Monte Carlo importance sampling and crude directional sampling are approximately equally efficient.

2.5 Level III, Directional Importance sampling

For directional sampling, basically, sampling in u-space is replaced by sampling in a limited number of directions. Equation (2.18) is rewritten as:

$$P_f = \int P\{g(\lambda \underline{\kappa}) \leq 0\} \frac{f(\underline{\kappa})}{h(\underline{\kappa})} h(\underline{\kappa}) d\underline{\kappa} \tag{2.25}$$

where $h(\underline{\kappa})$ is the importance sampling density of the vector $\underline{\kappa}$.

An estimate of the probability of failure is calculated from sample values:

$$P_i = P\{g(\lambda_i \underline{\kappa}_i) \leq 0\} \frac{f(\underline{\kappa}_i)}{h(\underline{\kappa}_i)} = (1 - \chi_n^2(\lambda_i^2)) \frac{f(\underline{\kappa}_i)}{h(\underline{\kappa}_i)}, \tag{2.26}$$

$$E(P_f) = \frac{1}{N} \sum_{i=1}^{N} P_i$$

The distribution $f(\underline{\kappa})$ has an uniform density. The density of $h(\underline{\kappa})$ can be computed numerically. The computation of $f(\underline{\kappa})/h(\underline{\kappa})$ requires considerable computational effort. Performing this operation for high n is therefore discouraged.

Several authors have suggested methods for importance sampling in combination with directional sampling [Kija92], [Dit88], [Dit90] and [Bje88]. All methods require prior knowledge on the influence of variables on the limit state function. In general, in structural reliability, there is little prior knowledge on the influence of variables on the limit state function. Even little knowledge may however speed up the computations considerably.

In general there are five methods of importance sampling:

- Decrease variance of unimportant variables.
- Truncate distribution function of variables with known importance to the limit state function.
- Apply weighting functions.
- Skip unimportant variables.
- Shift variables.

These methods will be discussed in the next sections.

2.5.1 Decrease the variance of unimportant variables

One of the importance sampling methods is decreasing the variance of non-dominating variables, which can be performed in combination with a shift of the mean value. This requires that non-dominating variables are known on forehand, or are recognised by the procedure itself.

Choosing a variable to be non-dominant where in fact it is dominant leads to an erroneous result. The procedure can therefore only be generally accurate when a possible incorrect choice of non-dominating variables is recognised and adjusted. Figure 2.8 shows an example with two standard normal variables. An importance sampling density $h(\underline{\kappa})$ is used instead of the original sampling density $f(\underline{\kappa})$. The importance density is based on a reduced variance of variable u_1, which is totally unimportant to the limit state function.

Figure 2.8: Decreasing the standard deviation of non-dominating variables.

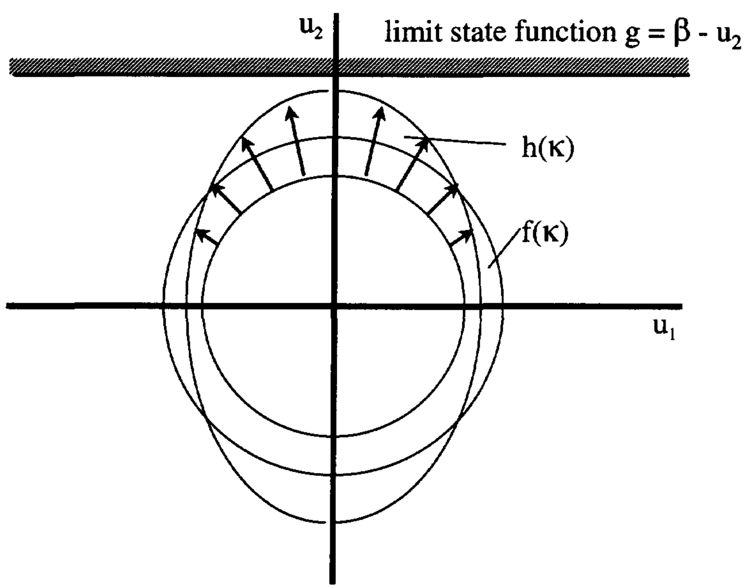

Figure 2.9 shows the results (required number of samples) of an example with two standard normal variables u_1 and u_2, using a limit state function $g = 4 - u_1$. Variable u_2 is totally unimportant to the limit state function. Here, a required accuracy of $V(\beta) = 0.005$ is used instead of $V(\beta) = 0.05$, because $V(\beta) = 0.05$ would give a number of samples which is too low to show the influence of decreasing the variance. Since variable u_2 is totally unimportant to the limit state function, it seems reasonable to assume that its variance can

be reduced to zero. Figure 2.9 shows that reducing the variance leads to a reduction of $V(\beta)$ indeed. Fewer samples are needed for the same $V(\beta)$ when $\sigma(u_2)$ is reduced. Using a very low $\sigma(u_2)$, may lead to an expected value for the reliability index β that is higher or lower than it should be. This is because the $V(\beta)$ is low, already for a low number of samples, also in cases where enough directions have been sampled to get a reliable estimate of β itself. This effect occurs for $\sigma(u_2) < 0.2$. Reducing $\sigma(u_2)$ below 0.2 does therefore make no sense and is represented by the dashed line in Figure 2.9. For 2 variables, the maximum reduction in the required number of samples is approximately 25 % compared to the original crude directional sampling procedure.

Figure 2.9: Number of samples needed for $V(\beta) = 0.005$, 2 variables, $g = 4 - u_1$.

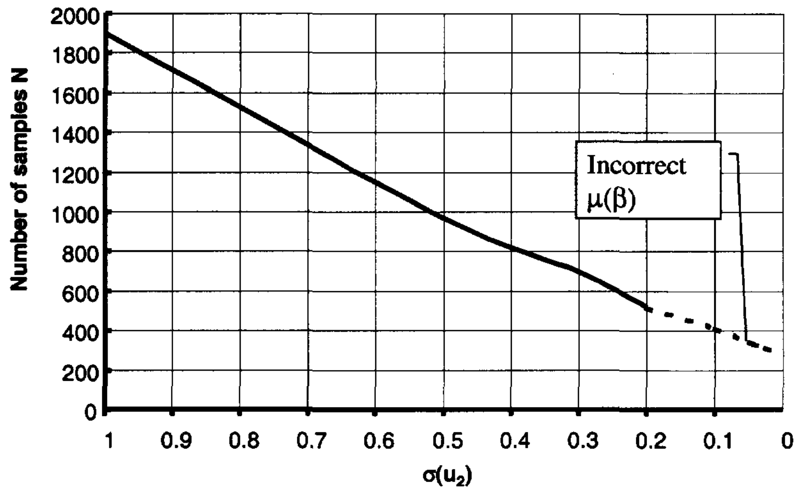

Figure 2.10 shows the required number of samples for limit state function $g = 4 - u_1$, with n standard normal variables (n-1 totally unimportant). Here $V(\beta) = 0.05$ is used. A number q unimportant variables have reduced standard deviation (0.5, 0.25 or 0.125). This number of unimportant variables q is plotted on the horizontal axis. It shows that, in the case of 10 random variables, approximately 700 samples are required when the non-dominant variables are not given a reduced standard-deviation ($q = 0$). This agrees with Figure 2.5. Obviously there is no difference in the required number of samples for limit state functions where all variables have equal importance and limit state functions where only few variables have importance.

Figure 2.10: Effect of reducing the standard deviation $\sigma(u_q)$ (eq. 2.27, $\beta = 4$, $V(\beta) = 0.05$).

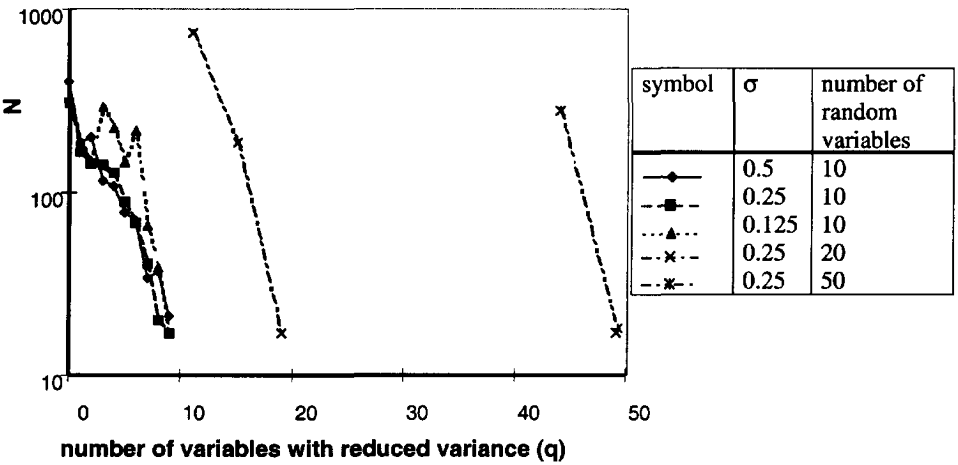

Reducing the standard deviation of all 9 non-dominating (out of 10) variables ($n = 10$, $q = 9$) to $\sigma(u_q) = 0.25$ leads to approximately 20 samples. The combination $n=50$, $q = 49$ and $\sigma(u_q) = 0.25$ needs approximately 20 samples as well. When $n = 50$, $q = 44$ and $\sigma(u_q) = 0.25$, still some 300 samples are required. Clearly nearly all unimportant variables should be recognised and considered as such to get down to a small number of samples.

The behaviour of variables with little instead of no importance to the limit state function in comparison to totally unimportant variables is subsequently researched. This is investigated with the limit state function:

$$g = \beta - x_1 - \sum_{i=2}^{n} 0.05 x_i \qquad (2.27)$$

The result is the same as shown in Figure 2.10. It is concluded that the behaviour of both variables with little importance and totally unimportant variables is alike. Importance sampling can therefore be used on these kinds of limit state functions as well.

2.5.2 Truncate the variable distribution

Instead of reducing the variance, the distributions of the variables may also be truncated. This might for instance be useful when it is known that only the positive side of the distribution is of importance to the limit state function. For example, only positive parts of the standardised distribution function of the variable describing the loads can be used. In most cases the important direction of only a part of the variables is known. Equation (2.26) can not be used directly because a part of the importance sampling distribution is zero. Instead samples in the truncated directions are assumed to have a zero probability response ($P_i = 0$). Figure 2.11 shows that no error is made when one variable is truncated. A (small) error is made when two variables are of importance to the limit state function and both are truncated. Figure 2.12 shows that for some directions $P_i = 0$ is assumed where this is not the case. Annex C shows that truncating more than 10 equally important variables leads to errors that are higher than 8 % (the maximum acceptable in error in the reliability index, as explained in section 2.2).

Annex C shows that the number of samples approximately reduces by a factor 2 for each truncated variable. Given the 10 truncated variables, the reduction is maximum factor $2^{10} = 1024$. Furthermore, Annex C shows that the correct result can even be found if an incorrect truncation is used. The condition is that some samples (approximately 10 % of the total number of samples) are chosen in the truncated directions. Sampling is continued until $V(\beta)$ is sufficiently low. The fact that only few samples are performed in the correct direction leads consequently to many required samples.

Figure 2.11: Limit state function with two variables, where only one (truncated) is important to the limit state function.

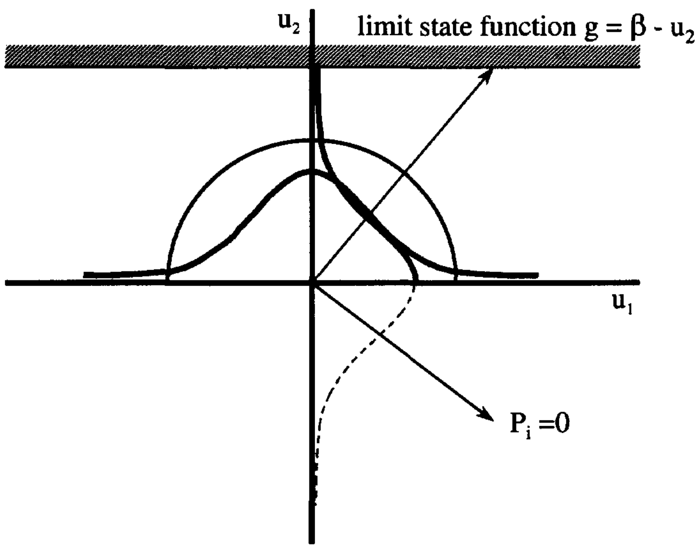

Figure 2.12: Limit state function with two variables, where both (truncated) are important to the limit state function.

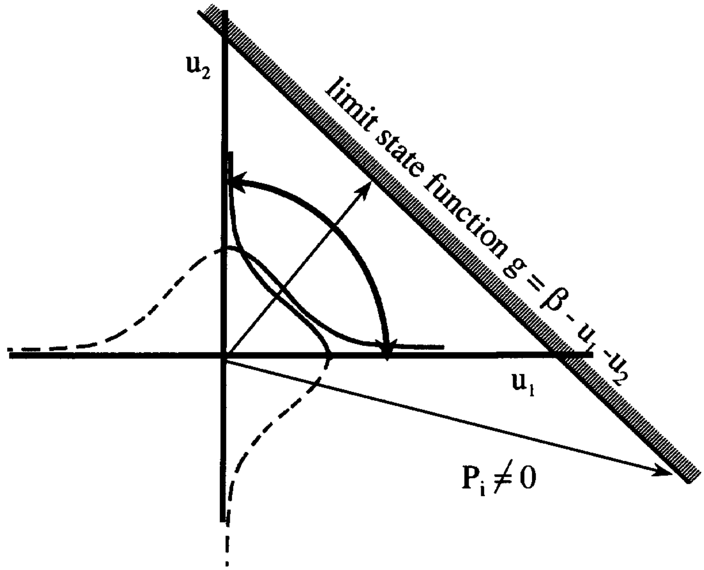

2.5.3 Apply weighting functions to directional sampling

In [Kya92] a weighting function is used to direct h(κ). The weighting function is based on previous results of the directional sampling procedure. Every time a sample has been performed, the weighting function is updated. As such an adaptive importance sampling procedure is obtained. According to [Kya92] there is a possibility of overlooking an important region when the weighting function method is used on its own. For low dimensional problems, [Kya92] therefore suggests to use 90 % adaptive importance sampling and 10 % uniform directional sampling (see also Annex C). For high dimensional problems a 50 - 50 % division is suggested. A 50-50 division however leads to a very high number of samples. For low dimensional problems [Kya92] suggests to find the important regions in the starting procedure.

2.5.4 Skip variables

The required number of samples depends on the number of random variables (see section 2.3.1) even when the random variables are not of importance to the limit state function. Since these non-dominating variables do not influence the result (β), it would be best to omit these variables entirely. A method that recognises these non-dominating variables is not yet found. A suggestion might be to use level II probability method FORM results (see section 2.6). Figure 2.13 shows two examples where this would and would not be a good suggestion.

Figure 2.13: Important variables found by FORM.

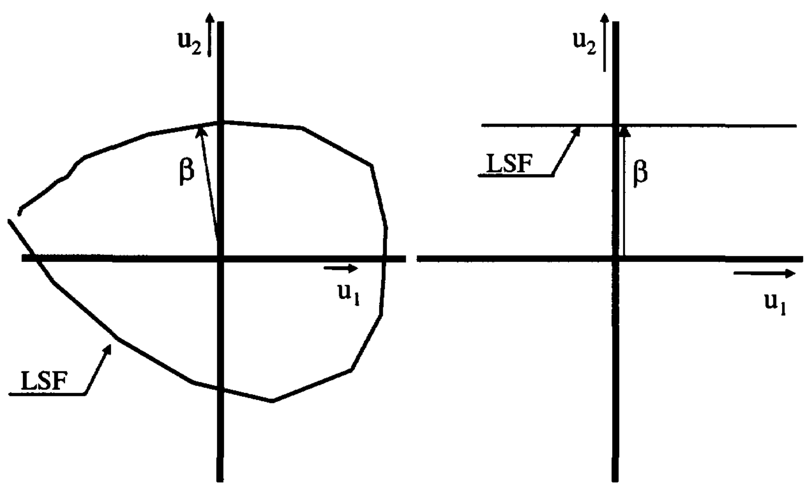

Two variables have importance where FORM finds only one

Only one variables has importance, The second (x_1) can be skipped

2.5.5 Shift variables

Next to truncating and reducing the variance, the mean value of the variable can be shifted as well. In fact, it is possible to focus the directional sampling on a certain region. Annex D gives an example of a system of four components where the sampling is focussed on a certain point. The example shows that other regions than the region of this design-point are not taken into account due to the focussing. The lesson is that importance sampling reduces the number of samples but may lead to erroneous answers that are not recognised. This method of importance sampling can only be performed when it is certain that important regions are not forgotten. This condition does not fit in the global aims of the thesis (where no prior knowledge is assumed to be needed).

2.6 Level II reliability methods

2.6.1 First and Second Order Reliability Methods

The present standard in level II methods is the First Order Reliability Method (FORM), according to [Has74], [Rack78] and [Mad86]. The FORM computes the probability of failure by means of linearising the limit state function in the so-called design-point or β-point. According to [Bje91], FORM has proven to be highly efficient in use with only few variables (< 50) and smooth limit state functions. The limit to 50 variables is not a physical limit. There is only little experience with higher numbers of variables.

Figure 2.14 shows a two-dimensional u-space (see section 2.1) with a limit state function. The point of the limit state function that is closest to the origin is called the design-point. The FORM linearises the limit state function in this design-point. Since the joint probability density function rapidly decreases with the distance $|u|$ from the origin, the main contribution to the probability integral (2.1) originates from the region that is closest to the origin. The probability of failure P_f can be computed from:

$$P_f = \Phi(-\beta) \tag{2.28}$$

where Φ is the standard normal distribution.

The design-point is to be found with a minimisation procedure that iterates to the vector $\underline{\alpha}\beta$ with the smallest distance from the origin to the failure surface (see Figure 2.14). Since the α values ($|\alpha| \leq 1.0$) show the influence of variables on the limit state function, they are called influence factors.

Several methods have been introduced to find the design-point. All of them originate from minimisation procedures. A general overview of these minimisation procedures is found in [Him72] and [Jud80]. The minimisation procedures can be divided into gradient and non-gradient methods. In general, gradient methods use less iterations than non-gradient methods. On the other hand, the gradients have to be delivered at cost of analytical differentiation or by means of numerical differentiation (at cost of LSFE).

Figure 2.14: Two-dimensional illustration of u-space, LSF and design-point.

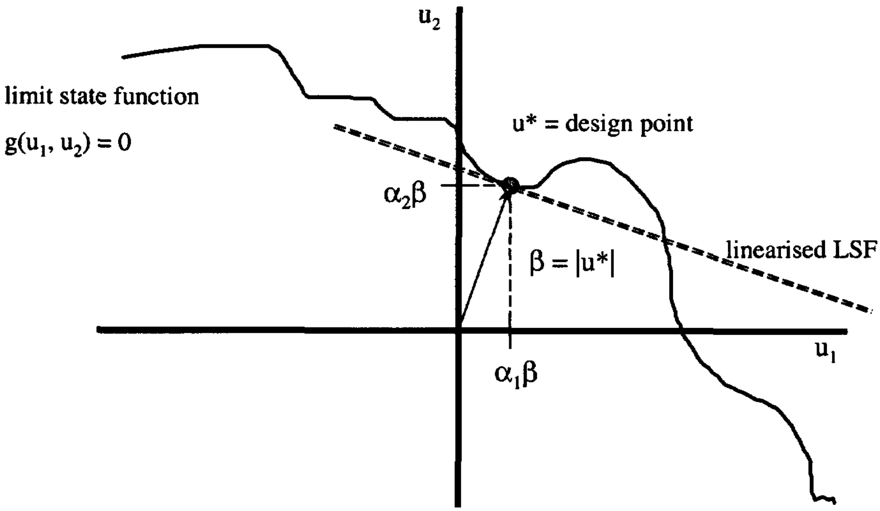

Figure 2.15: Some shapes of limit state functions in 2-dimension space.

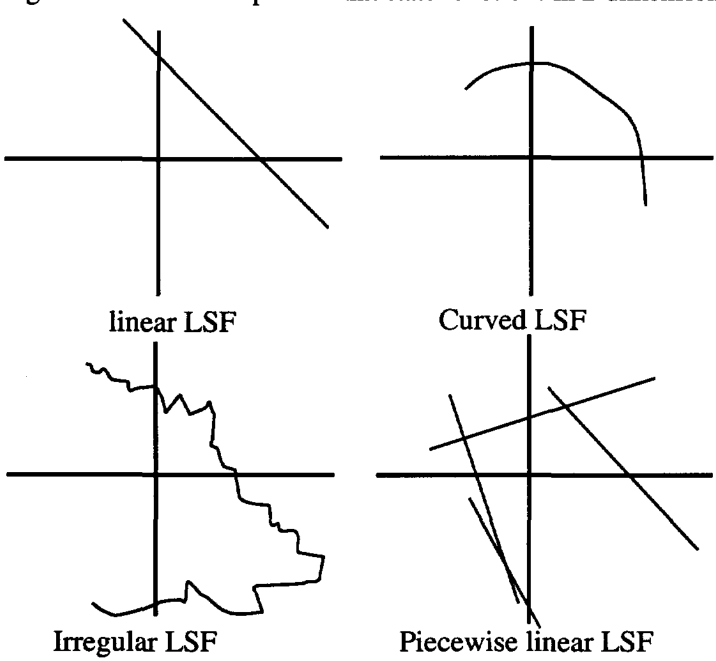

A linear approximation in the design-point will be accurate in cases of linear or relatively flat limit state functions. For strongly curved but smooth limit state functions (see Figure 2.15), [Bre84] introduced the Second Order Reliability Method (SORM). Instead of a linear approximation of the limit state function, a second order function (parabola) is fitted through the limit state function in the design-point. Information on the computation of the SORM probability of failure is given in [Tve90].

The irregularly shaped limit state functions (shown in Figure 2.15) may be a problem for the iteration process as well as for the accuracy of the answer. Whether or not irregularly shaped limit state functions are a problem for FORM or SORM depends on the iteration procedure used. As a solution for irregularly shaped limit state functions the importance sampling technique has been introduced in [Hoh88]. The probability of failure estimate is improved by importance sampling (standard importance sampling, see section 2.4) in the neighbourhood of the design-point found by FORM or SORM.

FORM and SORM are unable to cope adequately with piecewise linear limit state functions, shown in Figure 2.15. For these types of limit state functions a systems analysis has to be performed, which will be explained later in section 2.6.5.

2.6.2 Numerically computed gradient method

In order to find the unknown design-point, a minimisation procedure is used which iterates to the vector $\underline{\alpha}\beta$ with the smallest distance from the origin to the failure surface. The numerical computed gradient method is the original FORM procedure proposed by [Has74], [Rack78] and [Mad86]. A simple but instructive procedure is visualised for a problem with one random variable x_1 in Figure 2.16. In the starting point (point 0) the gradient of the limit state function to the variable is computed (by numerical differentiation using point 0^a). Point 1 is found as an estimated zero point. Here the gradient is computed again and a new zero point is estimated. This continues until the limit state function in a zero point equals zero and the point does not shift anymore. This last point is known as the design-point.

In some cases, this standard procedure does not lead to convergence. In the standard FORM procedure this may be improved by means of a relaxation factor v ($0 < v \leq 1$). Instead of going directly to the new estimated zero point, a point between the old $\underline{u}^{(k)}$ and new estimated zero point $\underline{u}^{(k+1)}$ is used:

$$\underline{u}'^{(k+1)} = v\,\underline{u}^{(k+1)} + (1-v)\underline{u}^{(k)} \tag{2.29}$$

According to [RCP97], the algorithm almost surely converges for the sequence v = 1, 0.5, 0.25, 0.125, … . Consequently, for low v the convergence requirements are performed at cost of low efficiency.

Several authors have suggested procedures to improve the search for the design-point. Minimisation algorithms are mostly the so-called sequential quadratic programming algorithms (which do not need relaxation factors). Well-known algorithms that are implemented in commercial FORM codes are RFLS [Abd90a], NLPQL [Sch85] and VMCWD [Pow82]. All algorithms claim to be robust and efficient. They all claim to use less LSFE. A discussion on the performance of RFLS and NLPQL can be found in [Abd90b]. Chapter 1 compares the number of LSFE used in the optimisation algorithms.

Figure 2.16: FORM iteration procedure for one random variable and one limit state function.

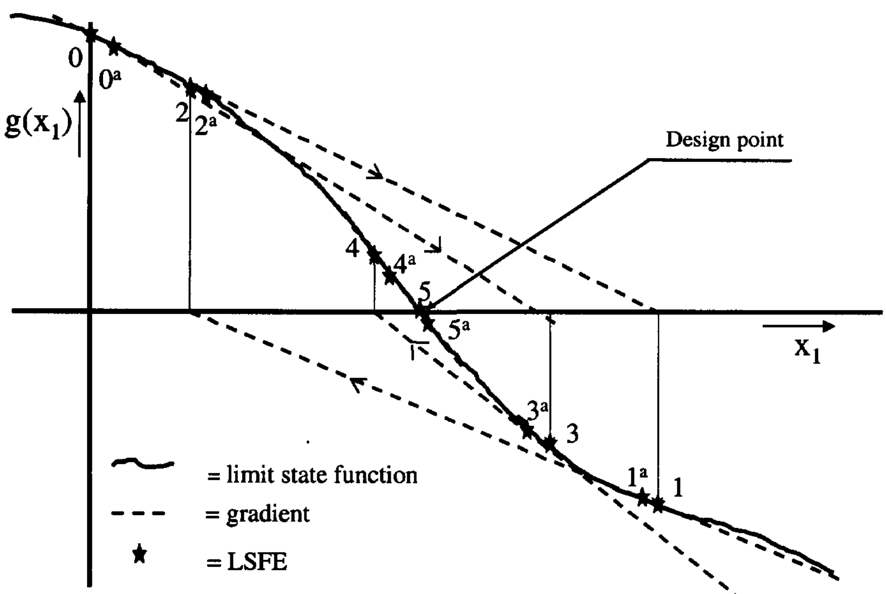

In case of non-linear FE analysis, the limit state may represent the collapse of the system. In that case, negative g-values are normally not explicitly quantified. Furthermore, the gradients can not always be calculated in the collapsed state. In the iteration process of the non-linear FEA the increment property may be used as variable. For instance in a load controlled iteration process, the limit state function can be rewritten as:

$$g = \tau - 1 \tag{2.30}$$

Here τ is the final load increment factor in the load controlled FEA iteration process (see Figure 2.17). Failure occurs for $\tau < 1$. Varying the variables u_i separately with Δu_i leads to a change in the maximum load factor $\Delta\tau$. The iterations to find the design-point for this limit state function are performed by computing the gradients: dg/du_i.

Not all non-linear FE analysis have a load (or deformation) controlled iteration process. A practical solution is to add a displacement limit state. In many cases, full collapse of the structure occurs only in connection with a very high displacement. Adding a displacement constrained in all directions equal to approximately 10 to 25 % of the measure of the structure solves most problems. It is expected that for most cases, the resulting probability of failure is only just slightly too high.

Figure 2.17: Non-linear load displacement graph.

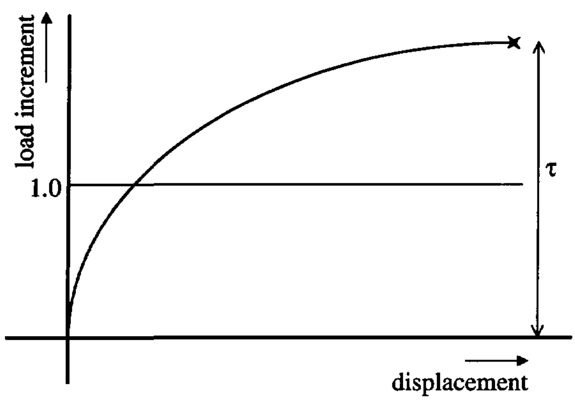

2.6.3 Analytically computed gradient method

The main contribution to the computational time in reliability analysis is the numerical calculation of the gradients of the limit state function to all variables. The basic concept is to replace the numerical calculation by an analytical calculation. The adjoint or variational principle is a direct method to compute the gradients. Examples can be found in [Yam88], [Liu88], [Reh91], [Tei91] and [Gut99]. It can be used for both linear and non-linear structural behaviour. At the expense of long derivations and computer coding it offers both computational efficiency and accuracy [Liu91]. For each finite element in the FE analysis, each (material) behaviour and each limit state (deformation, stresses), a new analytical derivation has to be performed. The method is explained for the simplest limit state: constrained displacement (deformation) for a structure with linear behaviour. It can also be applied to structures with physically and geometrically non-linear behaviour (see for instance [Liu88], [Reh91], [Tei91], [Fra96b], and [Gut99]).

The basic equation of FEA is:

$$K\underline{v} = \underline{f} \tag{2.31}$$

where K is the stiffness matrix, $\underline{v}$ is the displacement vector and $\underline{f}$ the load vector.

Differentiating the FEA equation to the random variables $\underline{u}$ leads to:

$$K\frac{d\underline{v}}{d\underline{u}} = \frac{d\underline{f}}{d\underline{u}} - \frac{dK}{d\underline{u}}\underline{v} \tag{2.32}$$

The limit state function equals:

$$g = \underline{v}_{lim} - \underline{v} \tag{2.33}$$

Pre-multiplying with $\left(\frac{dg}{d\underline{v}}\right)^T K^{-1}$ result in:

$$\left(\frac{dg}{d\underline{v}}\right)^T \frac{d\underline{v}}{d\underline{u}} = \left(\frac{dg}{d\underline{v}}\right)^T K^{-1}\left\{\frac{d\underline{f}}{d\underline{u}} - \frac{dK}{d\underline{u}}\underline{v}\right\} \tag{2.34}$$

In the direct differentiation method, the calculation of $\left(\frac{dg}{d\underline{v}}\right)^T \frac{d\underline{v}}{d\underline{u}}$ is performed. This method only needs the inverse of the stiffness matrix K, and the derivatives of K to $\underline{u}$. For examples of the derivations of $dK/d\underline{u}$ see for instance [Liu91] and [Liu87].

2.6.4 Non-gradient methods

Some FEA codes contain optimisation procedures that can be utilised to find the design-point. The implementation of such procedures in the commercial FEA code ANSYS is described in for instance [Moh96] and [Bor97]. In the ANSYS code the optimisation routine 'Sequential Unconstrained Minimisation Technique' (SUMT) is implemented [Him72]. The minimisation technique only requires the limit state function; the computation of gradients is avoided. The performance for non-linear systems has yet to be investigated [Bor97].

Another non-gradient method that is applied in combination with FE analysis is the Response Surface Method (RSM). In combination with FORM, the response surface method has been used by, for instance, [Far89] and [Buc88b]. The response surface method will be explained in chapter 3.

2.6.5 FORM combined with system analysis

By definition, level II methods are performed on component level or on single failure modes. Structural reliability analysis covers the complete failure domain. Consequently, an additional combination procedure of all failure modes has to be performed. The difficulty is to identify the system of failure modes and to compute the systems reliability index. In combination with FORM, it is customary to analyse the reliability of the system by means of the Branch-and-Bound method [Tho85]. For the Branch-and-Bound method, the reliability indexes of all failure modes have to be analysed. Furthermore, the structure has to be re-analysed after failure of one component. The full procedure is explained in annex B.1. The identification of the failure components is to be decided by engineering judgement. For frame structures this might be an option. For continuous structures this is not a realistic alternative.

An overview of the various methods is presented in [Kus99]. In [Kus99] it is concluded that there is no generally applicable method to identify all failure mechanisms. The best strategy depends on the problem at hand, i.e. on the limit state function shape in the transformed space. A combination of strategies is regarded to be the best, at the expense of very many limit state function evaluations.

In general, systems of failure modes can be modelled either as parallel or series systems or as a combination of both, see Figure 2.18 and 2.19. A parallel system is defined as an intersection of failure domains. A series system is defined as a union of failure domains.

Given the reliability of the separate failure modes, the systems failure probability can be evaluated [Hoh87]. The evaluation depends on the type of system. For unions, the failure probability can be bounded by the Ditlevsen bounds [Dit79]. For intersections the Hohenbichler approximation [Hoh82] may be used. Annex B.2 gives an explanation of both methods. Another customary method ([Dit87], [Lin87], [Dit90]) to obtain the system failure probability is to perform directional sampling on the linearised component limit state functions.

Figure 2.18: Union (series system) defined by 3 components.

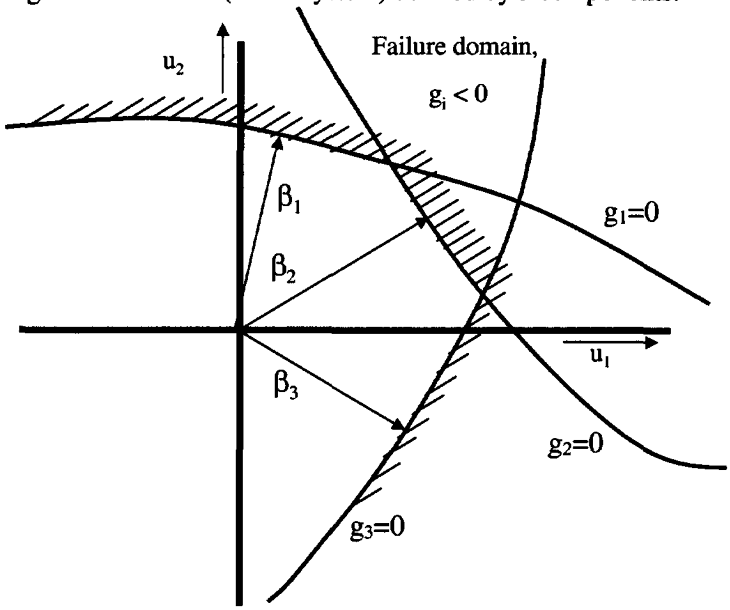

Figure 2.19: Intersection (parallel system) defined by 3 components (mechanisms, failure modes).

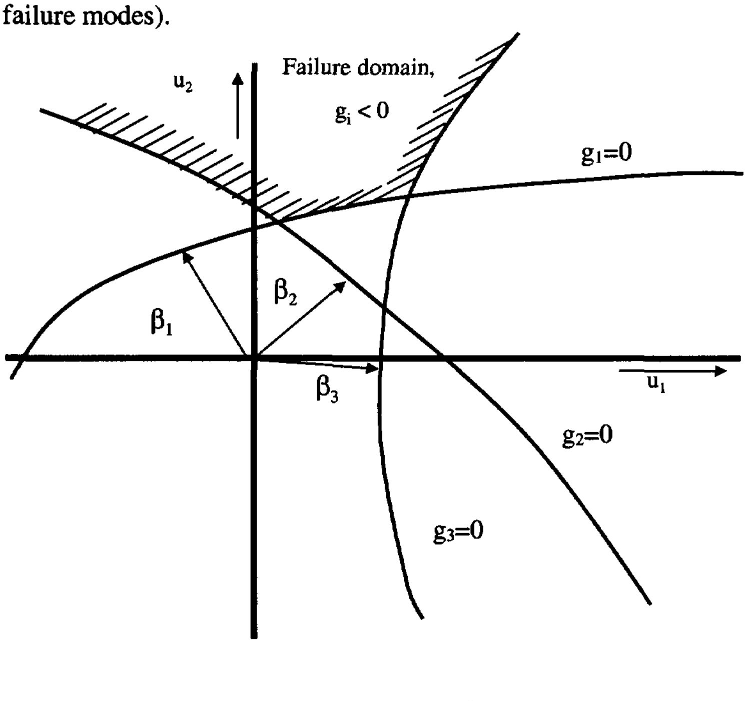

2.7 Level I reliability methods

Level I reliability methods compute only whether or not the reliability is sufficient instead of computing the real probability of failure. Combinations of variables are taken in such a way that the failure surface is likely to be outside the boundary defined by the reliability index. In the Eurocode [ENV91] it is suggested that the limit state function is checked in the point (-0.7β, 0.8β) for resistance R and load S respectively. For a structural system with one load and one resistance variable, the system of Figure 2.20 results: only one point has to be checked.

When there are more variables, the above mentioned procedure only holds for the dominant variables. For non-dominant variables, the coordinate point has to be multiplied with 0.4. In general it is not known whether a variable is dominant or not. In that case all combinations of possible dominant and non-dominant variables are to be checked.

For practical use, the checkpoints are translated into partial safety factors. The probability of failure is supposed to be sufficiently low if in neither point the value of the limit state function is negative. The more check points are used along the space with $r = \beta$ (see Figure 2.20) the more likely it is that the limit state function will not enter the space.

Figure 2.20: Example of check points in a 2-dimensional case.

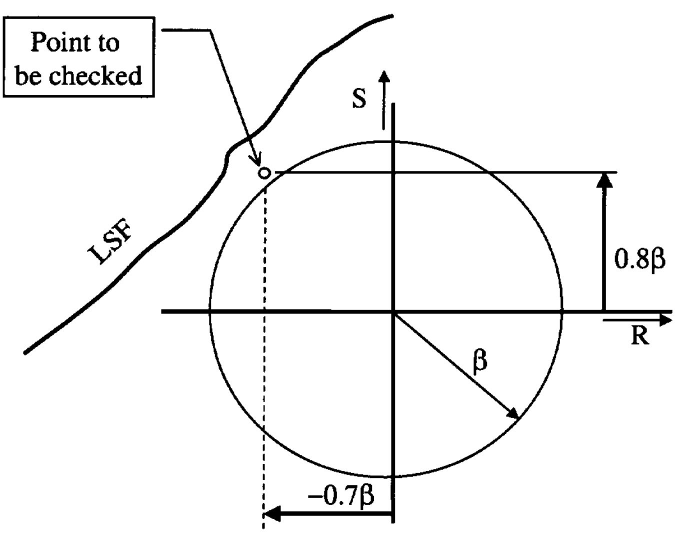

When the influence of the variables on the limit state function is not known to be either resistance or load (which is generally the case in complex structures), both possibilities have to be checked. For a structural problem with only two variables this results in the coordinates: (+0.7β, +0.8β), (+0.7β, -0.8β), (-0.7β, +0.8β) and (-0.7β, -0.8β). In general the number of points to be checked is equal to: $N = 2^n$

In practise this high number of points to be checked is never used. Mostly only a few points are checked. The more experience there is with the type of structure, the less points are checked. The following strategies can be used if the experience is not available:

1. Every load and resistance variable is set to be dominant once. In general it is not known beforehand whether the other (presumed non-dominant) variables x_i are either resistance or load. In that case, the positive or negative influence of a variable on the limit state is checked by means of a FEA calculation. When many limit states are to be considered the influence of a variable can be checked by means of calculating the influence lines.

   As a result, for every limit state considered, a limit state function $g = \sum_i^n \alpha_i x_i$ is obtained. The influence factor α is set to 0.8 and -0.7 for the presumed dominant load and resistance variables respectively. For non-dominating variables, the coordinates are multiplied by a factor 0.4. Considering one limit state this means that, as maximum, n coordinates are used (every variable is presumed to be dominant once). For k limit states the number of coordinates is limited to k n. Since there are many corresponding combinations, a number of approximately 3 n coordinates is more likely to be applicable.
2. A procedure described in [Vro99] is not limited to linear behaviour. The procedure starts setting all variables to their minimum or maximum design-value, depending on the designer's choice of influence on the limit state function. As a result, the starting coordinate is (+/-0.7β, +/-0.7β, …., +/-0.7β). One limit state function evaluation (LSFE) is performed in this starting point. For all n variables the coordinate values are subsequently individually changed to the opposite value. It is checked whether the value of the limit state function in this point is lower than in the starting point. When all coordinates show a higher limit state function value, it is concluded that the starting point was a good estimate and the procedure is stopped. When this is not the case, then the coordinate with the lowest value is used as a new starting point and the procedure is repeated. This procedure requires a minimum of 1+n points to be checked. For every extra starting point an additional n-1 points have to be checked. Examples in [Vro99] show that approximately 3 starting points are to be used. The number of points to be checked is therefore approximately equal to 3 n. It should be noted, however, that still combinations with lower limit state function values might exist.
   The multiplication factor 0.4 is not used here. This means that this approximation is on the safe side as far as this point is concerned.

Procedures used in practise use approximately 3 n coordinates to be checked. Compared to the level III methods (without importance sampling) this is a very low number of limit state evaluations. Directional sampling for instance uses N = 160 n. Directional sampling computes the actual probability of failure where a level I method only checks whether the reliability is sufficient. The only way to find an estimate of the failure probability is to slowly increase β until the value of the limit state function becomes negative.

2.8 Discussion

The aim of structural reliability methods is to compute the total structural reliability. Sections 2.3.1 and 2.4 showed (for $\beta \approx 4$) the following number of samples in the level III methods:

- Numerical integration: 9^n
- Monte Carlo simulation: $3/P_f$
- Monte Carlo importance sampling: 300 n
- Directional sampling: 160 n

Level II methods compute the component or single failure mode reliability instead of the total reliability computed by the level III methods. Level II methods can only compute the systems failure probability indirectly. First, the system behaviour is to be analysed, for instance by the Branch-and-Bound method. The Branch-and-Bound method requires many component FORM and system analysis. Afterwards, the systems reliability is analysed by for instance the Hohenbichler approximation. The component failure probabilities all require a FORM procedure, where the Limit State Function Evaluation (LSFE) can only be performed by FE analysis.

Let every FORM gradient procedure take approximately 10 iterations before reaching convergence. Then, for every failure path, the numerical computed gradient methods take 10(n+1) FE computations. The amount of failure paths is not known in advance. Simple examples of frame structures easily show 100 failure paths. Consequently, the number of FE computations will go up to 1000 n.

Analytical computed gradient methods require less FE computations. Compared to the numerically computed gradient methods the number of FE computations reduces to 1000. The disadvantage is that for all element types, the gradients to all variables or limit state functions have to be worked out analytically. In some FEA codes, these gradients are already implemented in the code. Most codes do not have this opportunity. For physical and geometrical non-linear behaviour, the analytical derivation of gradients requires a lot of effort (see for example [Gut99]).

The non-gradient methods can be divided into response surface methods and standard optimisation methods (for example SUMT). It is doubtful whether the standard response surface methods can be used for the analysis of systems reliability. The number of FE computations is approximately 4n. There is little experience with limit state function containing many variables. The accuracy depends on the data where the response surface is built on and the goodness of the fit (response surface). A response surface approach without possibility of checking whether it gives the right result seems not good enough.

The standard non-gradient optimisation methods have the same disadvantages as the response surface methods: There is little experience with these methods in combination with (non-linear) FE analysis.

The several level III and level II procedures are difficult to compare. Whether one or the other performs better depends on the number of random variables and the system behaviour. Table 2.1 shows the required number of FE computations. For sake of comparison an arbitrary structural reliability problem with 100 random variables is used, having a reliability index $\beta = 4$. The Branch-and-Bound method is supposed to take 100 FORM procedures.

The aim in this thesis is to compute the probability of failure with sufficient accuracy as fast as possible using standard FE code. Considering the results of Table 2.1, directional sampling, Monte Carlo importance sampling or a more accurate non-gradient FORM method is most likely to fulfil these aims. The possibilities of these options are discussed in the next chapter.

Table 2.1: Approximate comparison of the standard reliability methods (for $n = 100$, $\beta = 4$).

Method	Number of LSFE	Comment
NI	9^{100}	Exact solution
MC	100.000	Exact solution ($V(\beta) < 0.05$)
MC importance	30.000	Exact solution ($V(\beta) < 0.05$)
DS	64.000 (4 times 16000)	Exact solution ($V(\beta) < 0.05$)
FORM- Numerical gradient	100.000	Good approximation when system behaviour is recognised and acted on
FORM Analytical gradient	1000	Good approximation, lots of analytical derivations and computer coding
FORM non-gradient	400	Doubtful accuracy
Level I	300	Only check on sufficient reliability

3. Reliability methods using Response Surfaces

The previous chapter indicated that a fast reliability method should be searched in directional sampling, Monte Carlo importance sampling or FORM. In this chapter the use of these methods in combination with response surface methods will be investigated. First the conventional use of response surfaces is described.

3.1 Response surface method

The standard Response Surface Method (RSM) is used when response is only available from experiments or complex FE computations (for example large highly-non-linear FE models). An analytical limit state function replaces the real response function. The main idea is that the response consisting of a complex function of input variables is approximated by a simple function of the input variables. In combination with FEA, the RSM technique is used by, for instance, [Far89] and [Buc88b]. A general explanation of the response surface method can be found in [Box78].

In combination with FEA, the standard procedure is as follows:
1. Select the most important random variables on the basis of engineering judgement;
2. The value of each important random variable is varied individually and an FEA is performed (the other variables remain unchanged);
3. A response surface is constructed through the response data;
4. A reliability calculation is carried out using the response surface instead of the real response.

The type of reliability method used is of little importance since the time consuming LSFE (using FEA) are replaced by analytical expressions. Of main importance to the accuracy of the reliability method is the accuracy of the response surface compared to the real response.

Examples found in literature show a maximum of some 10 random variables. For instance, 6 random variables are used in [Far89]. Setting up the data took 50 to 92 FEA computations, depending on the desired accuracy. The question always remains whether every important random variable has been taken into consideration and whether the response function is accurate enough in the neighbourhood of the estimated design-points.

The response surface is generally constructed by fitting a quadratic function to the sampling points. There have been many suggestions the choices of these sampling points as well as the function to be used. In the simplest case, the value of each random variable is varied individually in positive and negative direction with a factor f σ. As a result, the sampling points are located at $\mu_i + e_i\,\sigma_i$, where $\underline{e}$ is the vector (0, 0, 0, 0, ... ±f, ..., 0). The factor f is advised to be equal for all variables [Box78].

[Buc90] suggests fitting a quadratic function without cross terms to these sample points:

$$g^* = a + \sum_{i=1}^{n} b_i u_i + \sum_{i=1}^{n} c_i u_i^2 \tag{3.1}$$

This response surface is used to find an estimate of the design-point $\underline{u}^*$ using FORM. As a next step this estimated design-point is used as a new centre point for sampling $u_i^* + e_i\,\sigma_i$. In both steps, 2n+1 sampling points are required. This method does not at all guarantee a reliable response surface. For non-linear limit state functions (multiple failure modes, see Figure 3.1), the first estimated design-point directs all further output to the mode belonging to this design-point. Other modes are unlikely to be found.

To fit in u-space is an arbitrary choice. Fitting in any other space may perform as well. For instance in some cases, fitting in x-space or in a rotated u-space may perform much better. In literature however, hardly any other space than u-space is used.

Figure 3.1: Non-linear limit state functions.

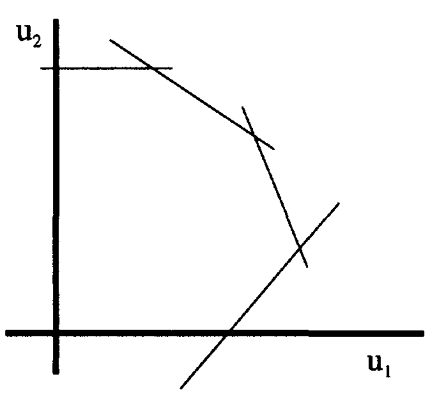

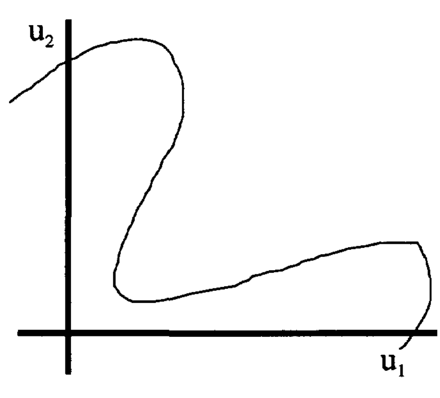

Using equation (3.1) means that the fitted response surface is sensitive to the choice of the coordinate axes. Several authors suggest therefore to include the cross terms in equation (3.1). This way, the interaction between variables is taken care of:

$$g^* = a + \sum_{i=1}^{n} b_i u_i + \sum_{i=1}^{n} c_i u_i^2 + \sum_{i=1}^{n} \sum_{j=1, j\neq i}^{n} d_{ij} u_i u_j \tag{3.2}$$

This so-called "Central Composite Design" requires $2^n + 2n$ LSFE. For a high number of variables, this leads to an enormous increase of the required number of sample points (FE computations) and is therefore not advisable. Improving the first step with relevant samples near the limit state is probably a far better option. In fact, samples should be searched on the limit state surface and close to the origin in the u-space. This is equivalent to the finding of the parameter λ in the directional sampling procedure. The procedure is further explained in section 3.2. Special care should be taken in case of non-convex limit state functions and limit state functions that have cross terms only. In these cases the response surface may not find all important regions (see Figure 3.1). The performance of the response surface techniques in case of non-convex limit state functions is further discussed in chapter 4

The response surface response is not exactly the same as the real response (introduced by the lack of fit). Performing a reliability method on a response surface introduces therefore a (reliability) model uncertainty. This uncertainty can be taken into account by introducing an extra random variable. This random variable can be expressed as the relative error in distance λ:

$$\varepsilon_\lambda = \lambda_{RS} - \lambda_{FEA} \tag{3.3}$$

It is assumed that the variable ε_λ is normally distributed with mean μ and standard deviation σ, equal to:

$$\mu(\varepsilon_\lambda) = \sum_{i=1}^{n(\theta)} \varepsilon_{\lambda_i} \tag{3.4}$$

$$\sigma^2(\varepsilon_\lambda) = \sum_{i=1}^{n(\theta)} \left(\varepsilon_{\lambda_i} - \mu(\varepsilon_{\lambda_i})\right)^2 \tag{3.5}$$

The model uncertainty can be taken into account regardless the reliability method applied.

3.2 Adaptive response surface combined with directional sampling

3.2.1 Procedure

In this section a procedure is suggested and demonstrated, combining the advantages of directional sampling, response surface and importance sampling. In section 3.1 the following starting procedure was suggested for the response surface method:
1. Increase the value of each random variable individually until the limit state is reached;
2. Fit a quadratic response surface;
3. Perform FORM on the fitted response surface.

Step 1 can be seen as a coarse directional integration procedure. Since the sampling is only performed in the coordinate axis directions in the u-space, it is called Axis Direction Integration (ADI). The ADI result already gives an estimate of the failure probability. The method for finding the root (at a distance λ) in a direction is explained in Annex A.1. A finite element computation is performed in the origin of the u-space (0, 0, 0, 0,…., 0) and the point (0, 0, f, 0, …., 0). When known, the factor f is set equal to the expected reliability index β. Experience shows that f = 3 performs good as well. Mostly after approximately 3 or 4 iterations (FE computations) the root is found. In some cases, no roots will be found in the u-space coordinate axis directions. This problem will be dealt with later.

Consequently, a response surface can be fitted to the data points. It has been chosen to fit the response surface to the data in:
- origin (0, 0, ………., 0)
- the points (0, 0, ±3, …., 0)
- the roots (0, 0, $\pm\lambda$, …., 0) (when available).

These data points are most times sufficient to fit a quadratic response surface to. Otherwise a linear surface has to be fit to the data (only first two terms of equation 3.2).

In section 2.4 importance sampling was suggested to improve the performance of directional sampling. The importance sampling was based on prior knowledge of the behaviour of the variables in the limit state function. Since it is hard to find this knowledge, it is preferred to let the probabilistic method produce this knowledge. A suggestion, mentioned in section 2.4, is to direct the directional sampling (importance sampling) by means of the FORM results of step 3. The influence factors can be used to find dominating variables which can be truncated in the directional sampling procedure. The rest of the variables can be adjusted such that they are focussed on the design-point. In most structural reliability problems, this will result in an enormous reduction in the number of variables and, in consequence, in the required number of samples. It is however unpredictable (for example in case of more than one important region) whether the correct answer is found.

In [Kya92] a weighting function is suggested to identify important regions. This weighting function is adapted every time a sample is produced. The procedure to construct this weighting function procedure requires many samples and is therefore rejected for the aims of this thesis.

Instead of using a weighting function, the response surface can be used to direct the samples. The Directional Sampling (DS) procedure can be performed on the response surface. Only in directions with, according to the response surface, a relatively high probability P_i an FEA is used instead of the response surface to compute the distance λ. Consequently, the accuracy of the DS procedure is high in important regions and low in non-interesting regions.

The question whether or not a failure probability is relatively high can be transformed into a measure γ on the minimum found distance λ_{min} (a direction is not important when $\lambda_{RS} > \gamma\, \lambda_{min}$). Harbitz proposes in [Har86] to skip a direction when $\lambda > \lambda_{min} + \lambda_{add}$, with $\lambda_{add} = 3$. Contrary to this proposal, the direction here is not skipped but the real λ_{FEA} is replaced with λ_{RS}.

In short the total procedure is:

1 Perform Axis Directional Integration (ADI)

2a Fit response surface on data (0, 0,.. f, ...0), using f = ±3 and f = ±λ (when available)

2b Perform coarse directional sampling on the response surface

- if $\lambda_{RS} < \lambda_{min} + \lambda_{add}$
  - Calculate $P_i(FE) = \chi^2(\lambda_{i,FE}, n)$
  - Update the response surface with new (FE) data, using only the point on the limit state ($g(\lambda\underline{\theta}) = 0$), when available
- else
  - Calculate $P_i(RS) = \chi^2(\lambda_{i,RS}, n)$.

If it is certain that only a positive or negative part of the distribution of a variable will be of importance to the limit state function (for example in the case of loads), the opposite direction can be skipped in the ADI starting procedure ($P_i = 0$). The skipping of a direction has no consequences in the following directional sampling procedure. This is because it is of no use to apply importance sampling in the directional sampling procedure. There will be no effect of truncating or shifting weighty dominant variables since the response surface would eliminate a sample in a non-important direction anyway and the computational effort for the elimination is negligible compared to an FE analysis

The procedure has similarities with the IFM (iterative fast Monte Carlo) procedure of [Buc88a]. The IFM procedure searches for areas to perform importance sampling. Monte Carlo sampling is carried out for one variable, where the others are kept at the mean value. This leads to an importance sampling area. The importance sampling region is found as a weighted average of all areas found. As such, the IFM method can be seen as the Monte Carlo equivalent of the proposed directional sampling procedure.

The proposed procedure uses the response surface only to direct its samples to important regions. The model uncertainty ε_λ described in section 3.1 is therefore not applicable to this procedure.

The proposed directional sampling procedure can not be applied under the following circumstances:

1. The failure domain is highly convex (see Figure 3.3a);
2. The origin in u-space is inside the failure domain (see Figure 3.3b);
3. The failure domain is non-coherent (see Figure 3.2c).

A highly convex failure domain results for instance if only combinations of variable changes lead to failure, whereas changes of the variables individually do not lead to failure. A special case occurs when the value of the limit state function in the ADI procedure is equal for every LSFE. Consequently the ADI procedure will result in a perfectly flat constant response surface. The DARS procedure will never find a direction where $\lambda_{RS} < \lambda_{min} + \lambda_{add}$ (λ_{RS} and λ_{min} are infinite) in this case. A solution may be to complete the ADI procedure with an equal number of samples in random directions. It is however questionable whether highly convex failure domains exist in structural reliability. These questions can only be solved in practice and will be discussed in chapter 4 and 5.

Figure 3.2: Failure domains that are not supported in the adaptive response surface sampling procedure (= failure domain).

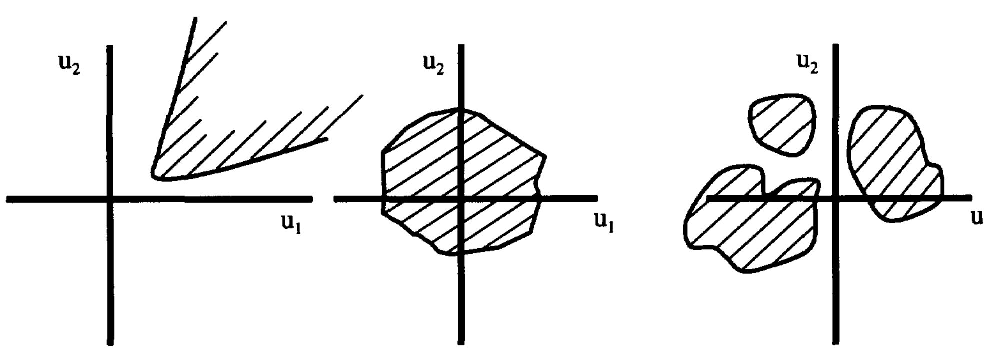

a: convex failure domain b: Origin inside failure domain c: Non-coherent failure domain

3.2.2 Example

The procedure is clarified by an example of a frame structure (Figure 3.3), adapted from [Kim97]: a 6-storey, 2-bay building under a random horizontal load and a deterministic vertical floor load. The limit state considered is yield stress in point A:

$$g = f_y - \sigma_A \tag{3.6}$$

In total there are 9 random variables (see Table 3.1): 6 forces, 2 Young's moduli and 1 yield stress. The correlation coefficient between the Young's moduli for beam and column $\rho = 0.9$. The distributions of the Young's moduli are truncated at zero, providing the Young's moduli to remain always positive (the FE code can not handle negative Young's moduli).

Only positive loads and negative yield stress can effect the limit state function. The opposite directions are therefore skipped in the ADI procedure.

Table 3.1: Statistical properties of random variables [Kim97].

Variable	Unit	Mean	St.dev	Lower bound	Distribution type	Importance in ADI
E beam	MN/m^2	$2.1\ 10^5$	$8.4\ 10^3$	0.0	Truncated Normal	-
E column	MN/m^2	$2.1\ 10^5$	$8.4\ 10^3$	0.0	Truncated Normal	-
F_1	kN	32	8.0	-	Normal	positive
F_2	kN	31	7.75	-	Normal	positive
F_3	kN	30	7.5	-	Normal	positive
F_4	kN	29	7.25	-	Normal	positive
F_5	kN	28	7.0	-	Normal	positive
F_6	kN	25	6.25	-	Normal	positive
f_y	MN/m^2	240	22	27	Lognormal	negative

To show the correctness of a quadratic response surface compared to the real response, crude directional sampling is performed until convergence to a sufficient low $V(\beta)$. A quadratic response surface (without cross terms) is fitted to all the crude directional sampling data (FE responses). In Figure 3.4 the response (distances λ where a vector $\lambda\underline{\theta}$ touches the limit state) of the fitted response surface and the distance using the FE analysis results are compared. The small distances are the most important for the calculation of the probability of failure. Clearly there is little difference between the distance according to both the response surface and the FE response.

Instead of distances, the probabilities $P_i = \chi^2(\lambda,9)$ can be compared. Figure 3.5 shows the difference between the estimated (response surface) and the real (FEA) probability of failure. Most of the times, the probability according to the response surface probability is slightly lower than according to the FEA, though the difference is small.

Replacing the FE computations with response surface results for directions where the response surface results in a distance λ less than a certain minimum seems reasonable.

Figure 3.3: 6 story frame structure [Kim97].

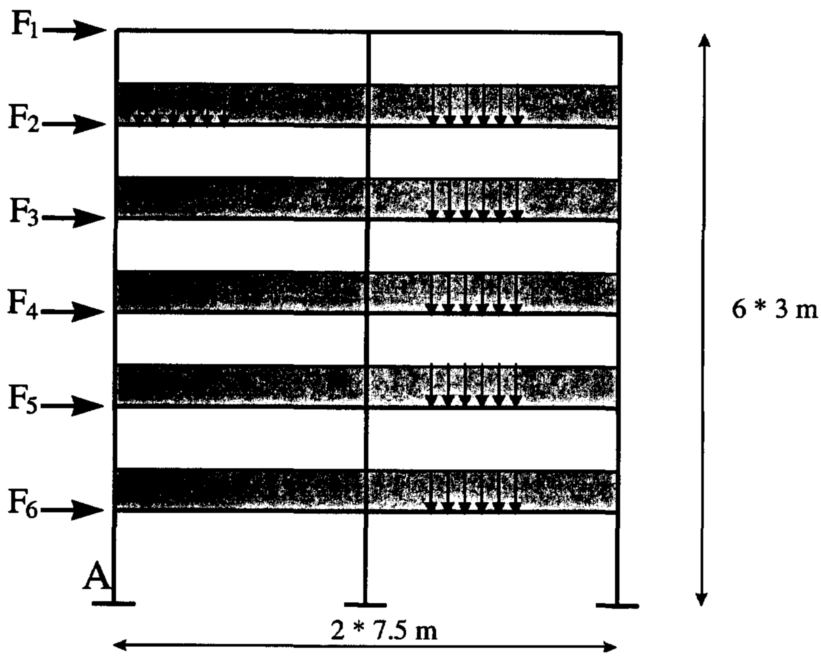

In the ADI procedure, there are 9 variables of which 7 have only one important direction. The ADI procedure therefore requires 9 + (9 - 7) = 11 samples. The iteration procedure for these 11 samples requires 44 FE computations. Table 3.2 gives the number of samples when using the subsequent DS procedure. The table shows that after the ADI procedure, for $\gamma = 1.3$, only 6 samples are using the real FE results. These 6 samples require 22 FE computations. In total 44 + 22 = 66 FE computations are used for $\gamma = 1.3$.

In Table 3.2 the factor γ on the distance is translated into a factor κ on the probability. It shows that there is little error when directions with probabilities of failure larger than 10 times the minimum ($\kappa = 1/10$) are discarded. In that case, after the starting procedure, only 4 simulations have to be performed. Since the estimated and real P_i (Figure 3.5) can differ by nearly a factor 10, a factor $\kappa = 1/100$ as a criterion is better used. Table 3.2 shows that only 6 FEA samples ($\kappa = 1/100$) are needed subsequent to the response surface construction. The factor $\kappa = 1/100$ means that $\gamma = 1.3$. Compared to the additional distance $\lambda_{add} = 3$ according to Harbitz [Har86], for $\beta = 3.6$, the factor $\gamma = 1.3$ means that $\lambda_{add} = 1.1$.

Each time a limit state function (FE) evaluation has been carried out, the response surface is updated.

The updated respons surface may involve that previous directions that were rejected for FEA before updating could be accepted using the new updated response surface. Therefore it is advisable to redo the complete sampling procedure from the beginning with this new condition. Of course, samples that were already analysed with FE computations are not analysed again in this adapted procedure. As such this procedure is called the Directional Adaptive Response surface Sampling (DARS). In fact it is also a kind of importance sampling since sampling using FEA is only performed in (according to the adaptive response surface) important directions.

Table 3.2: Results of directional sampling using response surface.

γ	κ	β	ADI samples	FEA in ADI	Samples using FEA after ADI	FEA after ADI
2.0		3.6	11	44	25	67
1.5	1/1000	3.6	11	44	12	33
1.3	1/100	3.6	11	44	6	22
1.16	1/10	3.6	11	44	4	13

All directional samples, including the ADI results, are used in the estimate of the probability of failure. The sampled directions during the ADI procedure, however, are not randomly taken but equally spaced on a uniform distribution. These sampling points are not random but coincide with the u-space coordinate axis directions. As a consequence it can be argued that these samples are not to be used in the directional sampling procedure.

The effect of including the ADI samples is analysed in Annex I. The ADI samples can be added without effect on the reliability estimate when all variables are equally important to the limit state function. When only one variable is important and the others are totally unimportant, then the reliability index is underestimated when using the ADI samples. In most cases there will not be only one important variable but many slightly important variables. In that case, it is expected that the error in the estimate is small.

Since many samples are used ($N \approx 160$ n) and only $N = 2$ n samples result from ADI, it can be argued that in that case the effect from the ADI samples is small. Since the number of samples is to be minimised, and every sample contributes, the ADI samples are not excluded from the directional samples.

Figure 3.4: λ-values (distances in u-space) of the response surface versus FEA.

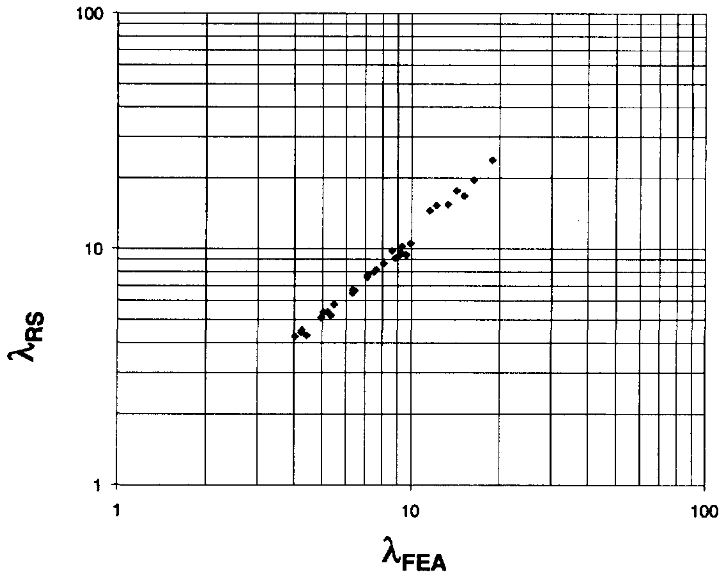

Figure 3.5: Sample probability (P_i) of the Response Surface (RS) versus FE (DIANA).

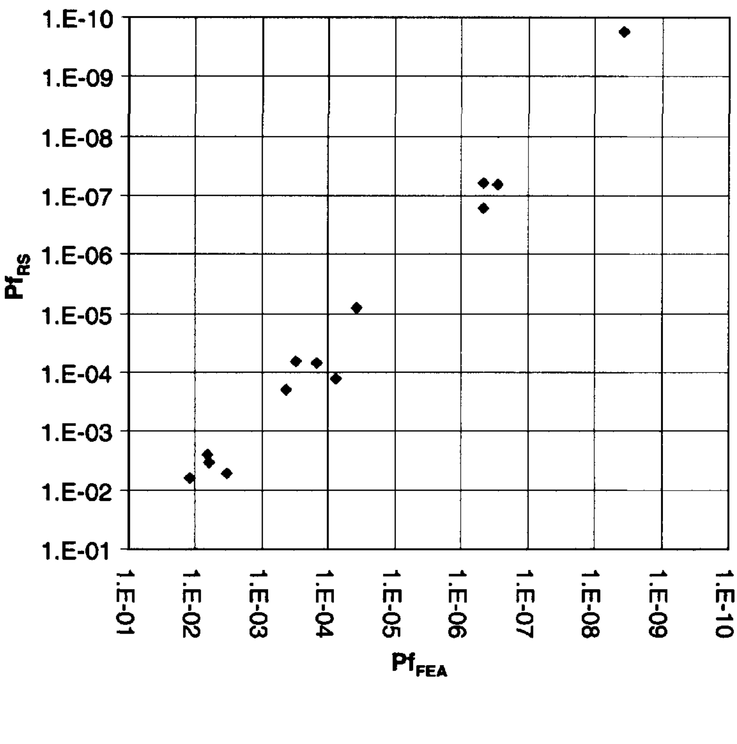

3.2.3 Antithetic directional sampling

As explained in section 2.3.3, directional sampling performs N simulations of the $\underline{\theta}$-vector. The directions are distributed uniformly in u-space. For most systems, $P_f(\underline{\theta})$ and $P_f(-\underline{\theta})$ are negatively correlated. For most limit state functions, only one of the positive and negative direction is of importance to the limit state function. It is therefore advisable to improve the performance of the directional sampling procedure by using a method of antithetic variables [Dea80]. For this purpose, for each simulated direction $\underline{\theta}$, a positive and negative distance (λ^+ and λ^-) is computed. The probability P_i of equation (2.18) is replaced by the average $[P_i(\lambda^+) + P_i(\lambda^-)]/2$. According to Deak [Dea80], the resulting variance is smaller than when using one direction and twice the number of simulations.

Figure 3.6: Number of samples for antithetic sampling compared to standard DS.

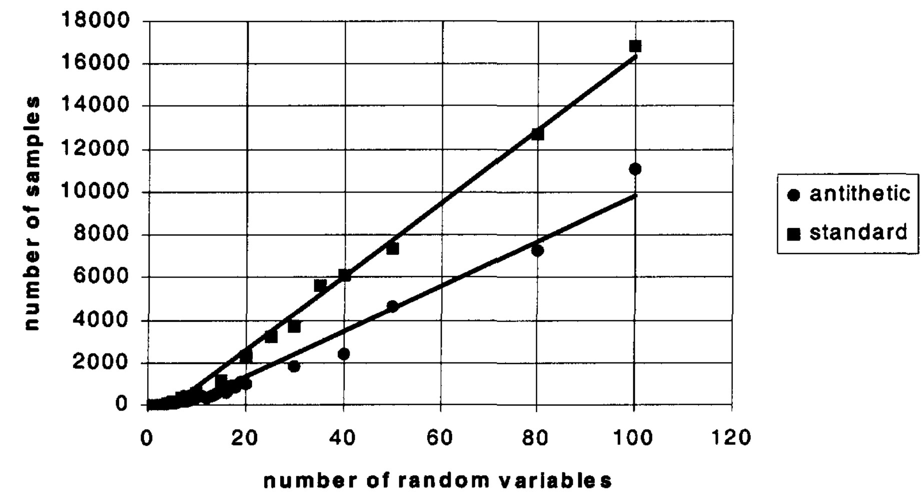

The number of samples required for standard directional sampling is equal to 160 n (see section 2.3.1). Figure 3.6 shows the number of samples for antithetic sampling compared to standard directional sampling for the case with equal importance to the limit state function of all variables and $\beta = 4$. Clearly, the required number of samples is lower than for standard directional sampling. The number of samples reduces to approximately 70 % ($N = 100$ n). The reduction however is less than expected by Deak [Dea80].

In the DARS procedure antithetic sampling is of even more use. In the ADI procedure, the number of samples is reduced to half. It is however expected that the number of limit state function evaluations will have less reduction. This is due to the fact that in uninteresting directions (with $P_i = 0$), mostly only two limit state function evaluations have to be performed (see Annex A).

Antithetic sampling can only be performed on systems where $P_f(\underline{\theta})$ and $P_f(-\underline{\theta})$ are negatively correlated. In general (in structural reliability) it is not known whether this negative correlation exists. It is therefore not advisable to use antithetic sampling by default.

3.2.4 Improvement of efficiency in combination with FEA

In combination with FE analysis, the efficiency of a reliability method is not only related to the number of samples. The number of LSFE per sample and the type of LSFE are important as well. In structural applications, an LSFE may be a linear as well as a non-linear FE analysis. In case of non-linear behaviour, for some samples, a linear computation can be used instead of a non-linear computation.

Suppose an elasto-plastic structural behaviour and limit state 'collapse'. It may not be useful to compute the distance λ_{col} to collapse, if the distance λ_{lin} for the start of yielding is relatively large.

In the ADI procedure, first only the distances λ_{lin} are computed. The limit state 'collapse' (including non-linear behaviour) will always lead to a higher distance λ than the distance λ_{lin}. The ADI procedure for the real limit state (collapse) starts with the variable with the lowest λ_{lin}. From this point on, non-linear LSFE have to be performed only in directions where $\lambda_{lin} < \lambda_{col} + \lambda_{add}$. This way, the non-linear computations are probably performed in fewer directions.

It may be useful to investigate the possibility of deriving the "linear" distances using analytical gradients. The effort in coding for linear gradients is relatively small, where the increase in computational speed may be considerable.

Another possibility to improve the efficiency is to combine the procedures to find the parameter λ and the iterations in the non-linear FE analysis. In the present procedure, to find the distance λ, the iterations for the non-linear computations are started all over again for every iteration of λ (see Figure 3.7a). When combining both iteration procedures, the non-linear combinations can start at the end of the previous calculations.

In a load-controlled non-linear FE analysis, the load F is incremented stepwise until failure. Suppose that in the ADI procedure there is one variable describing the load. Incrementing the load is equal to incrementing the parameter f in the directional sampling procedure (see Annex A.1: $F = \mu(F) + f\sigma(F)$). Supposing a normally distributed variable, the final load increment factor τ is then equal to $\mu(F) + \lambda\sigma(F)$. When the load is incremented from the mean value onwards, the distance λ is equal to the final load factor τ divided by $\sigma(F)$.

The same procedure can be used for other variables or combinations of variables. Combining both iteration procedures for FEA and λ leads to the reduction of the number of LSFE to one per direction.

Figure 3.7 : combining iteration processes.

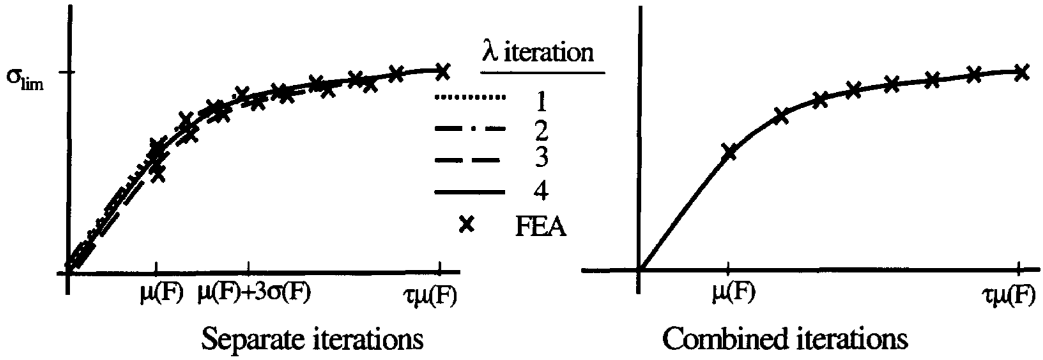

3.3 Adaptive response surface combined with Monte Carlo importance sampling

Chapter 2 showed that Monte Carlo importance sampling is approximately equally efficient compared to crude directional sampling. The adaptive response surface technique, described in the previous section can be applied to Monte Carlo sampling as well: only samples close to a relevant limit state are computed by FEA and all others are computed by means of the response surface.

The start of the procedure can be the same as for directional sampling: A response surface is build on the basis of ADI results. The question is what the condition should be when using FEA for sampling. For directional sampling the distance λ_{min} was taken as a measure. For Monte Carlo sampling, this measure can not be used. Figure 3.8 shows a possible procedure for the condition of sampling using FEA (for the one-dimensional case). If the sampled coordinate is outside the range $\lambda_{RS} \pm \lambda_{add}$, an FE analysis is to be performed and the response surface is updated. An optimal λ_{add} is to be found.

The use of a Response Surface already directs the FEA samples to a certain (important) region. This is a kind of importance sampling (for FEA samples) as well. The samples in the non-important regions (according to the response surface) are computed by means of the response surface function and cost relatively little effort to compute. Since the response surface already directs the FEA sampling, the use of extra importance sampling (increase σ_h) may be redundant and left out.

The technique is the DARS procedure alike, only the condition for sampling differs. The directional sampling technique always finds a sample at the limit state where Monte Carlo sampling finds a positive or negative value of the limit state function. A preference for either procedure can not be given at this stage. Since there is little difference only DARS is further researched

Figure 3.8: Condition for sampling in combination with Monte Carlo sampling.

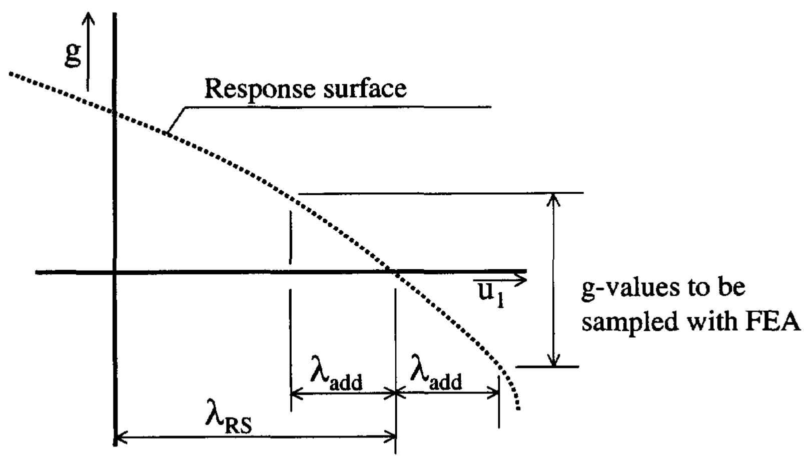

3.4 FORM performed on an Adaptive Response Surface

Structural reliability can generally only be analysed with a FORM analysis when it is combined with a system identification procedure such as the Branch-and-Bound method (see section 2.6). The Branch-and-Bound method requires the reliability index of every limit state considered. This means that many FORM analyses have to be performed. A FORM analysis can be performed on a response surface. The problem with this approach is the fact that the response surface might not be accurate enough in the neighbourhood of the estimated design-point. Consequently, the reliability index might not be accurate. For the latter [Rac78] and [Kar87] suggest an adaptive technique where FORM calculations on the response surface are extended with evaluations of the real (FEA) response.

An approach is here suggested where the reliability indices of all limit states considered by the Branch-and-Bound method are computed in one procedure instead of each one separate. The approach is a mixture of a numerical computed gradient and a non-gradient minimisation procedure. The FORM method is acting on the response surface only. As such, FE results are not used by FORM directly. The response surface is built using the FE results and updated every time a FORM iteration has taken place. The improvement of the present method to standard response surface techniques lies in an enhanced accuracy of the response surface in the neighbourhood of the latest estimate of the design-point and the simultaneous treatment of all limit state functions under consideration. The advantage of the scheme is that, compared to standard FORM, the number of time-consuming Limit State Function Evaluations (LSFE = FE analysis) is reduced.

In short the method is described as follows (see also Figure 3.9):

1. A starting point $\underline{x}_1$ is defined, $\underline{x}$ being the vector with random variables. Normally the starting point coincides with the origin in u-space.
2. The gradients for all limit states functions (or g-functions) are determined numerically. This requires (1+n) LSFE, where n is the number of random variables.
3. For each individual limit state function, a design-point is estimated using the standard FORM procedure. The g-values of all limit state functions in all estimates of the design-points are evaluated. This brings the total number of LSFE to (1 + n + k), where k is the number of limit state functions.
4. A linear (or if possible a quadratic) response surface is constructed on the basis of the (1 + n + k) results.
5. An iteration procedure is initiated, each iteration consisting of three sub-steps:
   (a) a standard FORM calculation based on the current (adapted) response surface, leading to a new set of k design-point estimates;
   (b) an FE computation in each new estimated design-point and LSFE in these new estimated design-points for all k limit state functions;
   (c) the construction of a new Adapted Response Surface (ARS) based on the extended database of LSFE.

   After N iterations the number of LSFE is (1 + n + Nk).
6. The iteration process is terminated when the value of the limit state function in the design-point for all limit states is sufficiently close to zero. The design-points themselves were found via an iteration procedure on the response surface in step 5a. It is implicitly assumed that the correct design-point is found when both the response surface and FE response are equal and near zero.

The gradients in point 1 are computed numerically. It is chosen to perform this operation in the points μ and $\mu + 3\sigma$. This way, local variations near the origin will hardly influence the gradients.

Any function may be used to construct the fitted surface g^*. Here a quadratic response surface including cross terms is proposed (equation 3.2).

Figure 3.9: Steps 2 to 4 of the proposed procedure for two limit state functions g_a and g_b: Finding the first estimated design-points and fitting Response Surfaces.

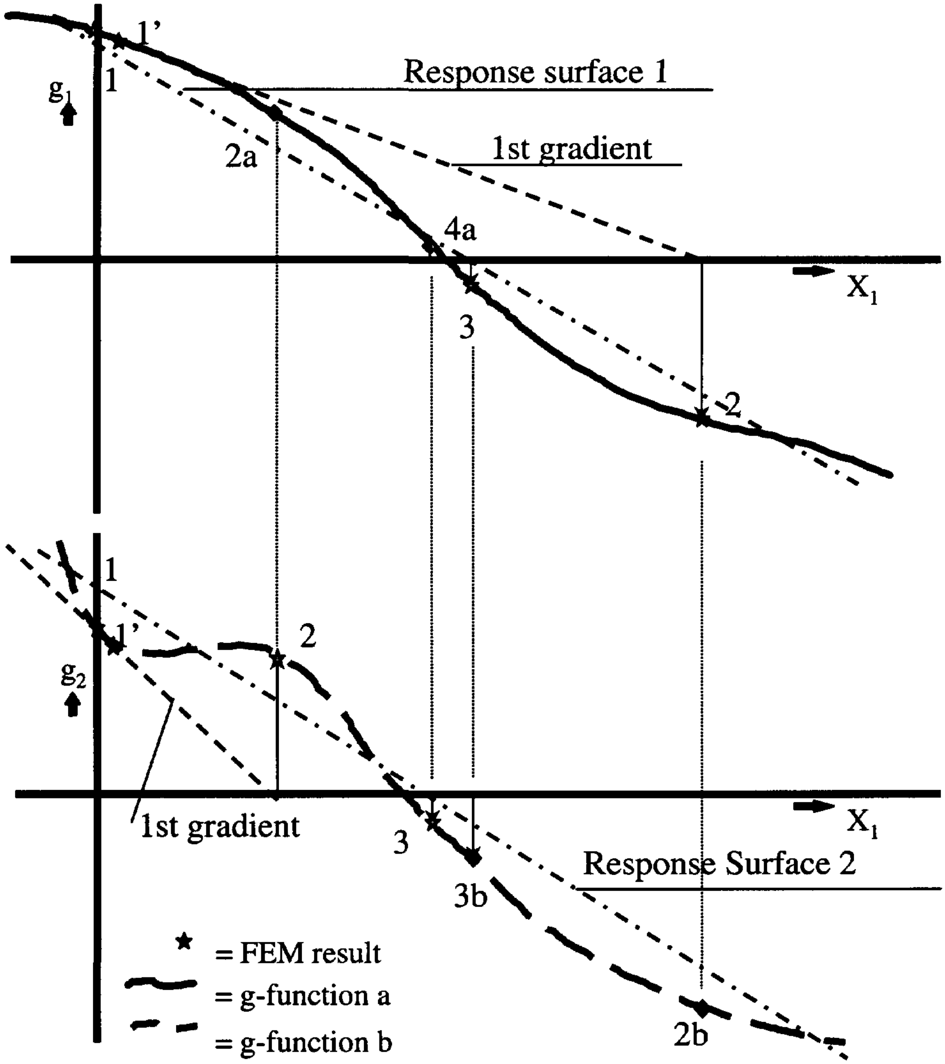

The gradients for both limit state functions are computed numerically in point 1 (point 1'). Based on the gradients a design-point is found in point 2. In both estimated design-points 2 a FE computation is performed. The limit state function is evaluated in the points 2, not only for the limit state function considered but for the other limit state function as well (points 2a and 2b). Now for each limit state function a response surface is fitted to four points: 1+1', 2 and 2a. A FORM procedure on this response surface leads to point 3.

The number of terms of the equation is limited by the number of data (LSFE). There should always be redundancy. For example with n = 2 variables the complete equation can already be used when the number of data is higher than 5. The number of terms should be kept low in order to prevent oscillations between data points. Sometimes a linear equation (only the first two terms of eq. 3.2) performs better and faster than a quadratic one. It has been chosen to use higher terms only when there is a 50 % redundancy in data points.

The fitted response surface should be most accurate in the neighbourhood of the latest estimated design-point. Data that have a large distance to this design-point should have less influence on the fit than data at close range or in the design-point.

After the FORM procedure has been completed, a combination procedure has to be applied to compute the system reliability. In addition, the procedure has to be repeated until all failure paths have been investigated. This can be performed using the Branch-and-Bound method described in Annex B. The method is further referred to as FORM-ARS.

4. Comparison of the reliability methods

4.1 Evaluation criteria

In the previous chapters the following reliability methods were found suitable for use in structural reliability:
1. Crude Monte Carlo simulation (MC),
2. Monte Carlo importance sampling (MCI)
3. Crude Directional Sampling (DS),
4. First and Second Order Reliability Method (FORM and SORM), combined with system analysis,
5. FORM through an Adaptive Response Surface (FORM-ARS), combined with system analysis,
6. Directional Adaptive Response surface Sampling (DARS).

For the analysis of one smooth limit state function, without system effects, the level II method FORM is generally regarded as the standard method giving the best mix of efficiency and accuracy [Sch97]. By way of introduction, in this section, all methods are compared based on relatively simple artificial limit state functions, most of them found in literature. In the next chapter, the most suitable reliability method will be tested for use in real structural reliability problems. In order to judge the different reliability methods, the following criteria are used from [Eng93] to select the artificial limit state functions:
1) Robustness against multiple critical points;
2) Robustness against noisy boundaries;
3) Capability to handle unions and intersections;

Efficiency and accuracy with respect to:
4) the number of variables (space dimension);
5) the probability level;
6) strong curvatures of the limit state function;
7) not finding roots in u-space coordinate axis directions.

Table 4.1: Overview of examples (all variables are normal, except for the Noisy LSF).

Description	Limit State Function	β	n	crit.	ref.
Linear LSF					
Standard R-S	$g = R - S$	3.5	2	-	
Noisy LSF	$g = x_1 + 2x_2 + 2x_3 + x_4 - 5x_5 - 5x_6 + 0.001\sum_{i=1}^{6}\sin(100x_i)$	2.3	6	2	Eng93
Non-linear LSF					
1 quadratic term	$g = R - S^2$	3.5	2	4	
10 quadratic terms	$g = R - \sum_{i=1}^{10} S_i^2/i$	3.0	11	4,6	
25 quadratic terms	$g = R - \sum_{i=1}^{25} S_i^2/i$	2.6	25	4,6	
Convex failure domain	$g = 0.1(u_1 - u_2)^2 - (u_1 + u_2)/\sqrt{2} + 2.5$	2.6	2	7	Bor97
Oblate Spheroid	$g = R - \sum_{i=1}^{10} S_i^2/(1 + i/10)$	1.1	10	1,4,5	
Saddle surface	$g = 3 - u_1u_2$	2.3	2	3,6,7	
Degenerated LSF					
Discontinuous LSF	$g = -0.5 + \sqrt{R - S} \cdot\cdot \quad \forall R \geq S$ $g = -0.5 \quad \cdots\cdots\cdots\cdots \quad \forall R < S$	3.8	2	3	Vro87
Two branches	$g = x_1 - x_2 - x_3 \cdot\cdot \quad \forall x_3 \leq 5$ $g = x_3 - x_2 \cdots\cdots \quad \forall x_3 > 5$	5.0	3	3	Vro87
Concave failure domain	$g = -0.5(u_1 - u_2)^2 - (u_1 + u_2)/\sqrt{2} + 3.0$	1.3	2	2,3 4,6	Kat94
Series system	$g_1 = 0.1(u_1 - u_2)^2 - (u_1 + u_2)/\sqrt{2} + 3.0$ $g_2 = 0.1(u_1 - u_2)^2 + (u_1 + u_2)/\sqrt{2} + 3.0$ $g_3 = u_1 - u_2 + 3.5\sqrt{2}$ $g_4 = -u_1 + u_2 + 3.5\sqrt{2}$ $g \;= \min\{Z_1, Z_2, Z_3, Z_4\}$	2.9	2	1,3	Kat94
Parallel system	$g \;= \max\{2.67 - u_1 - u_2, 2.50 - u_2 - u_3, 2.32 - u_3 - u_4, 2.25 - u_4 - u_5\}$	3.5	5	1,3	Eng93

It is well known that FORM/SORM analysis can fail when more than one design-point exists. Furthermore, FORM/SORM can fail in cases where the Limit State Function (LSF) contains numerical noise. SORM can fail in cases of discontinuous LSF. Most reliability methods are designed and tested on simple component reliability problems. In reality many reliability problems consist of systems of components, thus intersections and unions of the failure domains have to be taken into account.

The efficiency of the reliability methods can be expressed in the number of Limit State Function Evaluations (LSFE) since they take the main part of the computational time in FE applications. In the level II methods (FORM/SORM), the number of LSFE increases with the number of random variables. The number of LSFE used for Monte Carlo sampling depends only on the probability of failure. Both the number of random variables and the probability of failure are important when using directional sampling and Monte Carlo importance sampling (MCI). The performance of the DARS method is expected to be comparable to standard directional sampling when all directions have the same importance. In most reliability problems this is not the case and it is therefore expected that the number of LSFE used by DARS only depends on the number of important variables (and the probability of failure).

The initial response surface used for DARS is based on finding roots λ in coordinate axis directions. For some cases, there are only roots in other directions. Roots in the u-space coordinate axis directions may not exist ($\lambda = \infty$). Examples in this section will show how DARS handles these cases. The adaptive response surface technique in combination with Monte Carlo sampling is not used here. DARS is expected to perform better in efficiency (see section 3.3).

An overview of the selected limit state functions is given in Table 4.1. The criteria for choosing these examples are shown in the table as well. The examples are chosen such that it is expected to have a good selection to analyse the above mentioned criteria. Detailed description and results of the examples can be found in Annex E.

Additional to the examples summarised in Table 4.1, in section 4.6, a set of LSF is simultaneously analysed. Since the FORM-ARS procedure analyses all LSF at once instead of one by one, an increase of efficiency is expected, compared to standard FORM procedures.

4.2 Evaluation procedure and used reliability methods

The crude directional sampling (DS) result is considered to be the 'exact' result when the theoretical reliability is not available. The crude Monte Carlo technique has been applied only in case the various methods give different results. The results of the crude directional sampling procedures are the mean of 5 arbitrary runs. The coefficient of variation of the probability of failure $V(P_f)$ is chosen such that $V(\beta) = 0.05$. The efficiency of Monte Carlo importance sampling (MCI) depends on the number of variables and the correctness of the estimate of β. Since β is not known beforehand, here the importance sampling is optimised for $\beta = 4$. As a result, for other outcomes of the reliability index β, the importance sampling will not be optimal.

The basic (numerical gradient based) FORM iteration procedure has been described in chapter 2. Two other optimisation procedures to find the design-point are available in the commercial computer code COMREL: RFLS and NLPQL. According to [RCP97], the RFLS method is performing best at limit state functions with many random variables. NLPQL is said to perform best for a limited number of variables ($n < 20$). All FORM procedures start their iteration by default in the origin of the u-space. The COMREL code offers the opportunity for adaptive Monte Carlo sampling (adsamp). This is a kind of adaptive importance sampling. The mean value of the sampling density $h(\underline{x})$ is chosen in the point that has the absolute minimum g-value. For sake of completeness, this method is added to the comparison. The number of samples has been set equal to 10^5 in all cases.

The importance sampling option discussed in section 2.6.1 is an option in the COMREL code as well. By default 100 importance samples are used after the FORM or SORM iterations. The performance of this option will be discussed in the concluding remarks at the end of this chapter.

Two varieties of the FORM-ARS procedure are used: the quadratic response surface is fitted to the results in x-space and in u-space. The response surface is fitted to the computed data by means of the ODRPACK software, based on weighted orthogonal distance regression [Bog92]. Parameters of a response function are found by minimising the sum of the squared weighted orthogonal distances from the set of LFSE to the surface determined by the parameters.

In the DARS procedure, the limit state function results are used when according to the response surface the vector length λ is less than the minimum value found so far plus 3 ($\lambda_{add} = 3$) otherwise λ_{RS} is used. Antithetic sampling (section 3.2.3) is not used.

The results (except importance sampling) are summarised in Table 4.2 as a reference. Detailed information on the limit state function and results is found in Annex E. Intermediate results of the DARS procedure, such as the minimum found distance λ and the results of a FORM analysis on the final response surface, are presented in Annex E as well.

Table 4.2 shows a wide range of required LSFE. In the next sections, the results are discussed individually with regard to the criteria mentioned in section 4.1.

Overall, FORM (especially using ARS) is the best in efficiency. The problem with FORM is the robustness (accuracy). For some cases, an erroneous answer is found without error message or warning.

Level III methods can not give an error message. As a result, it is not sure whether DARS finds the correct answer. The results in Table 4.2 show however little reason for doubt. All level III procedures lead to the correct answer where DARS is the best in efficiency.

Table 4.2: Number of LSFE needed by the various reliability methods.

	FORM Standard	FORM NLPQL	FORM RFLS	FORM-ARS (u-space)	FORM-ARS (x-space)	SORM	MC	adsamp§	MCI	DS	DARS
Linear LSF											
Standard R-S	6	7	9	6	6	12	10^4	10^5	122	100	18
Noisy LSF	40	44	452	37	15	71	10^2	10^5	1125	925	271
Non-linear LSF											
1 quadratic term	12	19	14	7	6	24	10^4	10^5	267	60	38
10 quadratic terms	65	61	74	14	16	151	10^3	10^5	2868	1132	221
25 quadratic terms	#	#	#	#	#	541	10^3	#	6501	2540	188
Convex failure domain	8	7	9	7	7	14	10^3	10^5	513	208	47
Oblate Spheroid	#	#	#	#	#	*	10^2	#	1682	170	160
Saddle surface	#	47	36	33	33	#	10^2	#	385	299	225
Degenerated LSF											
Discontinuous	*	#	*	11	13	#	10^5	10^5	325	333	55
Two branches	*	#	*	*	29	253	10^7	10^5	2787	728	135
Concave failure domain	#	#	#	#	#	#	10^2	10^5	1172	260	240
Series system	#	7	8	8	8	12	10^3	10^5	166	227	175
Parallel system	*	#	*	*	*	523	10^4	10^5	2778	581	127

* *error convergence message*

\# *erroneous answer without error message ($\Delta\beta > 0.08\ \beta$)*

§ *adaptive sampling is performed with $N = 10^5$*

4.3 Linear limit state Functions

Standard Resistance-Solicitation problem

$$g = R - S \tag{4.1}$$

All reliability methods, of course, come up with the correct answer. The level II methods (FORM) perform best with respect to the number of LSFE. Annex E.1 shows that standard FORM is the fastest method. It requires only 6 LSFE: In the starting point the LSF is evaluated and the numerical derivatives to the two variables are computed. This first step requires 3 LSFE. Because of the linear LSF, the design-point is found at once. In the program, however, it is checked whether the result of the LSF is sufficiently near zero and the design-point does not shift anymore. This step again requires 3 LSFE. The minimum number of LSFE for a linear problem therefore equals N = 2 (1 + n). For this case where n = 2 this means N = 6.

The FORM procedures implemented in COMREL (NLQPL and RFLS) require more LSFE than the standard FORM procedure although both use two iterations (the same as standard FORM). NLPQL requires only one LSFE more, which is used for output. The RFLS uses one extra LSFE per iteration and one extra for output.

Level III reliability methods require far more LSFE. Crude MC uses the largest number of LSFE: 10,000. The best performing level III method is DARS. Compared to FORM, DARS requires approximately two to three times more LSFE. Annex E.1 shows that the DARS has found the minimum distance equal to the FORM reliability index. Furthermore it is shown that performing a FORM analysis on the final response surface ($\beta_{RS,FORM}$) leads to the same result as well. This is not surprisingly: the fitted response surface after finishing the ADI procedure is the same as the real limit state function.

Noisy limit state function

$$g = x_1 + 2x_2 + 2x_3 + x_4 - 5x_5 - 5x_6 + 0.001\sum_{i=1}^{6}\sin(100x_i) \tag{4.2}$$

The effect of adding noise to a linear LSF is investigated in this example (criterion 2 of section 4.1). Table 4.2 shows that all reliability methods come up with results within the tolerance specified. FORM however results in a slightly (5 %) too high reliability index. Level III reliability methods require far more LSFE than FORM. The best performing level III method is DARS. Compared to FORM, DARS requires about 6 times more LSFE. The effect of noise in the LSF on the accuracy can be neglected. Leaving the noise term out, influences only the number of LSFE of the FORM-RFLS procedure. The number of LSFE decreases to 12 % of the original number.

Annex E.2 shows the intermediate results of the DARS procedure. The minimum found distance λ_{min} = 2.54 which is higher than the exact result (β = 2.24). The FORM result based on the response surface is much better ($\beta_{RS,FORM}$ = 2.19). As in the standard FORM procedures, the noise on the limit state function influences the observed minimum distance. The response surface smoothens the noise on the limit state function. As a result, the $\beta_{RS,FORM}$ is fairly good as well.

4.4 Non-linear limit state functions

In this section LSF's are evaluated with one or more quadratic terms, see equation (4.3). The more quadratic terms (higher k) are included, the more non-linear the LSF becomes (criterion 6 in section 4.1). FORM linearises the LSF. The more non-linear the LSF the higher the error made by FORM. SORM does not linearise the LSF and should come up with the correct answer. The examples are also meant to investigate the performance for higher numbers of random variables (criterion 4).

Quadratic terms

$$g = R - \sum_{i=1}^{k} S_i^2/i \tag{4.3}$$

First an LSF with one quadratic term (k=1) is investigated. The results of the LSF with one quadratic term are approximately the same as for the standard Resistance-Solicitation problem. Intermediate results are given in Annex E.3.

An LSF having 10 quadratic solicitation terms (k=10) is used to investigate a moderate high number of variables. Each variable has a different importance in the reliability function. Annex E.4 gives the results of this LSF. FORM and SORM give different results because of the curvature of the LSF. SORM and directional sampling give the correct answer. FORM results in a 7 % deviation in β (which is acceptable). The FORM varieties using an ARS require far less LSFE than the other FORM procedures.

Finally an LSF with 25 quadratic solicitation terms (k=25), each having a different importance to the LSF, is analysed. Table 4.2 shows that the various FORM methods give erroneous results (without message). SORM leads to a result within the specified margin ($\Delta\beta/\beta = 0.04$). Adaptive Monte Carlo sampling focuses too much on a design-point found by FORM and leads to an equally incorrect answer.

Directional sampling results in the correct answer. The high number of variables leads to a high number of LSFE in crude directional sampling (DS). Use of the response surface (DARS) decreases the number of LSFE considerably. While using DARS, the disadvantage of directional sampling (the increase in number of samples with increasing dimension) seems to disappear.

The intermediate results of the DARS procedure are shown in Annex E.5. The minimum found distance $\lambda_{min} = 3.47$ which is higher than the exact result ($\beta = 2.65$). This minimum distance was already found during the ADI procedure. In 1217 samples, DARS did not find a lower distance. The FORM result ($\beta_{RS,FORM} = 3.17$) based on the response surface is higher than the exact result as well. Compared to the previous cases (one and ten quadratic terms), an increase of discrepancy between the exact result and λ_{min} and $\beta_{RS,FORM}$ can be observed. The cause of this discrepancy is that more than one region contributes to the probability of failure.

Convex failure domain

$$g = 0.1(u_1 - u_2)^2 - (u_1 + u_2)/\sqrt{2} + 2.5 \tag{4.4}$$

The case with a convex failure domain shown in Figure 4.1 may give problems to the DARS method. Since the sampling in u-space coordinate axis directions can not find any roots, the initial response surface of the DARS procedure is troublesome (criterion 7 in section 4.1). The FORM methods come up with approximately the correct results using about 10 LSFE. Level III methods need more LSFE and lead to the exact result as well. The intermediate results of the DARS procedure, described in Annex E.6, show that the final minimum distance λ_{min} and $\beta_{RS,FORM}$ are the same as the results of the various FORM methods.

Figure 4.1: Convex failure domain (roots of the LSF).

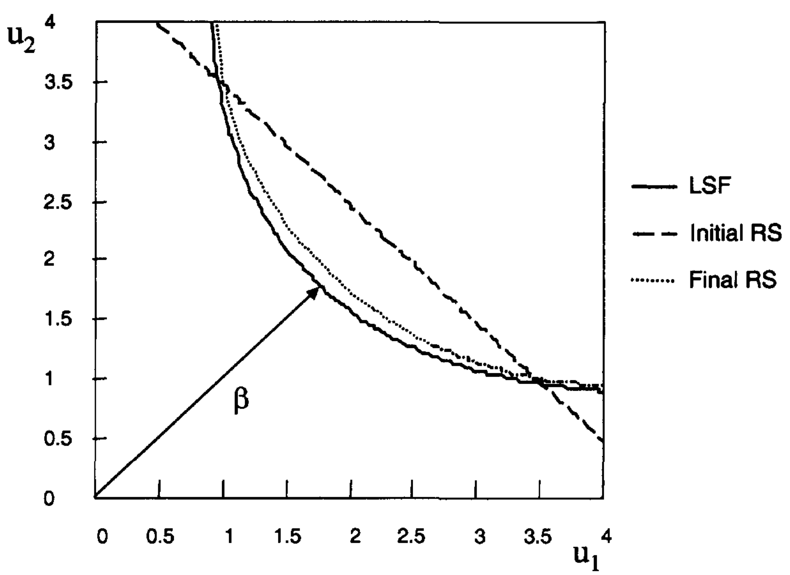

The DARS procedure is able to come to the correct result although the initial response surface did not give any roots. The response surface after ADI (initial RS) and the response surface after the last sample (final RS) are shown in Figure 4.1. The ADI procedure can not find a root in the coordinate axis directions ($\lambda = \infty$). In the iterations, however, intermediate limit state function values are found. For the building of the initial RS the points (0, 0), (0, ±f), (±f, 0), (0, ±λ), (±λ, 0), are used. By default f = 3 is used. This means in this case that three points ((0, 0), (0, ±3) and (±3, 0)) are found after the ADI procedure to which a linear RS is fitted.

Figure 4.1 shows that the initial (linear) RS deviates from the real LSF. The deviation of the distance λ is however lower than λ_{add} (= 3). This is why the DARS procedure has little trouble with this LSF. The deviation between the first response surface distance λ_{RS} and the real distance λ does not need to be lower than λ_{add} for DARS to perform well. Using a much lower additional distance, for instance $\lambda_{add} = 0.5$, leads to same result as for $\lambda_{add} = 3$. The response surface is already adapted when some samples are performed in the edges of the LSF, for instance in the direction (0.3, 0.9).

The final RS is nearly the same as the real LSF. The final fitted RS function equals:

$$g^* = 2.38 - 0.82\, u_1 - 0.82\, u_2 + 0.1\, u_1^2 + 0.1\, u_2^2 \tag{4.5}$$

There may be cases where the LSF is such that no roots are found and the gradients in the origin (using points (0,f)) are zero. In this case $\lambda_{min} = \infty$ and crude directional sampling is to be performed at start, since λ_{RS} is less than $\lambda_{min} + \lambda_{add}$ for all directions. This case will be explained in the next chapter.

Oblate Spheroid

$$g = R - \sum_{i=1}^{10} S_i^2/(1 + i/10) \tag{4.6}$$

The LSF shaped as an oblate spheroid should cause trouble to the level II methods (criterions 1,3,6). All directions are of importance (although not all in the same degree) where level II methods focus only on one. Table 4.2 shows indeed errors in the FORM results. All FORM varieties result in $P_f = 4.7\ 10^{-4}$ whereas $P_f = 1.4\ 10^{-1}$ is the correct answer. This means an error of a factor 300 in P_f is found. SORM recognises a problem and gives an error message (see Annex E.7). The SORM error message even reports that FORM is likely to be erroneous. FORM itself does not give this error message.

Adaptive Monte Carlo sampling (adsamp) focuses on a certain region found by FORM and leads therefore not to the correct result. Crude directional sampling (DS) leads to the correct answer and needs only a few samples (no more than used by FORM).

Monte Carlo importance sampling (MCI) performs worse in efficiency compared to crude directional sampling because the importance sampling is optimised for $\beta = 4$, where $\beta = 1.1$ is the correct answer. The required LSFE by MCI is factor 10 higher than used by DS. The intermediate results of the DARS procedure are given in Annex E.7. Since all directions have importance, the DARS procedure has little advantage compared to crude directional sampling. The minimum distance found by DARS is equal to the FORM β result. Obviously an union of failure domains (series system behaviour) is at hand.

A FORM analysis on the response surface leads to an extremely high β (= 46.4). Clearly FORM is not a good tool to investigate these types of limit state functions.

Saddle surface

$$g = 3 - u_1 u_2 \tag{4.7}$$

This limit state function has been added to show the effect of having a limit state function with cross terms only and using equation 3.1 nevertheless as a response function. Table 4.2 (and Annex E.8) shows the results of the various procedures. Since there are two regions with contributions to the failure probability, where FORM finds only one, an error by a factor 2 (underestimation) is expected from all FORM varieties. On the otherhand, FORM overestimates the probability of failure due to the convex shape of the limit state function. So FORM itself results in a sufficient accurate result because of the balancing of both effects. SORM does not overestimate the probability of failure due to the convex shape of the limit state function. Consequently an error by a factor 2 remains in the probability of failure in SORM which is considered as insufficiently accurate for the aims in this thesis. The same effect results from the importance sampling procedure after FORM. Monte Carlo Importance sampling (MCI), directional sampling (DS) and DARS all lead to a sufficient accurate answer requiring approximately 300 limit state function evaluations. DARS can not find roots in any of the four coordinate axis directions (criterion 7). The value of the limit state function is equal to 3 for every limit state function evaluation. As a result only a flat response surface can be fitted these data. For this case the DARS procedure would never find a direction where $\lambda_{RS} < \lambda_{min} + \lambda_{add}$ (λ_{RS} and λ_{min} are infinite). In chapter 3 it was discussed that for this case (where every limit state function evaluation in the coordinate axis direction results in the same value), the sampling ADI procedure is completed by sampling procedure in random directions. Criterion 7 vanishes after this random direction sampling procedure and the DARS procedure is finished without problems. The DARS procedure has little advantage compared to standard directional sampling because nearly all directions are important.

4.5 Degenerated limit state functions

Degenerated reliability functions should be seen as a system of reliability functions. They are used to research criterion 1 and 3. Using level II reliability methods, the systems reliability should have been analysed with Ditlevsen Bounds or the Hohenbichler approximations. The idea of this section is that the systems behaviour might not be recognised by the user. For instance, some LSF in the previous section could have been considered as systems. The problem is to recognise these. In this section the system effect in the limit states is recognised but, on purpose, not acted on.

Discontinuous limit state function

$$\begin{aligned} & g = -0.5 + \sqrt{R - S} \cdots \forall R \geq S \\ & g = -0.5 \cdots\cdots\cdots\cdots\cdots \forall R < S \end{aligned} \tag{4.8}$$

Standard FORM methods may have problems with this discontinuous function because during iterations they might come in a region where g is negative and the derivatives to both variables is zero. Consequently the standard FORM does not know how to find a new estimate of the design-point. The results in Table 4.2 show that all standard and commercial FORM and SORM procedures give either no or an erroneous answer. The ARS-FORM procedures perform well because the limit state function is smoothed out. Consequently ARS-FORM never finds zero derivatives. Crude directional sampling (DS) finds the approximate correct answer but needs many more LSFE compared to FORM. Monte Carlo importance sampling (MCI) leads to the correct answer and requires a number of samples comparable to crude directional sampling. DARS leads to the correct result and needs little LSFE. The intermediate answers of DARS λ_{min} and $\beta_{RS,FORM}$ (Annex E.9) show the correct results as well.

Two branches

$$\begin{aligned} & g = x_1 - x_2 - x_3 \cdots \forall x_3 \leq 5 \\ & g = x_3 - x_2 \cdots\cdots\cdots \forall x_3 > 5 \end{aligned} \tag{4.9}$$

Figure 4.2: Limit state function with two branches (x_1 = 10).

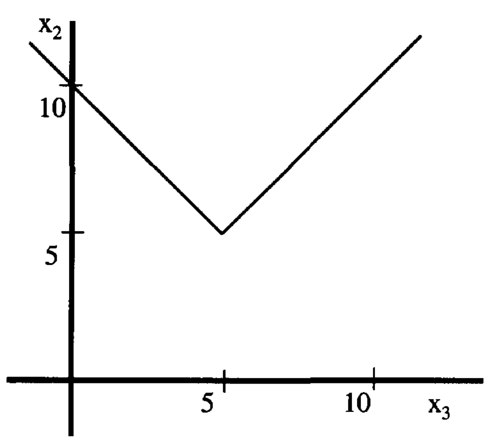

The case with two branches, shown in Figure 4.2, is of course not meant to be solved by level II reliability methods. The figure shows that an intersection is concerned. FORM should have convergence problems with this case because the estimated design-point moves constantly between the two branches. The ARS procedures smoothes the function and should therefore have less difficulty. The results in Table 4.2 show that the standard FORM methods have indeed serious problems. Only FORM-ARS in x-space performs reasonably well. The fitted RS in u-space does not converge. As a result there is no convergence in the FORM procedure. Crude directional sampling and DARS performs best with the correct answer (see Annex E.10).

Concave failure domain

$$g = -0.5(u_1 - u_2)^2 - (u_1 + u_2)/\sqrt{2} + 3.0 \tag{4.10}$$

Figure 4.3: Concave failure domain.

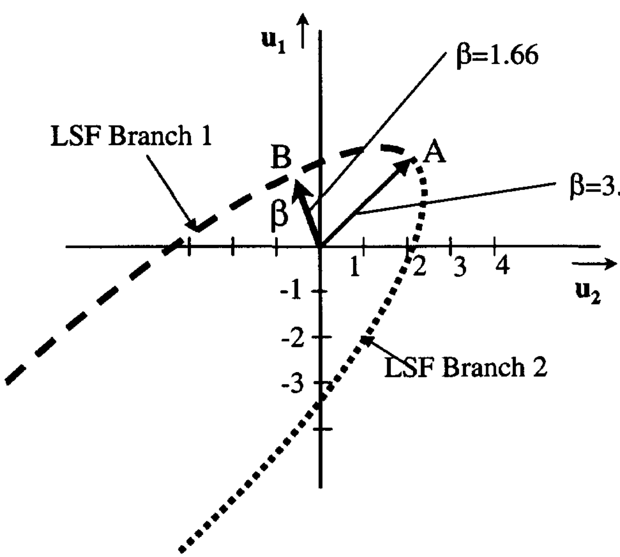

Figure 4.3 shows a limit state function with a concave failure domain. In fact, this is a system of the two branches of the parabola. FORM methods are likely to find design point A with a probability of failure, which is a factor 2 too low.

This case shows extremely erroneous FORM (and SORM) answers when the default starting point (0,0) is chosen. A reliability index $\beta = 3.0$ is found instead of the exact $\beta = 1.26$. Any other starting point leads to the correct $\beta = 1.66$ result (design point B). Most manuals of commercial FORM advise to use multiple starting points to avoid erroneous answers. The commercial code COMREL offers the possibility to select random starting points. This makes it possible to use multiple starting points in successive computations automatically. It is difficult to decide how many starting points are to be used. Unfortunately, it is sometimes possible for all trials to converge to the same point even when other solution points exist ([Kiu98]).

Crude directional sampling leads to the exact result. The DARS procedure has hardly any advantage in comparison to the standard directional sampling. Nearly all directions are of importance. Monte Carlo importance sampling (MCI) performs worse than crude directional sampling because the importance sampling is optimised for $\beta = 4$, where $\beta = 1.7$ is the correct answer (see Annex E.11).

Series system

$$g = \min\{0.1(u_1 - u_2)^2 - (u_1 + u_2)/\sqrt{2} + 3.0,\ 0.1(u_1 - u_2)^2 + (u_1 + u_2)/\sqrt{2} + 3.0,\ u_1 - u_2 + 3.5\sqrt{2},\ -u_1 + u_2 + 3.5\sqrt{2}\} \tag{4.11}$$

This series system with two non-linear and two linear branches was earlier analysed by [Kat94] and [Bor97]. Figure 4.4 shows the failure domain. Using the PROBAN code for reliability analysis, [Kat94] shows, that the union of four branches results in Ditlevsen bounds $2.84 < \beta < 3.0$.

Annex E.12 shows a clear difference between the level II and III method results. Level III methods calculate the system reliability instantly (β=2.85), where the level II methods calculate the component reliability (β=3.0). In this case, the difference is approximately a factor 1.4 in failure probability.

Figure 4.4: Series system with 4 branches.

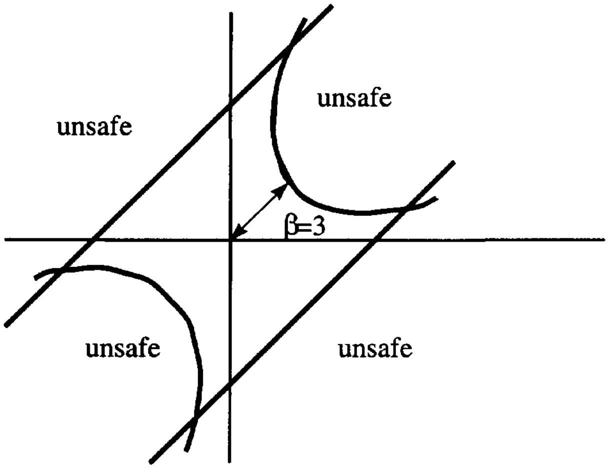

Parallel system

$$g = \max\{2.677 - u_1 - u_2, 2.500 - u_2 - u_3, \\ 2.323 - u_3 - u_4, 2.250 - u_4 - u_5\} \tag{4.12}$$

This is an intersection (parallel system) of four limit state functions. The FORM methods lead of course to an erroneous answer (see Table 4.2). These methods were never meant to deal with these kinds of problems. The limit state functions should be analysed separately and be combined in a system analysis. The fact that SORM is coming up with the correct result is surprising. The curvature of the LSF can not be evaluated since the design-point is found at an intersection of two (linear) components. The correct answer of SORM is coincidental. A change in differentiation method leads to another (but incorrect) result.

All level III methods lead to the correct result. DARS requires the least samples of the level III methods.

This example is also analysed in [Au99] with a Markov chain simulation based Monte Carlo importance sampling technique. It resulted in the (correct) reliability index $\beta = 3.53$ within 400 samples ($V(P_f) \approx 0.3 \Rightarrow V(\beta) \approx 0.03$). This number of samples is slightly higher than used by the DARS procedure (See Annex E.13).

4.6 Performance of FORM-ARS on a set of limit state functions

The FORM-ARS method is supposed to perform better (with respect to efficiency) in comparison to standard FORM methods in cases where many limit state functions (having the same variables) are to be investigated simultaneously. Where standard FORM computes the reliability index of the various limit state functions one by one, FORM-ARS computes them all at once. In this section, only the FORM varieties are compared. The performance of DARS may improve as well when a set of limit state functions is analysed simultaneously. The performance of the DARS method however is not further researched in this section.

Linear limit state functions

A case with $j = 9$ linear limit state functions and 10 random variables is investigated:

$$g_j = R_j - \sum_{i=1}^{10} S_i/(i/2)\,, \tag{4.13}$$

S_i has a standard normal distribution, R_j is a constant equal to j. All FORM varieties lead to the correct result. FORM-ARS needs 28 Limit State Function Evaluations (LSFE), where RFLS and NLQPL need 236 and 219 determinations respectively. The FORM-ARS procedure computes the reliability index of all 9 LSF at once. For 9 LSF this means an increase of speed by factor 9.

Quadratic limit state functions

A second example multiple limit state function has quadratic functions:

$$g_j = R_j - \sum_{i=1}^{10} S_i^2/(1+i/10) \tag{4.14}$$

The input is equal to the case mentioned above. The RFLS algorithm takes 6653 LSFE, NLPQL and FORM-ARS respectively use 1502 and 30 LSFE. The small number of LSFE of FORM-ARS compared to the others is perhaps a little coincidental. FORM-ARS fits a quadratic function to the data. The limit state function is perfectly quadratic, so after n+1 LSFE, the fit is equal to the limit state function. The other 9 limit state function evaluations are used to check whether the limit state function value is zero such that in this case no iterations are needed any further.

4.7 Conclusions

The performance of the reliability methods was analysed with respect to seven aspects mentioned in section 4.1. In Table 4.3 the performance is summarised.

Level II methods:

With respect to efficiency, the ARS combined with FORM performs the best of all level II methods. The degenerated limit state functions (section 4.5) show another advantage of the ARS procedure: the ARS method smoothens the reliability functions and finds the correct design-point, where other procedures have problems with zero derivatives at discontinuities. Besides, the ARS method has a big advantage in performance when analysing multiple LSF.

For FORM-ARS, fitting the response surface to data in x-space performs in nearly all cases better than fitting in u-space. Maybe this is coincidental since most cases have limit state functions that are linear or quadratic while normal distributions are used. It is doubted whether the same preference for fitting in x-space would occur when less smooth limit state and distribution functions were used. For instance using truncated distributions may give wide spaced points in u-space, where in x-space they are very narrowly spaced. Fitting a quadratic response surface to widely spaced data leads to a more realistic response surface than fitting to narrowly spaced data (Annex F).

Concerning the commercial FORM code it can be concluded that the NLPQL is more efficient than the RFLS algorithm. The number of iterations used by the standard FORM procedure is, on average, just a little smaller than the NLPQL method.

The cases with very curved limit state functions, for instance the "oblate spheroid" and the "concave failure domain", show that incorrect answers may result from FORM. These incorrect answers are found by all FORM procedures without error messages.

FORM is sometimes sensitive to the starting point. The remedy is to try several starting points and take the lowest β as result. How many and which starting points are to be used has never been sorted out. Furthermore it is not sure whether the real design-point is found this way.

SORM has the same problems as FORM with the exception of the performance on non-linear LSF. When the LSF get very non-linear (Oblate spheroid) then SORM drops out as well.

Table 4.3: performance of the various reliability methods.

aspect		FORM standard	FORM NLPQL	FORM RFLS	FORM-ARS (u-space)	FORM-ARS (x-space)	SORM	MC	adsamp	MCI	DS	DARS
1	multiple critical points	--	--	--	--	--	-	++	-	++	++	++
2	noisy boundaries	++	++	+/-	++	++	++	++	+	++	++	++
3	unions and intersection	-	-	-	-	-	+	++	-	++	+	+
4	space dimension	+/-	+/-	+/-	+/-	+/-	+/-	++	+/-	+/-	+/-	+
5	probability level	++	++	++	++	++	++	--	++	+/-	+/-	+
6	strong curvatures in the LSF	--	--	--	-	-	-	++	+	++	++	++
7	no roots in axis directions	++	++	++	++	++	++	++	++	++	++	+

++ *very little influence or very good*
+ *little influence or good*
+/- *moderate influence*
- *strong influence of less good*
-- *very strong influence or bad*

The COMREL importance sampling option discussed in section 2.6.1 is meant to improve the probability failure estimate for irrigularly shaped limit state functions. The only really irregularly shaped LSF discussed in this chapter is the "Noisy LSF" case. For this case the importance sampling in the neighbourhood of the FORM/SORM design point resulted in a better estimate of the probability of failure. The probability of failure estimate improved for the "25 quadratic terms" and "oblate speroid" cases as well. These cases do not have an irregularly shaped LSF but have a strongly curved LSF and many regions that contribute to the probability of failure near the design point found. In these cases, use importance sampling after FORM/SORM, increases the number of samples considerably, since it is nothing else than standard importance sampling.

For all other cases the importance sampling was superfluous because SORM already gave the correct answer or the importance sampling did not improve the reliability estimate. In all cases the use of the importance sampling option cost a considerable amount of LSFE.

Level III methods:

The performance of crude Monte Carlo sampling (MC), adaptive Monte Carlo sampling (adsamp), Monte Carlo importance sampling (MCI), crude Directional sampling (DS) and DARS has been investigated.

While the number of samples with DS and MC importance sampling (MCI) increases with dimension, DARS does not seem to have this disadvantage. Figure 4.5 shows the number of LSFE used by DARS and DS. It shows that after the starting procedure, the DARS procedure is quite insensitive to the dimension.

Figure 4.5: Number of LSFE versus the number of variables required by DARS and DS.

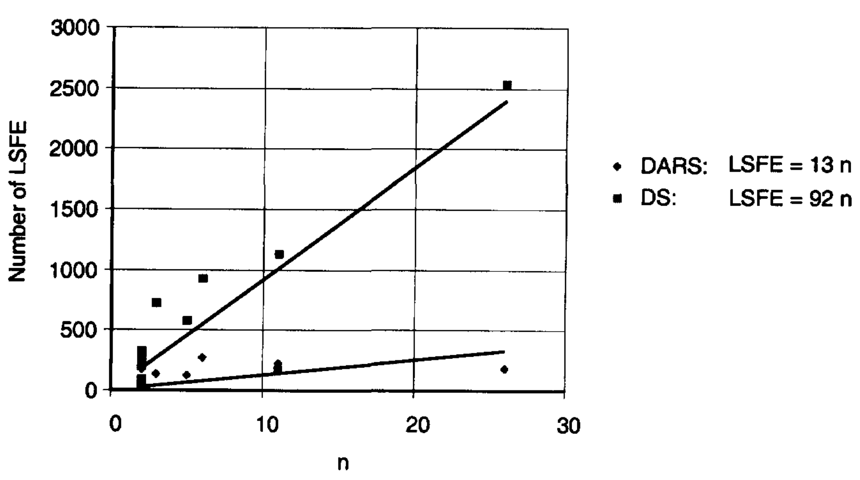

The number of LSFE used by MC importance sampling (MCI) is comparable to the number of LSFE used by crude directional sampling (DS). The number of LSFE is relatively large only when the reliability index is highly overestimated.

The DS procedure is without error. In case of LSF where all directions are of approximately the same importance, the DARS procedure has little advantage compared to the crude directional sampling procedure. The fact that all directions have importance results in a low $V(P_f)$ and a low number of LSFE anyway. The required LSFE for DARS vary from 0.5 till 5 per sample.

Level II compared to Level III procedures

FORM requires far less LSFE than the directional sampling (DS) procedure, sometimes however at the expense of accuracy. The examples show that an error of a factor 3 in reliability index (Oblate spheroid) may occur using FORM.

FORM finds the exact result for single design points in relatively flat limit state functions. For less flat limit state functions the errors can be reduced using importance sampling option in the neighbourhood of the design point or SORM. Irregularly shaped limit state functions should be analysed with the importance sampling option (requiring however many LSFE). An adaptive response surface combined with FORM (FORM-ARS) requires the least samples and solves irregularly shaped limit state functions as well.

For multiple design points (unions or intersections) a systems analysis is to be performed, for instance by means of the a Branch-and-Bound method (also at cost of many LSFE).

Level III methods do not have any drawbacks with respect to the shape of the limit state function. The number of LSFE only depends on the number of random variables and/or the probability of failure. It does not depend on the shape of the limit state function. In general however, level III methods use more LSFE than FORM, especially in the case of single relatively flat limit functions.

In structural reliability the limit state functions are often not flat but irregularly shaped and curved. From the foregoing it can be concluded that FORM has some drawbacks which can be overcome by using sophisticated measures as SORM, importance sampling and system analysis. The consequences are however a more complicated procedure and many LSFE. Although these sophisticated measures improve the accuracy and reliability of the FORM probability of failure estimates it is still not without doubt whether the correct answer is found.

Since efficiency is only useful when the correct answer can be guaranteed, DARS may be considered overall the best procedure. It gives the correct result with the least LSFE and uses no prior knowledge of the influence of variables on the limit state function. Only in cases where this prior knowledge is available, system behaviour is absent, and the limit state functions are not irregularly shaped, the FORM methods are clearly to be preferred.

5. Structural applications

5.1 Introduction

In the previous chapter, the efficiency and accuracy of the reliability methods on artificial limit state functions were analysed. The DARS (Directional Adaptive Response surface Sampling) procedure was considered to lead to the best combination of accuracy and efficiency given the requirement of not needing any preknowledge of the influence of variables on the limit state function. The shape of the limit state function of structural systems may be different from these artificial limit state functions. The efficiency and accuracy of the DARS procedure on real structures has yet to be proven.

Table 5.1 shows some examples of recent reliability studies on FE models by various authors. The table shows clearly that the number of random variables n in recent papers is hardly higher than 10. For this reason, these examples are not a good set of test cases for analysing the performance of a reliability method as intended in this thesis. They can only be used as benchmark to show the accuracy of the method. The papers on structural reliability based on the adjoint or variational principle show a number of variables up to 100. One of these examples [Gut94] is reanalysed in this chapter.

Set of structural examples

In order to test the performance of the DARS procedure, a number of structures have been chosen that are typical for civil engineering practice. In particular structures that have outspoken system behaviour, such as steel frames, and structures made out of material with a high uncertain behaviour such as ground and road structures have been selected. Furthermore, large and small structures have been chosen and structures with a geometrically and physically non-linear behaviour. This way, it is supposed to have a representative mixture of the civil engineering practise where a probabilistic FEA might be interesting.

The examples are meant to show the accuracy and efficiency of the DARS method. The results will be compared to the crude directional sampling method or results found in literature. The dimension n of the examples is maximised to 80 in order to keep the number of LSFE in crude directional sampling within practical limits. The condition for sampling is the same as used in chapter 4. The FEA results are used when $\lambda_{RS} < \lambda_{min} + 3$ [Har86]. It is referred to as DARS(3.0). Though it is a reliable condition to use this additional distance

$\lambda_{add} = 3$, it may result in less efficiency. Therefore, in the examples the effect of loosening the condition to an additional distance $\lambda_{add} = 1.1$ (section 3.1) is investigated as well, It is referred to as DARS(1.1). Antithetic sampling is not used.

For all cases intermediate results are given. First of all the results from the starting procedure are given. The DARS procedure starts sampling in the u-space coordinate axis directions. This sampling is comparable to (course) directional integration (ADI). This result gives a first impression of the probability of failure.

In the next step, a response surface is fitted to the ADI data. As an intermediate result, a FORM analysis is performed on this response surface ($\beta_{RS,FORM}$). Finally the DARS reliability $\mu(\beta)$ is given, together with the confidence limits belonging to $V(\beta) = 0.05$: β_{low} and β_{upper}.

For sake of comparison, the crude directional sampling (DS) result is given. Finally, for the sake of completeness, the minimum observed distance from origin to the limit state (λ_{min}) is given. For single linear limit state functions, this distance λ is comparable to the reliability index β, as would be found from FORM. For most cases, at the end of the DARS procedure, a FORM analysis is performed on the final RS. The difference between the FORM result and the DARS result gives some insight on the system behaviour of the structure. Besides, the FORM result gives insight in the influence factors.

As stated in section 3.1, the response surface response is not exactly the same as the real response (introduced by the lack of fit). Performing FORM on a response surface introduces therefore a (reliability) model uncertainty. The difference in the FORM reliability index because of the introduction of the extra random parameter.

The DARS procedure uses the response surface only to direct its samples to important regions. The model uncertainty is therefore not applicable to the DARS method.

Random fields models

Random fields are used for modelling spatial variations such as those in material properties, the random variation of the load on a structure or the spatial variation of the geometry of the structure (for instance coordinates or local dimensions). An overview of the use of random fields in structural engineering practise is given in [Van84] and [Fab88]. For use in combination with FEA, the random fields are to be translated in finite element properties.

Point discretisation methods represent the uncertainties of a random field by its value in one or more points. Most of the time the midpoint of the element (the so-called 'midpoint' method) is used for discretisation. Other methods are the:
- Weighted integral method [Deo90];
- Nodal point method [His81];
- Local averaging method [Van83];
- Interpolation method [Liu86].

Another representation is made by means of spectral or series expansion models. Proposed methods are:

- Basis random variable method [Law87]
- Kernel expansion method or Karlhunen-Loeve expansion [Gha91];
- Homogeneous chaos expansion method [Gha91];
- Perturbation method [Gha91].

The models described in [Gha91] may be very useful in combination with FEA. The number of stochastic parameters describing the stochastic fields can sometimes be far less then used by point discretisation methods. This especially occurs when a very fine (random field) mesh is used, where a course mesh would be appropriate as well. The spectral or series expansion models require some insight in the probabilistic structural response. Therefore, where applicable, the mid-point method is used for the structural application in this chapter.

Table 5.1: Some recently published FERM studies (n = number of variables).

Author	Reference	Reliability method	n
Vanmarcke	[Van83]	FORM	10
W.K. Liu et al	[Liu87]	adjoint SORM	30
Yamazaki et al	[Yam88]	adjoint FORM	100
P-L Liu & Der Kiureghian	[Liu91]	adjoint FORM	85
Gutierrez et al	[Gut94]	adjoint FORM	100
Vanmarcke	[Van94]	FORM	20
Zhang & Der Kiureghian	[Zha94]	FORM	5
Bouyssy & Rackwitz	[Bou95]	FORM	
Borri & Speranzani	[Bor96]	FORM	11
Colangelo et al	[Col96]	unknown	9
Frangopol et al	[Fra96a]	MCREL (MC)	8
Lemaire & Mohamed	[Lem96]	RYFES (FORM)	6
Moarefzadeh & Melchers	[Moa96]	DS	10
Pedersen	[Ped96]	FORM	6
Borri & Speranzani	[Bor97]	FORM	8
Bucher	[Buc97]	RS/MC	15
Guan & Melchers	[Gua97]	RS/FORM	13
Kim & Na	[Kim97]	unknown	10
Schuëller	[Sch97]	unknown	20
Val, Bljuger & Yankelevsky	[Val97]	FORM	9
Graham & Deodatis	[Gra98]	MC	2
Guan & Melchers	[Gau98]	DS	16
Mitteau	[Mit98]	SORM	5
Shao & Morotsu	[Sha98]	FORM	11
Shiao & Chamis	[Shi98]	IPACS	29
Gutierrez	[Gut99]	adjoint FORM	108

FE code and computer

The DARS procedure is implemented in a pilot version of the existing FE analysis code DIANA [DIA98] (see also Annex G). The input data for an FE computation are changed for every sample. The FE analysis itself is the same as a standard deterministic computation. For use in this chapter, as a standard, no optimisation on the FE computations (as suggested in section 3.2.4) is performed.

The computations are performed on a HP 9000, 160 MHz UNIX machine. For comparison of computational speed, the results of the cases show the total computational time (hh:mm). In Annex J, per case, the CPU seconds, File Access (FA), and Input-Output (IO) seconds are shown.

5.2 Beams

The cases in this section are chosen to show the performance of DARS on simple structures. The structures are designed using a code type level I reliability method (partial safety factors). The structural behaviour is chosen such that various difficulties to the reliability method are shown, while the FE analysis is rather simple and therefore fast. The following cases are analysed:

1. Simply supported beam.

   The behaviour of the beam is physically non-linear. Consequently, some random variables become only of importance near the limit state. In the origin of u-space they have no influence at all. Finding roots in all u-space coordinate axis directions (in ADI) may therefore be troublesome.
2. Simply supported beam with random Young's modulus

   The beam has a linear behaviour. The case is chosen to verify the performance of correlation along the beam and a high number (50) of random variables. The results are checked with results found in literature.
3. Stussi-Kollbronner beam.

   The Stussi-Kollbronner beam has a physically non-linear behaviour. This case has the same problems as case 1. This case is chosen because of available analytical results.
4. Central buckling.

   The central buckling case includes geometrically and physically non-linear behaviour. Besides, coordinates are treated as stochastic parameters to bring initial imperfections into account. Stochastic parameters become of importance only near the limit state. As in case 1, in the neighbourhood of the origin in u-space there is no influence of these parameters on the limit state function at all.

5.2.1 Simply supported I-Beam

A simply supported steel I-Beam (Figure 5.1) is investigated. A vertical load F is placed in the centre of the span. Both end points are supported in the vertical direction. The elementary load bearing capacity is simply given by:

$$F_y = 4\,M_y\,/\,\ell \tag{5.1}$$

F_y = mid span force at the yield point
M_y = bending yield moment of the beam
ℓ = span length

Figure 5.1: Simply supported beam.

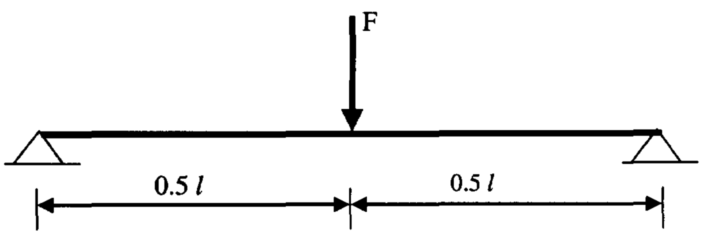

Figure 5.2: Stress-strain diagram.

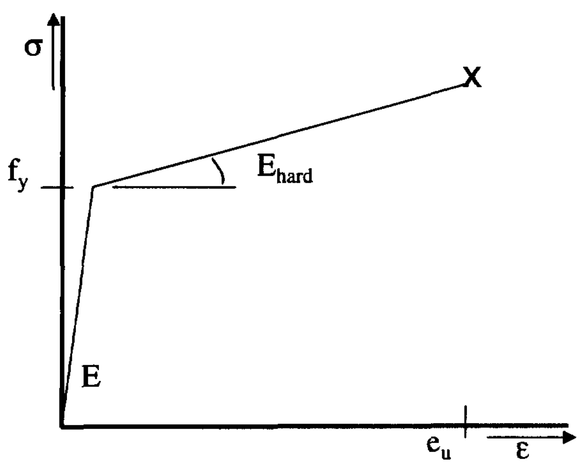

The mean value of the actual load F on the beam in the probabilistic analysis has been chosen in such a way that the following level I design condition is just fulfilled:

$$\gamma_f \, \mu(F) = 8 \, W_y \, f_{yk} / (\gamma_m \ell) \tag{5.2}$$

ℓ	= 10 m	= span
W_y	= 0.00126 m^3	= elastic section modulus (HE 300 A)
f_{yk}	= $\mu(f_y)$ - 1.64 $\sigma(f_y)$	= characteristic value of the yield stress
γ_f	= 1.5	= partial load factor
γ_m	= 1.1	= partial resistance factor

Table 5.2: Statistical properties of random variables.

Variable	Unit	Mean	St.dev.	Lower bound	Distribution type	Importance in ADI
E	MN/m^2	$2.1 \; 10^5$	$8.4 \; 10^3$	0.0	Truncated normal	-
F	kN	eq. (5.2)	$0.2 * \mu$	-	Normal	positive
f_y	MN/m^2	240	19.2	0.1	Lognormal	negative
e_u		0.2	0.05	0.01	Truncated normal	negative
E_{hard}	MN/m^2	120	9.6	1.	Shifted lognormal	-

The properties of the random variables are presented in Table 5.2. The shifted and truncated variables are chosen to prevent the variables to become zero or negative. This would lead to a fatal error in the FEA analysis because it is physically impossible. The mean value and standard deviation given for the truncated distributions are the parameters of the untruncated distribution.

The coefficient of variation of the load is chosen as some kind of weighted average for all loads (self-weight, wind, snow and/or live load). The mean values and coefficients of variation of the material behaviour are used from [Vro87]. All material related variables are fully correlated over the length of the beam. The yield stress f_y and the hardenings modulus E_{hard} are assumed to be negatively correlated with $\rho(f_y, E_{hard}) = -0.5$ (see Figure 5.2).

Exceedance of the ultimate strain leads to collapse of the beam. The limit state therefore is ultimate strain, which itself is a random variable:

$$g = e_u - \varepsilon\{E, f_y, E_{hard}, F\} \tag{5.3}$$

This case is chosen to verify the performance of DARS in a case where some random variables (E_{hard} and f_y) become only of importance near the limit state. Changing these variables individually from μ to μ - f σ (f = 3), while the other variables keep their mean value, leads to the initial conclusion that the variables E_{hard} and f_y have little influence on the value of the limit state function. Consequently the search for λ is stopped because of this initial conclusion and roots are not found (assumed to be at infinite distance).

The resulting initial response surface is then nearly flat with respect to these variables. For higher values of f, these variables may however have large influence on the probability of failure. It is investigated whether the DARS procedure is able to correct the response surface such that the correct result is found.

The computations are performed using a FEA model with 10 numerically integrated beam elements (with 17 integration points over the height of the beam).

Table 5.3: Results of the simply supported beam (n = 5).

		ADI	DARS λ_{add} =1.1	DARS λ_{add} =3.0	DS
Results	$\mu(\beta)$	3.88	4.84	4.67	4.47
	β_{low}-β_{upper}	(3.67 - ∞)	4.71 - 5.50	4.33 - 5.03	4.32 - 5.02
	λ_{min}	4.69	4.69	4.69	4.69
	$\beta_{RS,FORM}$	7.63	4.91	5.00	7.70
Samples	LSFE	18	274	435	1294
	samples	10	1799	384	384
Computer	hh:mm	00:04	01:07	01:31	04:24

Table 5.4: Influence factors α belonging to $\beta_{RS,FORM}$.

	E	F	f_y	e_u	E_{hard}
ADI	+0.00	+0.65	–0.10	–0.75	+0.00
DARS(1.1)	+0.21	+0.12	–0.08	+0.95	–0.02
DARS(3.0)	–0.16	+0.83	–0.24	+0.45	+0.19
DS	–0.17	+0.75	–0.26	+0.54	+0.22

Table 5.3 shows the results of the probabilistic analyses. For n = 5 variables, ADI uses 2n = 10 directional samples. Three variables have only one a priori important direction in the ADI procedure (see Table 5.2), so seven directions remain. To find the roots in these seven directions, 18 LSFE are used. One LSFE is used in the origin of u-space. In 5 directions, 5 LSFE are used (see Annex H). For these directions a change in f does not lead to a significant change in limit state function value g. As a result it is supposed that the distance λ from origin to the root is infinite. In the other two directions, in total 12 LSFE are used to find the root.

Crude directional sampling (DS) leads to $\beta = 4.47$ and is here regarded as the exact result. The ADI procedure results in $\beta = 3.88$ which is too low. The FORM performed on the initial (ADI) response surface leads to $\beta = 7.63$ which is far too high. The main cause of the difference between λ_{min} and $\beta_{RS,FORM}$ is the fact that a linear RS is used on a strong non-linear behaviour. A quadratic RS would probably perform better. Details are explained in Annex H. Table 5.4 shows the influence factors α, calculated by FORM.

After performing the full DARS analysis, again a FORM analysis is performed on the fitted RS. Because of the large set of data, now a quadratic function can be fitted to the data (see Annex H). This quadratic response surface clearly helps to improve the β estimate. DARS(3.0) shows a $\beta_{RS,FORM}$ decreased from 7.63 (ADI) to 5.00. The FORM result is therefore better but still too high.

The results of DARS(3.0) show that the procedure is able to correct the response surface and leads to the correct result. DARS(3.0) uses only 33 % of the LSFE compared to crude directional sampling. DARS(1.1) does not lead to the correct result. For this case it can be concluded that the additional distance $\lambda_{add} = 1.1$ is too low. That the $\beta_{RS,FORM}$ is relatively better for DARS compared to DS can be explained by the fact that in DARS only relevant samples are used for the construction of the response surface. Roots at high distances in less important directions computed by DS make the RS less good in the neighbourhood of the design point.

This effect can also be visualised by including the lack of fit random variable (realibility model error, introduced in section 3.1). The reliability index resulting from this model variable is shown in Table 5.5.

Table 5.5: Effect of including the lack of fit factor ε to the FORM on the RS.

	$\mu(\varepsilon)$	$\sigma(\varepsilon)$	$\beta_{RS,FORM}$	
			without ε	including ε
FORM on RS after DARS, $\lambda_{add} = 1.1$	-0.25	0.65	4.91	4.33
FORM on RS after DARS, $\lambda_{add} = 3.0$	-0.16	0.76	5.00	4.11

Including the model error (lack of fit), leads to a lower reliability index because of the extra uncertainty in (reliability method) modelling. The DARS procedure does not have an error term because of the lack of fit of the response surface. The DARS method will therfore always lead to a better estimate than the FORM on RS estimate including ε.

5.2.2 Simply supported I-Beam with random Young's modulus

A simply supported steel I-Beam, reported in [Gut94], is investigated. The deflection of a uniformly loaded beam with a random distributed Young's modulus is analysed. The beam has a length of 10 m, a rectangular cross section $A = 0.02\ m^2$ and a moment of inertia $I = 6.67\ 10^{-5}\ m^4$. The Young's modulus E is normally distributed and varies randomly along the beam. The correlation between the value of E at two different locations on the beam is expressed as:

$$\rho(\Delta x) = \exp\left(-\frac{|\Delta x|}{\alpha L}\right) \tag{5.4}$$

where L is the length of the beam and α a dimensionless measure of the so-called correlation length. The uniform distributed vertical load equals $q = 1000$ N/m. The mean value of Young's modulus equals $\mu(E) = 3\ 10^{10}\ N/m^2$. The standard deviation is $\sigma(E) = 10^9\ N/m^2$. The (serviceability) limit state function equals:

$$g = 0.07\ \text{m} - \delta_{mid} \tag{5.5}$$

where δ_{mid} is the displacement at mid span

In [Gut94], the structure is discretised in 100 elements. In order to study the behaviour under different mesh sizes, the random field is discretised in 2, 4, 5, 10, 20, 25, 50 and 100 equally spaced stochastic elements. The parameter α is varied: 0.1, 0.25 and 1.0. In [Gut94] it is shown that 10 stochastic elements are sufficient for higher values of α. For $\alpha = 0.1$, approximately 50 stochastic elements are required for an accurate result.

Table 5.6: Results of the beam with random Young's modulus (n = 50).

		ADI	DARS $\lambda_{add} = 1.1$	DARS $\lambda_{add} = 3.0$	DS*
Results	$\mu(\beta)$	2.33	3.42	3.82	3.90*
	β_{low}-β_{upper}	(2.00 - ∞)	3.27 - 3.74	3.68 - 4.13	3.74 - ∞
	λ_{min}	4.77	4.77	4.77	4.77
	$\beta_{RS,FORM}$	4.18	4.18	4.20	
Samples	LSFE	390	390	417	111299
	samples	100	6760	27195	30990
Computer	hh:mm	00:05	00:10	00:32	44:02

* *no convergence to $V(\beta) = 0.05$*

The case with $\alpha = 0.1$ and 50 stochastic elements is reanalysed with the DARS method. The results in Table 5.6 show that after the initial ADI procedure, DARS(3.0) only requires 417 FEA computations, where crude directional sampling requires 111,299 FEA computations (without leading to convergence). DARS reduces the number of FEA computations to less than 1 %. The example shows that DARS is really performing well for high numbers of variables. The computational time compared to DS is reduced to 1%.

Using FORM, a reliability index $\beta = 3.8$ was found in [Gut94] which compares well with the DARS results. DARS(1.1) leads to a 10 % discrepancy in reliability index. As in the previous section, it can be concluded that $\lambda_{add} = 1.1$ is a too low additional distance.

The fact that the number of LSFE computations in DARS(1.1) has not increased after ADI shows that in non-of the 6760 DARS samples the condition $\lambda_{RS} < \lambda_{min} + \lambda_{add}$ is fulfilled. Maybe the procedure should be changed in such way that at least once this condition is fulfilled and the FEA in this direction leads to a finite value for λ_{FEA}. This ensures that the response surface is adapted and new important regions may be found.

The FORM procedure applied to the response surface leads to $\beta_{RS,FORM} = 4.2$ for both $\lambda_{add} = 3.0$ and $\lambda_{add} = 1.1$. Since there is no system behaviour in this case, the FORM result should be the same as the DS result. A quadratic response surface is clearly not capable to describe the real response of this structure very well.

A fully correlated Young's modulus leads to a reliability index $\beta = 2.3$. The random field Young's modulus increases the reliability index from $\beta = 2.3$ to $\beta = 3.9$. In this case (with a very low α) the parallel system of Young's moduli has a large influence on the reliability.

5.2.3 Stüssi-Kollbrunner beam

A well-known phenomenon in structural plasticity theory is the influence of the rotational capacity on the plastic resistance of structures. Results of elementary plastic analyses are valid only if the structure has sufficient deformation capacity. In some cases, this deformation capacity even has to be infinite. Fortunately, insufficient deformation capacity can be compensated for by some hardening properties of the material. In [Waa97], one of the famous examples to show the necessity of deformation capacity (the Stüssi-Kollbrunner beam [Stu35]) is investigated in a probabilistic manner. The I-beam (see Figure 5.3) consists out of three adjacent spans; the middle span loaded by a concentrated force in the centre of the span.

Figure 5.3: Stüssi-Kollbrunner beam.

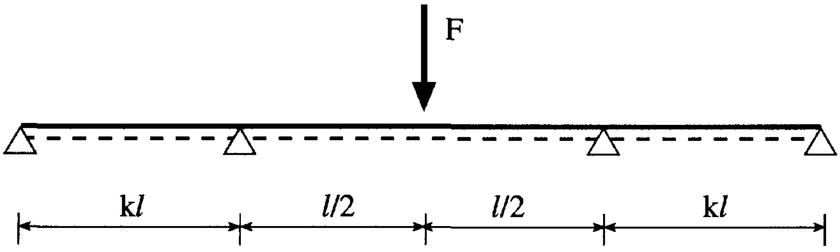

According to the theory of plasticity, the load bearing capacity is given by:

$$F = 8\, M_y / \ell \tag{5.6}$$

F_y = mid span force
M_y = fully plastic moment of the beam
ℓ = central span length

The point of discussion is that the load bearing capacity does not depend on the length of the outer spans. Normally the load deflection diagram shows two changes of direction. The first change corresponds to the forming of a plastic hinge midspan, the second to the forming of plastic hinge at the supports. It turns out that for all values of k (= ratio of the span lengths) the elementary load bearing capacity of 8 M_y/ℓ can be reached, except for $k = \infty$. In that case the load bearing capacity is only 4 M_y/ℓ, which means only 50 percent. This is called the Stüssi-Kollbrunner paradox.

Figure 5.4: σ-ε diagrams for various material properties.

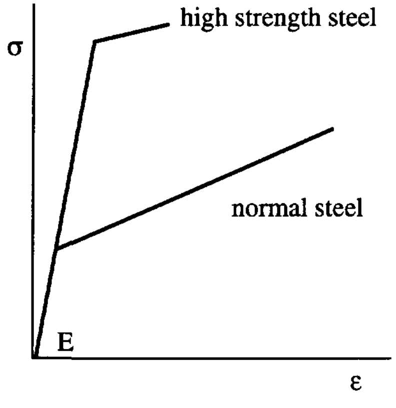

In [Waa97] the beam has been investigated using a special purpose finite element model including the finite deformation capacity of the material. The following two types of material were considered (see Figure 5.4):

- normal steel: $f_u / f_y = 1.5$ and $e_u = 0.5$
- high strength steel: $f_u / f_y = 1.1$ and $e_u = 0.2$

where f_y and f_u represent the yield and rupture strength respectively and e_u is the strain at rupture.

The critical limit state in this problem is failure of the outer fibre at mid span. It is assumed that beyond this point no more load can be added. Formally, the limit state function can be written as:

$$g = e_u - \varepsilon\{f_y, E_{hard}, F\} \tag{5.7}$$

The computations do not include local buckling of flanges or similar mechanisms.

The mean value of the load F on the beam in the probabilistic analysis has been chosen such that normal design conditions are fulfilled:

$$\gamma_f \, \mu(F) = 8 \, W_y \, f_{yk} / (\gamma_m \ell) \tag{5.8}$$

where:

ℓ	$= 10$ m	= span
W_y	$= 0.00126$ m^3	= elastic section modulus (HE 300 A)
f_{yk}	$= \mu(f_y) - 1.64\,\sigma(f_y)$	= characteristic value of the yield stress
γ_f	$= 1.5$	= partial load factor
γ_m	$= 1.1$	= partial resistance factor

Table 5.7: Statistical properties of random variables.

Variable	Unit	Mean	St.dev.	Lower bound	Distribution type	Importance in ADI
E	MN/m^2	2.1 10^5	8.4 10^3	0.0	Truncated normal	-
F	kN	eq. (5.8)	0.2 * μ	-	Normal	positive
f_y	MN/m^2	240	19.2	0.1	Lognormal	negative
e_u		0.2	0.05	0.01	Truncated normal	negative
E_{hard}	MN/m^2	120	9.6	1.	Shifted lognormal	-

Figure 5.5: Reliability index β for normal and high strength steel as a function of k ($k\ell$ = side span length); FEA and simplified calculation (from [Waa97]).

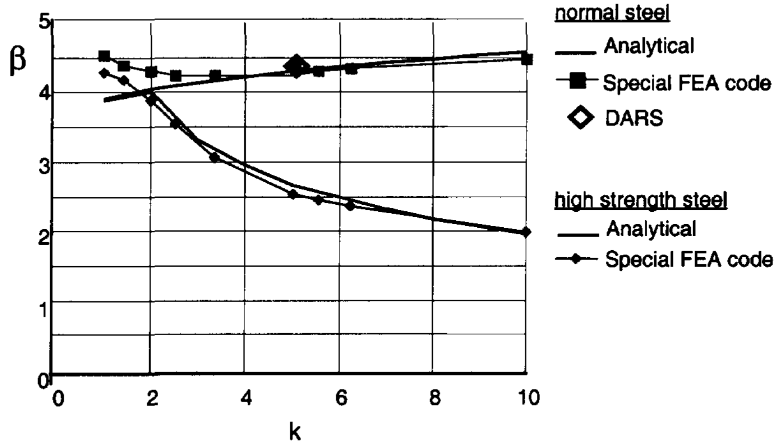

The random variables are presented in Table 5.7. All material related variables are fully correlated over the length of the beam. The yield stress f_y and the hardenings modulus E_{hard} are assumed to be negatively correlated with $\rho(f_y,E_{hard}) = -0.5$. The results of the reliability analysis [Waa97] are shown in Figure 5.5 (FEA lines) where for both materials the reliability index β is given versus the span ratio k. The probability of failure was calculated by means of FORM and crude directional sampling on a special purpose FEA model. The reliability index does not decrease with increasing k for normal steel due to its large deformation capacity. High strength steel has a lower deformation capacity which is reflected in the results by a decrease of reliability with increasing k. Already for $k > 2$ it drops below the $\beta = 3.8$ limit that has been specified informally in the Eurocode [ENV91] as a target value.

In [Waa97] the FEA code results are compared with results from a simplified analytical model. The results of the analytical model are presented in Figure 5.5 as well. In this section, for one case, it is investigated whether the DARS procedure using the FE code DIANA performs the same as the special purpose code. Table 5.8 presents the results for the case with normal steel and k = 5. The results are the same as computed by the special purpose code and the analytical results. DARS(3.0) performs as good as crude directional sampling (DS). The DARS(1.1) results are nearly as good and require only 61 % of the LSFE required by DARS(3.0). The confidence interval of DARS(1.1) is however very large and the FORM reliability index $\beta_{RS,FORM}$ is negative. Both aspects do not make the outcome of DARS(1.1) very trustworthy. It is therefore concluded that $\lambda_{add} = 1.1$ is too little a distance in this case.

Table 5.8: Results of the Stüssi-Kollbrunner beam out of normal steel and k = 5.

		ADI	DARS λ_{add} =1.1	DARS λ_{add} =3.0	DS
Results	$\mu(\beta)$	3.79	4.51	4.39	4.41
	β_{low}-β_{upper}	(3.51 - ∞)	4.34 - ∞	4.24 - 5.24	4.26 - 5.23
	λ_{min}	4.60	4.60	4.59	4.59
	$\beta_{RS,FORM}$	5.60	negative	4.26	4.49
Samples	LSFE	23	245	399	1950
	samples	10	549	450	501
Computer	hh:mm	00:25	04:30	07:50	36:18

Table 5.9: Influence factors α belonging to $\beta_{RS,FORM}$.

	E	F	f_y	e_u	E_{hard}
ADI	+0.00	+0.57	–0.07	–0.73	+0.36
DARS(1.1)	–0.05	+0.89	–0.15	–0.38	+0.18
DARS(3.0)	–0.04	+0.67	–0.17	+0.69	+0.21
DS	+0.03	+0.48	–0.12	+0.85	+0.16

Compared to the performance of the simply supported beam in section 5.2.1, it is remarkable that there is obviously little error in the initial response surface. A cross section is already plastic in the case that the parameters have their mean values. As a result, changing variables leads to a change in limit state function value. Consequently the response surface is non-flat with respect to these variables.

Other remarkable outcomes are the influence factors presented in Table 5.9: Both DS and DARS(3.0) show a positive influence factor for the variable e_u (ultimate strain). It was expected, from an engineering point of view, that this variable would perform as a strength parameter and a negative influence factor would have resulted. This expectation is strengthened by the fact that the minimum observed distance λ_{min} (= 4.59) is indeed found in the negative direction of variable e_u. The reason for the positive influence factor is not clear. The resulting reliability index ($\beta_{RS,FORM}$) is rather good. As a consequence, completely wrong influence factors are not expected. Given the results of the previous cases the option of an erroneous response surface is most likely to be the cause of the strange influence factors.

5.2.4 Central elastic plastic buckling

This case is added to show the performance of DARS on a structure with a geometrically non-linear behaviour. The beam of section 5.2.1 is now axially loaded (see Figure 5.6). Only half of the beam is modelled. The beam has a physically non-linear behaviour because of the bi-linear stress-strain diagram (see Figure 5.2).

Figure 5.6: Beam axially loaded.

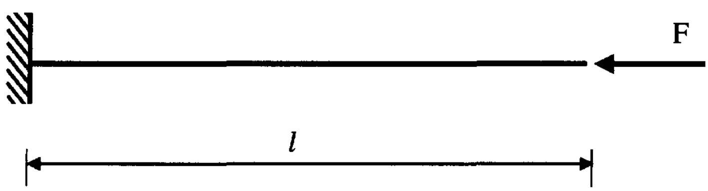

The mean value of the load on the beam in the probabilistic analysis has been chosen such that normal design conditions are fulfilled:

$$\gamma_f \, \mu(F) = F_d \tag{5.9}$$

where:

ω	$= f(\lambda)$	= buckling coefficient
λ	$= 2\ell / i$	= slenderness
F_d	$= f_{yk} A / (\omega \, \gamma_m)$	= design load
ℓ	$= 5$ m	= span
A	$= 0.01125$ m^2	= cross section (HE 300A)
i	$= 0.0749$ m	= radius of inertia
γ_f	$= 1.5$	= partial safety factor for the load
f_{yk}	$= \mu(f_y) - 1.64\,\sigma(f_y)$	= characteristic value of the yield stress
γ_m	$= 1.1$	= partial safety factor for the resistance

All material related variables are fully correlated over the length of the beam. The yield stress f_y and the hardenings modulus E_{hard} are assumed to be negatively correlated with correlation coefficient $\rho(f_y, E_{hard}) = -0.5$ (see Figure 5.2). The initial displacement or curvature is taken into account via a shift of y-coordinates. The mean value of the shift of the y-coordinates equals 0.0 m. The standard deviation is taken such that the characteristic value (1.64 σ) of the deviation is equal to 0.1 % of the length. The standard deviation increases linear from support until end. At the end of the beam the standard deviation equals $\sigma = 0.006$ m (0.06 % of double the length of the beam). The beam is built up out of 4 elements. The correlation coefficient between two y-coordinates is assumed to be:

$$\rho(y_i, y_j) = \exp\left(-\frac{|x_j - x_i|}{2\alpha\ell} \right) \tag{5.10}$$

where ℓ is the length of the beam and α a dimensionless measure of the so-called correlation length chosen to be $\alpha = 1.0$.

Table 5.10: Statistical properties of random variables.

Variable	Unit	Mean	St.dev.	Shift	Distribution type	Importance in ADI
E	MN/m^2	$2.1\ 10^5$	$8.4\ 10^3$	-	Truncated normal	-
F	kN	eq. 5.9	$0.2 * \mu$	-	Normal	positive
f_y	MN/m^2	240	19.2	0.1	Lognormal	negative
E_{hard}	MN/m^2	120	9.6	1.0	Shifted lognormal	-
y_{end}	m	0.0	0.006	-	Normal	-
$y_{3/4}$	m	0.0	0.045	-	Normal	-
$y_{2/4}$	m	0.0	0.003	-	Normal	-
$y_{1/4}$	m	0.0	0.0015	-	Normal	-

$y_{i/4}$ means y coordinate at x-position of i/4 of the length of the beam

The coefficient of variation of the load is chosen as a weighted average for all loads (self-weight, wind, snow and live load). A summary of the random variables is given in Table 5.10. Exceedance of the ultimate strain leads to collapse of the beam. The limit state therefore is ultimate strain, which in itself is a random variable:

$$g = e_u - \varepsilon\{E, f_y, E_{hard}, F, y\} \tag{5.11}$$

The results are shown in Table 5.11. The time needed for crude directional sampling to reach convergence is too long. The computations have therefore been stopped manually after 20 days of computations. At that stage 4741 samples were computed. After the full amount of samples, DARS(3.0) results in $\beta =$ 4.16. The DS result is not in the confidence interval of DARS(3.0) The difference is however small.

DARS(1.1) leads to a too high reliability index. As in previous cases, it can be concluded that the distance $\lambda_{add} = 1.1$ is too low.

For sake of comparison, the results of the DARS(3.0) computations have been analysed after 4741 samples as well. For the same number of samples, DARS(3.0) and DS come up with approximately the same result ($\beta \approx 3.9$).

The FORM performed on the response surface after the ADI ($\beta_{FORM,RS}$) results in a much too high reliability index. The influence factors are shown in Table 5.12. The main influence is because of the shift of the y-coordinates.

This central buckling case is a good example of a case where antithetic sampling (section 3.2.3) would have lead to erroneous results. The initial displacement of the beam is symmetric. $P_f(\underline{\theta})$ and $P_f(-\underline{\theta})$ are positively instead of negatively correlated.

Table 5.11: Results of the central buckling case (n = 8).

		ADI	DARS* $\lambda_{add}=1.1$	DARS $\lambda_{add}=3.0$	DS*
Results	$\mu(\beta)$	1.89	4.43	4.16	3.87
	β_{low}-β_{upper}	(1.45 - ∞)	4.25 - ∞	3.95 - ∞	3.63 - ∞
	λ_{min}	3.00	3.00	3.00	3.00
	$\beta_{RS,FORM}$	6.27	-	4.67	-
Samples	LSFE	58	101	385	14009
	samples	16	11735	2659	4741
Computer	hh:mm	01:20	01:47	09:31	500:40

*no convergence to sufficiently low $V(P_f)$

Table 5.12: Influence factors α belonging to $\beta_{RS,FORM}$.

	E	F	f_y	E_{hard}	Σy
ADI	+0.00	+0.61	+0.10	+0.00	+0.78
DARS(1.1)	-	-	-	-	-
DARS(3.0)	+0.01	+0.57	+0.40	+0.05	+0.71
DS	-	-	-	-	-

5.3 Non-linear steel frame structures

Non-linear steel frame structures are chosen to show the performance of the DARS procedure on structures with non-linear behaviour and system effects. The reliability of several frame structures, adapted from [Dey98], is calculated. The loads F_i on the frame are the only random variables. There is no correlation between the loads. The Youngs-modulus equals 2.1 10^{11} N/m^2. The stress-strain diagram is presented in Figure 5.7. The limit state is collapse of the structure. This is translated into a constraint in stress of $\sigma_u = 360$ N/mm^2, in any point k of the structure. The limit state function therefore equals:

$$g = f_u - \max\{\sigma_K\} \tag{5.12}$$

Figure 5.7: Stress-strain diagram.

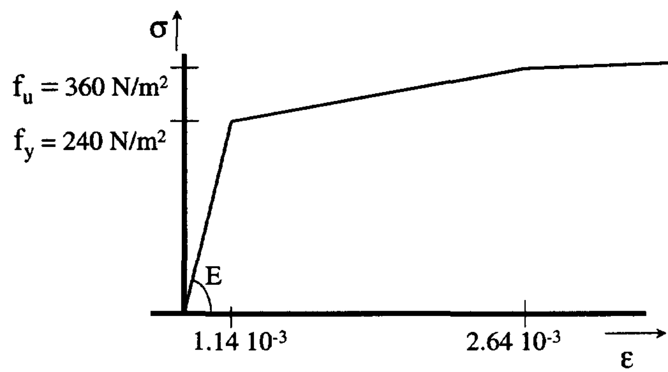

5.3.1 *One-storey, one-bay frame*

A one-storey, one-bay frame structure, shown in Figure 5.8, is examined. This case is adapted from [Dey98] and [Tho85], where yield moments are used as property. The yield moments are translated into yield stresses of standard steel profiles: HE180A beams and HE160A columns. The stochastic properties of the loads are listed in Table 5.13.

According to [Tho85], the failure of the beam is the dominant failure mechanism. There are five sequences leading to this mechanism. [Tho85] states, using the Branch-and-Bound method, that 18 FEA are necessary to identify these sequences. The significant sequences are identified as 7-4-8-2, 7-4-2, 7-8-4-2, 4-7-8-2 and 4-7-2. The union of the sequences leads, according to [Tho85], to a systems probability $6.5\ 10^{-3} < P_f < 6.6\ 10^{-3}$ ($\beta \approx 2.5$).

The results of the DARS and DS reliability computations are presented in Table 5.14. The resulting reliability index is the same as mentioned in [Tho85]. DARS gives the same answer as crude directional sampling (DS). The ADI (starting) procedure already gives nearly the correct result. DARS(3.0) uses 80 % of the LSFE used by DS. There is therefore little advantage in the use of the DARS method compared with the DS method.

The FORM result $\beta_{RS,FORM}$ based on the crude directional sampling (DS) response surface is nearly the same as the DS reliability index. The less LSFE are used (for instance in DARS(1.1)), the more the $\beta_{RS,FORM}$ deviates from the exact result.

Influence factors resulting form the FORM analysis on the final response surface are given in Table 5.15. DARS and DS methods come up with the same result.

Figure 5.8 shows the deformed structure at the minimum found distance λ_{min} which can be seen as the most likely failure mode. Plastic hinges occur at point 2, 4, 7 and 8, which is as found in [Tho85].

Figure 5.8: One-storey, one-bay frame structure, shown with the most likely failure mode (mode belonging to λ_{min}) according to DS.

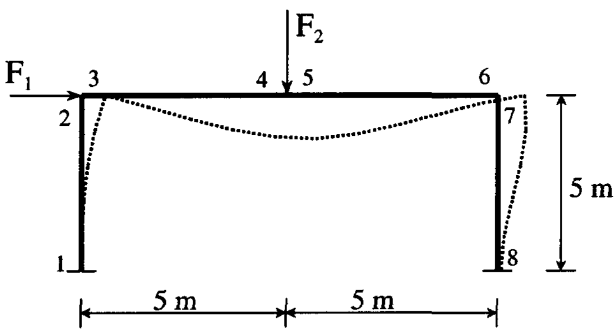

Table 5.13: Input for FEA of the one-storey, one-bay frame structure.

Variable	Unit	Mean	St.dev.	Distribution	Importance in ADI
F_1	kN	20.0	6.0	Lognormal	positive
F_2	kN	40.0	12.0	Lognormal	positive

Table 5.14: Results for the one-storey, one-bay frame structure (n = 2).

		ADI	DARS $\lambda_{add}=1.1$	DARS $\lambda_{add}=3.0$	DS
Results	$\mu(\beta)$	2.46	2.56	2.55	2.55
	β_{low}-β_{upper}	(2.05 - ∞)	2.46 - 2.68	2.46 - 2.68	2.46 - 2.68
	λ_{min}	2.69	2.68	2.68	2.68
	$\beta_{RS,FORM}$	2.28	2.71	2.62	2.40
Samples	LSFE	9	169	242	339
	samples	4	128	128	128
Computer	hh:mm	00:01	00:04	00:19	00:40

Table 5.15: Influence factors α belonging to $\beta_{RS,FORM}$.

	F_1	F_2
ADI	0.54	0.84
DARS(1.1)	0.50	0.87
DARS(3.0)	0.50	0.87
DS	0.50	0.87

5.3.2 One-storey, two-bay frame

The frame structure in Figure 5.9 is made up of IPE450 columns and HE360A beams. The probabilistic analysis of a similar case has earlier been reported in [Dey98] and [Xia94b]. As in the one-storey, one-bay case, the yield moments are translated into a yield stress of steel profiles. The loads are the only random variables. According to [Xia94b] there are 4 significant failure modes, leading to 93 significant failure sequences. The Branch-and-Bound method resulted in a system reliability $2.66 < \beta < 2.87$.

The random variables (loads) are summarised in Table 5.16. There is no correlation between the loads.

Table 5.16: Input for FEA of the one-storey, two-bay frame structure.

Variable	Unit	Mean	St.dev.	Distribution
F_1	kN	267.0	80.0	Lognormal
F_2	kN	445.0	133.5	Lognormal
F_3	kN	445.0	133.5	Lognormal

The results are presented in Table 5.17. The DARS results are the same as the crude directional results. The reliability index resulting from a FORM analysis on the response surface ($\beta_{RS,FORM}$) deviates from the directional sampling result. The difference between the DS result and $\beta_{RS,FORM}$ after DS can be explained by the fact that it concerns a series system of failure modes. The real reliability index has to be lower than β_{FORM}. The less LSFE are used (for example in DARS), the higher the $\beta_{RS,FORM}$ result. This is the same as observed in the previous cases. The difference in response surface can be observed in Table 5.18.

The resulting reliability index is lower than the bounds found in literature. Using a yield stress instead of yield moments can not explain such a difference. It may be that the bounding in the Branch-and-Bound method in [Xia94b] was a little too optimistic or there were more significant failure modes than recognised.

Figure 5.9: One-storey, two-bay frame structure, shown with the most likely failure mode (mode belonging to λ_{min}) according to DS (plastic hinges are shown as o).

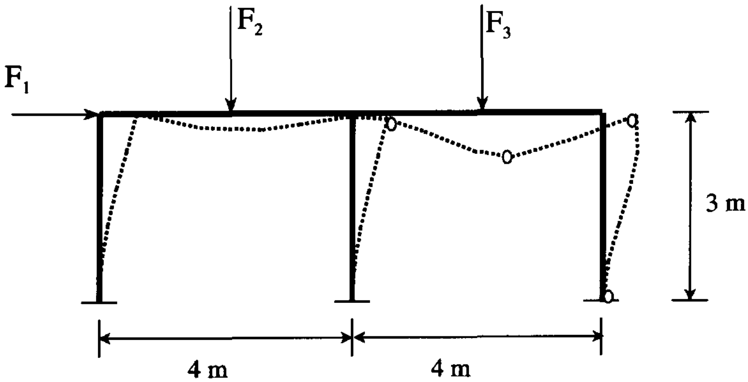

Table 5.17: Results of the one-storey, two-bay frame (n = 3).

		ADI	DARS $\lambda_{add}=1.1$	DARS $\lambda_{add}=3.0$	DS
Results	$\mu(\beta)$	2.19	2.44	2.41	2.41
	β_{low}-β_{upper}	(1.87 - ∞)	2.34 - 2.57	2.32 - 2.53	2.32 - 2.53
	λ_{min}	2.79	2.74	2.74	2.74
	$\beta_{RS,FORM}$	2.67	2.71	2.79	2.59
Samples	LSFE	12	115	269	422
	samples	6	156	156	156
Computer	hh:mm	00:01	00:11	00:26	00:42

Table 5.18: Influence factors α belonging to $\beta_{RS,FORM}$.

	F_1	F_2	F_3
ADI	0.53	0.57	0.63
DARS(1.1)	0.45	0.53	0.72
DARS(3.0)	0.45	0.53	0.72
DS	0.45	0.53	0.72

5.3.3 Two-storey, two-bay frame

The frame in Figure 5.10 is made up of HE260A columns and HE280A beams. The probabilistic analysis of a similar case has earlier been reported in [Dey98] and [Xia94b]. Contrary to the properties in [Dey98], the yield stresses of steel profiles are used instead of yield moments. The loads are the only random variables. According to [Xia94b] there are 3 significant failure modes, leading to 204 significant failure sequences. The Branch-and-Bound method resulted in a system reliability $2.34 < \beta < 2.65$.

Figure 5.10: Two-story, two-bay frame structure shown with the most likely failure mode (mode belonging to λ_{min}) according to DS.

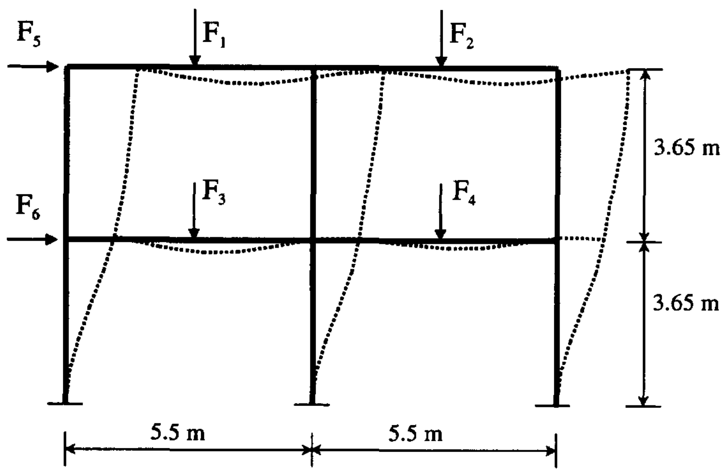

Table 5.19: Input for FEA of two-storey two-bay frame structure.

Variable	Unit	Mean	St. dev.	Distribution
F_1-F_4	kN	178.0	26.7	Lognormal
F_5	kN	44.8	16.5	Lognormal
F_6	kN	89.6	33.0	Lognormal

The random variables are summarised in Table 5.19. The results are presented in Table 5.20. The DS and DARS lead to the same results. The DARS(3.0) procedure takes 304 samples and 267 LSFE. Crude directional sampling (DS) needs 304 samples as well, but needs 1053 LSFE computations.

The FORM procedure applied to the response surface should result in a higher β than DS and DARS because of system effects. As in the previous cases the $\beta_{RS,FORM}$ resulting from the DS response surface is too high. FORM on the DARS response surfaces performs better but still results in a too high β. Influence factors given in Table 5.21 are very consistent (exclusive ADI results).

The reliability index $\beta = 2.84$ is a little higher than the one found in literature. The difference can be explained by some differences in geometry and the use of the yield stress instead of yield moment. Figure 5.10 shows the most likely failure mode. Plastic hinges occur at all three column footings.

Table 5.20: Results of the two-story, two-bay frame structure (n = 6).

		ADI	DARS $\lambda_{add}=1.1$	DARS $\lambda_{add}=3.0$	DS
Results	$\mu(\beta)$	2.17	2.86	2.86	2.84
	β_{low}-β_{upper}	(1.72 - ∞)	2.67 - 3.13	2.68 - 3.15	2.68 - 3.16
	λ_{min}	3.00	3.00	3.00	3.00
	$\beta_{RS,FORM}$	3.00	3.41	3.62	3.91
Samples	LSFE	31	86	267	1053
	samples	12	304	304	304
Computer	hh:mm	00:05	00:15	00:46	03:01

Table 5.21: Influence factors α belonging to $\beta_{RS,FORM}$.

	F_1	F_2	F_3	F_4	F_5	F_6
ADI	0.64	0.45	0.38	0.27	0.31	0.25
DARS(1.1)	0.80	0.49	0.31	0.03	0.15	0.05
DARS(3.0)	0.81	0.50	0.27	0.04	0.12	0.06
DS	0.82	0.48	0.26	0.02	0.16	0.03

This case has been chosen to show the effect of splitting the limit state into a linear-elastic and non-linear (plastic) part according to the suggestion in section 3.2.4, see Figure 5.11. Whether a (directional) sample has a positive or negative effect on the limit state function can be investigated using a linear FE analysis (leading to a distance λ_{lin}). The limit state "collapse" (including non-linear behaviour) will always lead to higher λ-values.

The basic idea is to carry out linear elastic computations first in all u-space coordinate axis directions. Consequently, the non-linear computations are performed in important directions only.

Table 5.22 shows the ADI results of the first (linear) limit state function. All negative coordinate axis directions result in an infinite distance to the limit state "non-linear behaviour" (lin -). The positive directions (lin +) result in a distance varying from 2.1 to 5.4. The linear ADI computations cost 33 seconds.

The non-linear computations are now first of all performed in the positive direction of variable 1, which leads to the minimum distance in the linear case ($\lambda_{lin} = 2.1$). The distance including non-linear behaviour (plastic collapse) equals $\lambda = 3.0$. When for a next direction the linear computations result in a λ_{lin} higher then $\lambda_{min} + \lambda_{add}$, the non-linear computations are of no use and can be skipped. In this case all negative directions can be skipped. Non of the positive directions can be skipped.

Figure 5.11: Linear-elastic and "collapse" limit state.

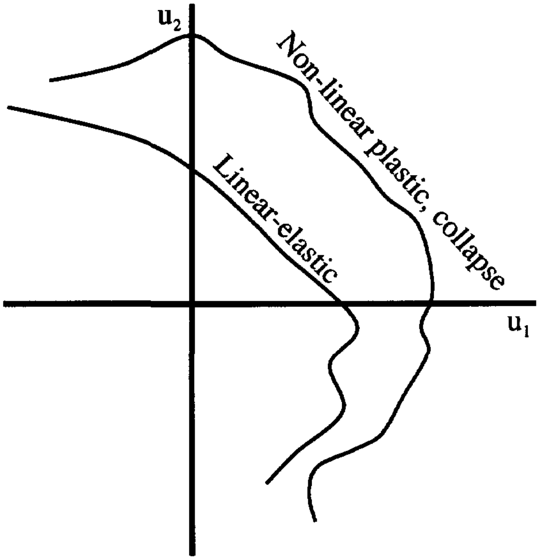

Table 5.22: Distances λ from origin to limit state.

Variable	λ_{lin}-	λ_{lin}+	λ +
1	∞	2.1	3.0
2	∞	3.1	4.2
3	∞	3.6	5.8
4	∞	5.6	7.6
5	∞	4.5	6.4
6	∞	5.4	7.0

The non-linear computations in 6 instead of 12 directions cost 216 seconds. Together with the linear computations, this results in 249 seconds (4 minutes) which is faster compared to the nearly 5 minutes according to Table 5.20. The computations in the ADI procedure become faster by approximately 20%.

After the ADI procedure, the same scheme is used. If $\lambda_{RS} < \lambda_{min} + \lambda_{add}$ then λ_{lin} is computed first. A non-linear FE analysis is only performed if $\lambda_{lin} < \lambda_{min} + \lambda_{add}$. It turns out that the condition $\lambda_{RS} < \lambda_{min} + \lambda_{add}$ is fulfilled in 62 of the 292 directions sampled. The distance λ_{lin} is computed first in these 62 directions. The linear computations cost 1058 s computational time. A distance λ_{lin} higher than $\lambda_{min} + \lambda_{add}$ is found in only one of the 62 directions. For this direction no non-linear computations have to be performed. The gain by leaving out this one non-linear computation is 42 s computational time. The balance is therefore against performing linear computations first. Apparently the response surface is sufficient to direct the samples. An extra condition to direct samples is not profitable with respect to computational time in this case.

5.4 Bridge structures

5.4.1 Orthotrope bridge deck

Figure 5.12 shows a side view and cross section of a normal lattice bridge. A part of a steel bridge deck between two cross beams has been modelled. The load (a truck wheel) is positioned exactly in the middle between two cross beams and right above a trough stiffener. The loaded area is 300 * 300 mm^2. Because of the stochastic properties of the deck, symmetry may not exist in the strict sense. Nevertheless, for simplicity, stochastic symmetry is assumed so that only half of the structure has to be analysed. This assumption is probably incorrect, but for sake of computational speed this incorrectness is neglected. The model is shown in Figure 5.13.

For the Ultimate Limit State (ULS) calculation, the anticipated lifetime of the structure has been set equal to 100 years. The distribution for the maximum axle load F in a period of 100 years can be approximated by a normal distribution with $\mu(F)$ = 250 kN and $\sigma(F)$ = 30 kN [Vro93]. This axle load is given exclusive of trends (traffic and vehicle growth) and dynamic effects. For trends and dynamic effects, factors equal to 1.2 and 1.3 respectively are applied. Both trends and dynamic effects are supposed to have no influence on the standard deviation. Consequently, the parameters of the distribution of a wheel load (half the axle load) are $\mu(F)$ = 180 kN and $\sigma(F)$ = 15 kN. As mentioned above, the wheel load is distributed over an area of 300 * 300 mm^2. The mean and standard deviation of the distributed load are 2167 kN/m^2 and 167 kN/m^2 respectively.

Table 5.23: Input of FEA [Vro87] and [Vro93].

Variable	n	Unit	Mean	St.dev.	Lower bound	Distribution type	Importance in ADI
f_y	24	N/mm^2	268.0	21.5	227.0	Shifted lognormal	negative
t (deck)	6	mm	12.0	0.48	0.1	Truncated normal	-
E	1	N/mm^2	$2.1\ 10^5$	$8.4\ 10^3$	0.1	Truncated normal	-
F	1	kN/m^2	2167	167	-	Normal	positive

Figure 5.12: Side view and cross section of a lattice bridge.

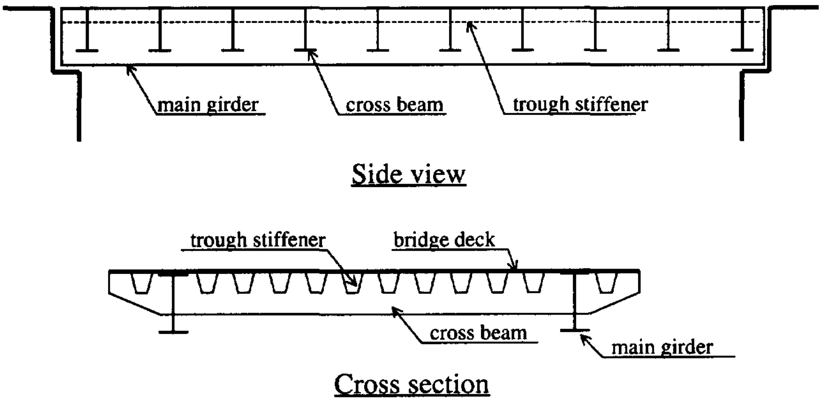

Figure 5.13: Part of bridge deck and correlated area's.

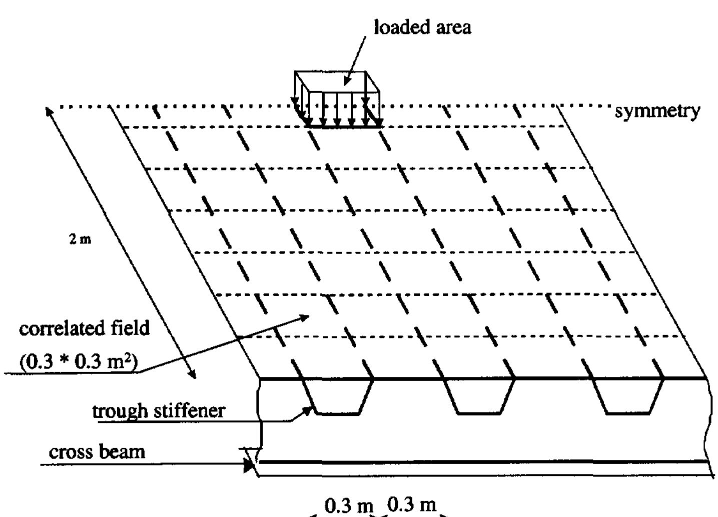

Figure 5.14: FEA mesh of bridge deck.

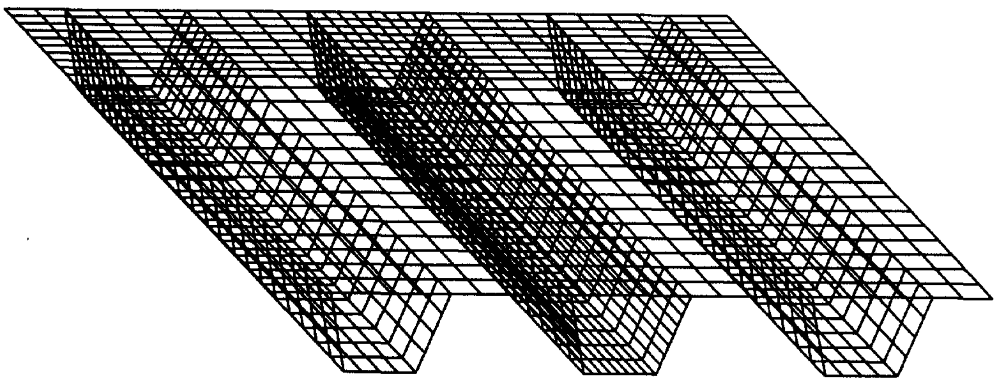

Figure 5.15: Random field mesh of bridge deck.

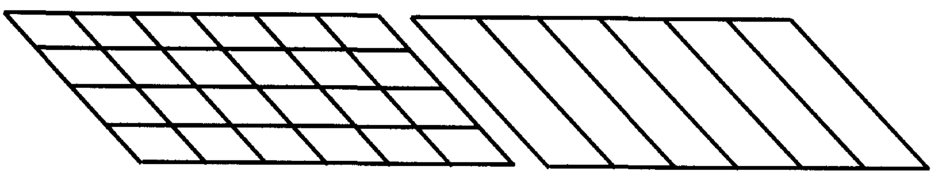

Random σ Mesh Random t Mesh

The FE model (Figure 5.14) consists of 1824 shell elements (8 noded elements, 27 integration points per element). In addition to the axle loads, the main stochastic parameters are thickness of the plate t, the Young's modulus E and the yield stress of the material. The random variables are summarised in Table 5.23. The Young's modulus E is fully correlated over the deck. The yield stress of the bridge deck is supposed to be fully correlated in areas of 300 * 300 mm^2 (see Figure 5.15: Random field mesh of bridge deck). The thickness of the plate is fully correlated in the length direction of the troughs.

The correlation between two areas for both deck plate thickness and yield stress is expressed by the correlation length a = 1.4 m (eq. 5.4). There is no correlation between the stochastic parameters (for example between yield stress and thickness). The troughs are supposed to have deterministic geometric and material parameters. The total number of stochastic parameters equals 32 (24 times yield stress, 6 times plate thickness, one Young's modules and one force).

The ultimate limit state (yielding in any part of the deck) equals:

$$g = \min(f_y - \sigma_{x,y}) \tag{5.13}$$

The limit state function can be seen as a series system of all separate elements to fail. The system reliability is computed instantly by the DARS procedure.

Table 5.24: Results of the bridge deck (n = 32).

		ADI	DARS $\lambda_{add}=1.1$	DARS $\lambda_{add}=3.0$	DS
Results	$\mu(\beta)$	2.06	2.73	2.45	2.41
	β_{low}-β_{upper}	(1.74 - ∞)	2.61 - 2.91	2.30 - 2.72	2.29 - 2.60
	λ_{min}	4.21	4.21	4.21	4.21
	$\beta_{RS,FORM}$	2.93	3.00	2.92	2.54
Samples	LSFE	83	83	150	2701
	samples	62	1366	939	939
Computer	hh:mm	02:23	02:27	04:07	69:23

Table 5.25: Results of the bridge deck with correlated t and σ (n = 4).

		ADI	DARS $\lambda_{add}=1.1$	DARS $\lambda_{add}=3.0$	DS
Results	$\mu(\beta)$	3.57	2.82	2.83	2.82
	β_{low}-β_{upper}	(3.28 - ∞)	2.65 - 3.20	2.65 - 3.21	2.65-3.21
	λ_{min}	4.20	2.75	2.75	2.75
	$\beta_{RS,FORM}$	2.98	2.25	2.25	2.51
Samples	LSFE	12	46	70	343
	samples	8	181	181	181
Computer	hh:mm	0:22	1:28	2:09	9:46

The results are shown in Table 5.24. According to crude directional sampling, the result is a reliability index $\beta = 2.4$, DARS(3.0) leads to the correct result using 8 % of the samples used by crude directional sampling. DARS(1.1) leads to an incorrect result.

The difference between λ_{min} and the reliability index β is rather high. The difference between $\lambda_{min} = 4.21$ and $\beta = 2.38$ means a difference in probability of failure by a factor 67. The failure of the troughs may be a series system. A factor 67 in failure probability can not be explained by this series system only. Maybe the found distance λ_{min} is not the real minimum.

The wheel load is the main stochastic parameter, according to FORM analysis subsequent to the DS procedure ($\alpha = 0.73$). Next important influence factor is the thickness of the deck plate near the wheel load area ($\alpha = 0.48$).

To analyse the random field effects of σ and t, the bridge deck is reanalysed with fully correlated σ and t variables. This means only four random variables remain: E, t, σ and F. The results are presented in Table 5.25. The full correlation between t and σ leads to an increase of the reliability index from $\beta = 2.4$ to $\beta = 2.8$. The difference is such that the effect of random fields can not be neglected.

5.4.2 Cable-stayed bridge

A cable-stayed bridge, designed in a level I manner is analysed. The design of this cable-stayed bridge is published in [Boe99]. A side-view of the cable-stayed bridge structure is given in Figure 5.16. The width of the bridge deck is 17 m, four traffic lanes of 3.25 m each and two maintenance lanes of 2 m width each. All supports are assumed to be springs, representing the soil's stiffness.

The cross-section of the main span has a composite character. The 148.4 m main span is build up with a beam grid of steel and is subdivided in sections with a length of 14.5 meter. Each bridge deck section consists of two main girders and four cross beam girders.

On top of the beam grid lies a concrete slab with a thickness of 0.25 m. The main girders have a centre to centre distance of 13 meter. The cross beam girders on both sides of the connection between the stay cable and the bridge deck are heavier then the other two cross beam girders of the section. Finally, the pylon is made out of concrete. The cable to deck connection is 1 m outside the centreline of the main girder. At this point, a rather rigid grid has been used to distribute the cable force into the bridge deck.

Figure 5.16: Side-view cable-stayed bridge.

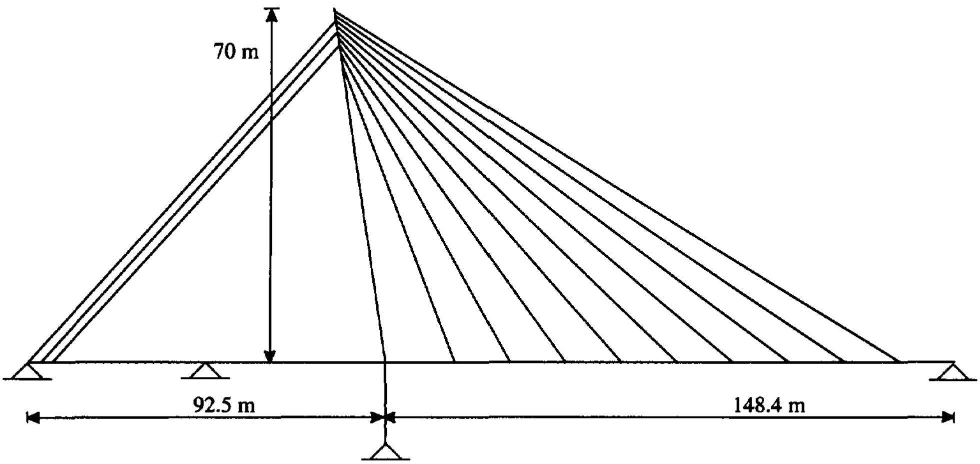

Figure 5.17: 3-D model.

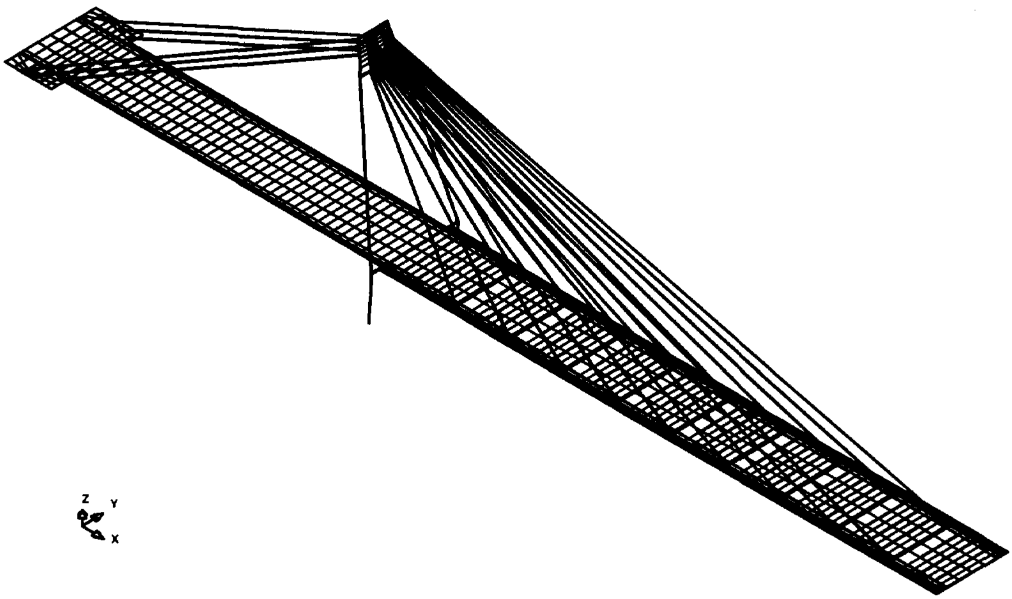

A 3-D FE model is presented in Figure 5.17. The model is such that global structural behaviour can be described. Local limit states such as local collapse of the bridge deck can hardly be described with this model.

The thickness of the concrete deck and Young's moduli of steel and concrete are random variables. Besides, the prestress force of the cables and material properties of the concrete pylon and pylon footing are random variables. The vertical supports under the bridge are modelled as springs. The random character of the soil stiffness is translated into random spring stiffness.

The stochastic properties are summarised in Table 5.26. Most geometric and material parameters are derived from [Vro87]. The traffic loads on the bridge are derived from [Vro93] and multiplied with a dynamic increment factor $\varphi = 1.1$. The traffic load is defined per lane on the main and side spans. This way both the torsion and the in plane bending of the bridge are automatically included.

The ultimate limit state is overstressing of either the cables, the steel girders or the concrete-steel deck:

$$g = \min\{f_{u,sc} - \sigma_{sc}, f_{u,s} - \sigma_{s,} f_{u,c} - \sigma_c) \qquad (5.14)$$

where:

σ_{sc} is the stress in the steel cables

σ_s is the stress in the steel girders
σ_c is the stress in the concrete deck
f_u is the ultimate stress

As mentioned before, the ultimate stress of the cables is supposed to be a random variable. The strength parameters ultimate stress in the 9 cables on the right and in the 3 cables on the left are supposed to be fully correlated. All variables presented in Table 5.26 have a truncated normal distribution. The 3-D model has 67 independent random variables in total. The limit state function can be computed using a linear FE analysis.

Table 5.26: Probabilistic properties of the cable-stayed bridge.

Variable	n	Unit	Mean	St. dev.	Lower bound	Dist	Imp. in ADI
Deck side spans							
$E_{concrete}$	6	N/mm^2	48000	4800	10.	N	-
t (thickness)	5	m	nom.val.	0.1*nom. val.	0.1	N	-
Deck main span							
$E_{concrete}$	3	N/mm^2	48000	4800	10.	N	-
t (thickness)	3	m	0.25	0.005	0.1	N	-
E_{steel}	8	N/mm^2	2.1 10^5	8.4 10^3	0.1	N	-
$f_{u,s}$	1	N/mm^2	397	31.7	0.	N	neg.
Footing pylon							
$E_{concrete}$	1	N/mm^2	38500	4800	10.	N	-
Pylon							
$E_{concrete}$	1	N/mm^2	38500	4800	10.	N	-
Stay cables							
E	1	N/mm^2	1.95 10^5	7.8 10^3	0.1	N	-
Prestress load	19	N/mm^2	nom. val.	0.1*nom. val.	0.0	N	pos.
$f_{u,s}$	2	N/mm^2	1500	100	700		neg.
Supports (springs)							
Vertical translation side span	4	N/mm^2	nom. val.	0.1 * nom. val.	0.5 * nom.val	N	-
Rotation under pylon foot	1	N/mm^2	nom. val.	0.1 * nom. val.	0.5 * nom.val	N	-
Load							
Long span slow lane	2	kN/m	38.0	5.0	0.0	N	-
Long span fast lane	2	kN/m	27.0	3.6	0.0	N	-
Short span slow lane	4	kN/m	39.0	5.6	0.0	N	-
Short span fast lane	4	kN/m	32.0	5.2	0.0	N	-

Table 5.27: Results of the cable-stayed bridge (n = 67).

		ADI	DARS λ_{add} =1.1	DARS λ_{add} =3.0	DS[1]
Results	$\mu(\beta)$	2.02	3.70	3.79	3.05[1]
	β_{low}-β_{upper}	(1.78 - ∞)	3.55 - 4.01	3.70 - 3.90	*2.71 - ∞[1]*
	λ_{min}	5.39	5.39	5.39	5.39
	$\beta_{RS,FORM}$	4.05	4.07	4.08	-
Samples	LSFE	214	229	231	10906
	samples	134	15160	29267	2575
Computer	hh:mm	02:59	03:30	04:10	163:45

[1]*Crude directional sampling has not reached convergence after 7 days of computation*

Table 5.28: Main Influence factors α belonging to $\beta_{RS,FORM}$.

	prestress load	prestress load	$f_{u,sc}$
ADI	+0.31	+0.58	−0.75
DARS(1.1)	+0.54	+0.53	−0.65
DARS(3.0)	+0.53	+0.52	−0.63
DS	-	-	-

The results are shown in Table 5.27. It can be seen that λ_{min} was found in the ADI procedure. The ADI procedure results in β = 2.02. This is the result of 134 samples in the u-space coordinate axis directions. Only three of 134 directions lead to a relatively small distance λ: two of the prestress loads (λ = 7.03 and λ = 7.10) and one strength parameter $f_{u,sc}$ (overstressing the cables) (λ = 5.39). Because of the many non-important directions ($\lambda = \infty$, P_i = 0), the resulting reliability index β becomes relatively low. Supposing that the 3 above mentioned variables are the only important ones, and the rest of the variables are left out, the ADI result would be β = 5.57.

The time needed for crude directional sampling to reach convergence is too long. The computations have therefore been stopped manually after 7 days of computations. At that moment 2575 samples were computed. The crude directional sampling starts in the 134 u-space coordinate axis directions and then explores the random directions. The result after 2575 samples is β = 3.05 (with interval $2.71 < \beta < \infty$). Annex I shows, that this is likely to be a lower bound estimate of β when λ_{min} is found in one of the coordinate axis directions. Excluding the ADI samples from the crude directional samples leads to an expected reliability index β = 5.63. As shown in Annex I, this is likely to be a kind of upper boundary of the reliability index.

DARS(3.0) leads to a reliability index $\beta = 3.79$. In total 29,267 samples (231 LSFE) were used to reach convergence. The result is in line with the crude directional sampling results. DARS(1.1) leads to $\beta = 3.70$, using 15,160 samples (229 LSFE).

The FORM analysis on the response surface (see Table 5.28) shows that only the variables describing the prestress and yield stress of the cables are of importance. The FORM result is the same for ADI and DARS.

Figure 5.18: Most likely deformations near the elastic limit state.

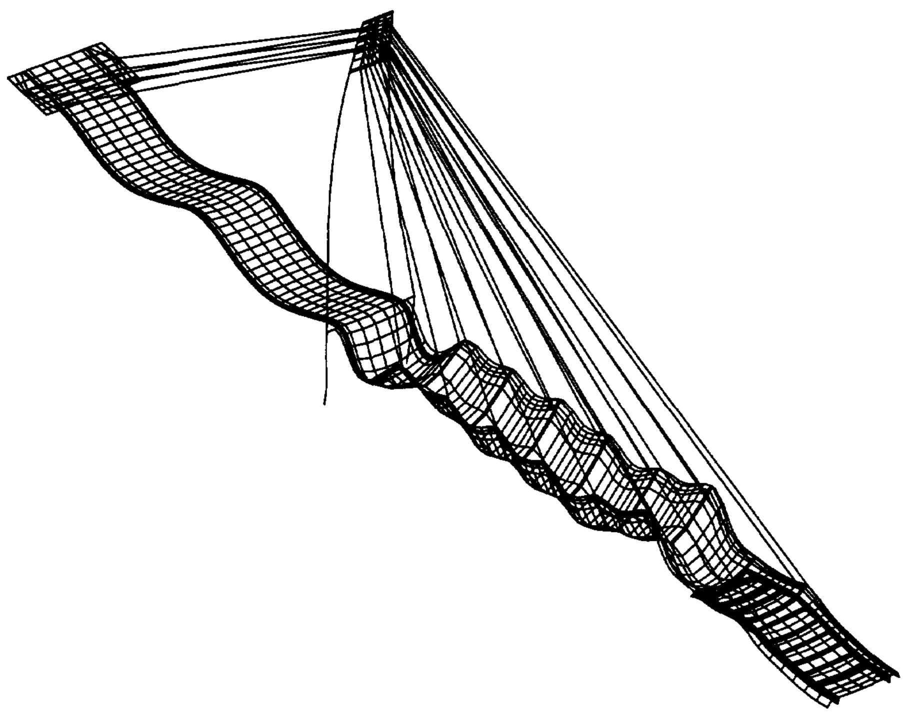

5.5 Soil structures

5.5.1 Asphaltic pavement structure

Most Dutch road structures consist of a top-layer of asphalt, a base of granular material and a subbase of sand. A typical cross-section of a road structure is shown in Figure 5.19. Standard design procedures in the Netherlands calculate the longitudinal strain in the bottom of the asphalt in points A, B and C and compare the maximum longitudinal strain with the ultimate strain. The limit state function is therefore:

$$g = e_u - \max\{\varepsilon_L\} \tag{5.15}$$

where:
e_u is the ultimate strain
ε_L is the longitudinal strain

Figure 5.19: Typical road structure.

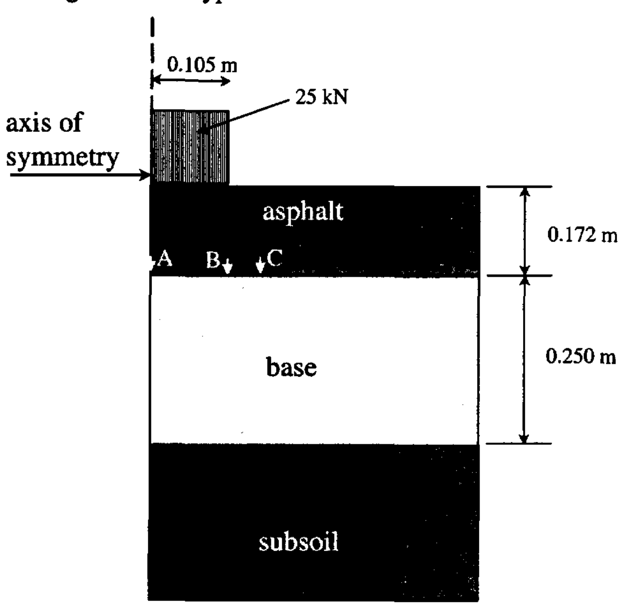

Table 5.29 shows the random variables of the structure. The Young's modulus E varies randomly along the base layer. To investigate the influence of correlation of this Young's modulus, a 3-dimensional model shown in Figure 5.20 is build. The correlation between the value of E at two different locations in the layer is expressed with the following equation:

$$\rho(\Delta x) = \exp(-\frac{|\Delta x|}{\alpha}) \tag{5.16}$$

where $|\Delta x|$ is the distance between the midpoints of two elements in horizontal direction and α a correlation length. In this case α is chosen to be 2 m. The value of the Young's modulus E is supposed to be fully correlated in groups containing elements with midpoints within a horizontal distance of 0.2 m. The Young's moduli in vertical direction are supposed to be fully correlated per layer. Furthermore, all other parameters are supposed to be fully correlated per layer. The total number of random variables n = 86 (E and υ in asphalt and subsoil, and 82 E-moduli in the base layer).

Table 5.29: Input for FEA road structure.

Material	Unit	Mean	St.dev.	Lower bound	Upper bound	Distribution type	Imp. in ADI
Asphalt							
E	N/mm^2	7950	3180	0.1		Truncated normal	-
υ	-	0.35	0.175	0.00	0.49	Beta	-
e_u	m/m	250 10^{-6}	75 10^{-6}		-	Lognormal	neg.
Base							
E	N/mm^2	400	160.	0.1		Truncated normal	-
υ	-	0.35	0.175	0.00	0.49	Beta	-
Subsoil							
E	N/mm^2	100	40	0.1		Truncated normal	-
υ	-	0.35	0.175	0.00	0.49	Beta	-

Two variants have been analysed to research the influence of the correlation of the Young's moduli in the base layer:

1. Fully correlated over the layer.
2. Random field (eq.(5.16)).

The crude directional sampling results, presented in Table 5.30 and Table 5.32, clearly show that the correlation type of the stiffness of the base has only little influence on the probability of failure.

Figure 5.20: 3-dimensional FE mesh.

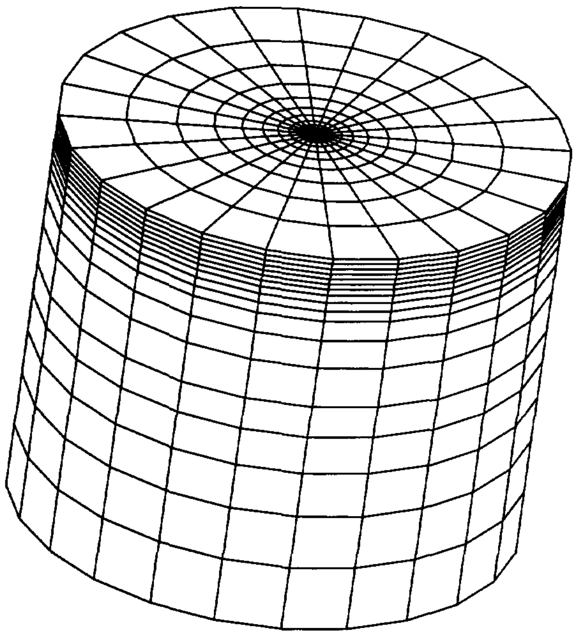

The DARS results for the partly correlated base case are not very good compared to the crude directional sampling results. Crude directional sampling (DS) finds $\beta = 2.14$ where DARS(3.0) finds $\beta = 1.85$. The DS result is not even within the confidence interval of DARS, although the confidence intervals do overlap.

Maybe the number of samples is chosen too low. The sampling continues until sufficiently low $V(\beta)$. The number of samples is approximately ten times the number of random variables only. This number of samples may be too low to be sure that the estimate of β is normally distributed (see section 2.3.4).

There may also be a problem with the handling of the correlation. As discussed in section 2.1, the result of the reliability method may depend on the arrangement of the eigenvectors. In this case, one variable is highly important while the others strongly depend on this main variable. When the arrangement is unfavourable with respect to the FE response, the ADI procedure will effect that only this main variable is important, and the others totally unimportant. The DARS can only correct this situation after very many samples. Before this, the convergence to $V(\beta) < 0.05$ is reached. Consequently the DARS procedure results in a too low reliability index, because some directions are supposed to be non-important, where in fact however they may give a small contribution.

Table 5.30: Results of the asphaltic pavement structure with fully correlated Young's modulus in the base layer (n = 7).

		ADI	DARS λ_{add} =1.1	DARS λ_{add} =3.0	DS
Results	$\mu(\beta)$	1.81	2.26	2.19	2.29
	β_{low}-β_{upper}	(1.40 - ∞)	2.06 - 2.63	2.01 - 2.50	2.17 - 2.54
	λ_{min}	2.52	2.52	2.52	2.52
	$\beta_{RS,FORM}$	1.41	2.21	2.19	2.09
Samples	LSFE	40	480	917	1015
	samples	14	240	240	240
Computer	hh:mm	02:58	48:03	60:43	66:17

Table 5.31: Influence factors belonging to $\beta_{RS,FORM}$.

	Asphalt			Base		Subsoil	
	E	υ	e_u	E	υ	E	υ
ADI	–0.98	–0.05	–0.17	–0.06	+0.01	–0.00	–0.01
DARS(1.1)	–0.70	–0.18	–0.68	–0.09	–0.01	–0.03	–0.05
DARS(3.0)	–0.67	–0.16	–0.69	–0.17	–0.03	–0.11	–0.00
DS	–0.86	–0.18	–0.43	–0.17	–0.10	–0.05	–0.00

Table 5.32: Results of the asphaltic pavement structure with partly correlated random field Young's modules in the base layer (n = 86).

		ADI	DARS λ_{add} =1.1	DARS λ_{add} =3.0	DS
Results	$\mu(\beta)$	2.27	1.67	1.85	2.14
	β_{low}-β_{upper}	(1.40 - ∞)	1.59 - 1.77	1.70 - 2.06	2.03 - 2.28
	λ_{min}	2.52	2.52	2.52	2.52
	$\beta_{RS,FORM}$	1.62	1.69	1.62	1.84
Samples	LSFE	552	603	552	2421
	samples	174	816	624	835
Computer	hh:mm	38:50	46:49	55:58	248:57

5.5.2 Installing sheet pile

The installation of a sheet pile wall is a good example of a geotechnical construction. This example will show a number of typical soil mechanic aspects. A calculation is selected with a fictitious, but for the Netherlands normal, soil profile. After the first excavation, followed by a water level reduction, the ground anchor is installed. A second excavation and water level reduction follows. Finally, the surface load is placed. Figure 5.21 gives an overview of the situation. The limit state is global instability during construction and in the final situation. The steel elements such as sheetpile and anchor are supposed not to fail.

This example gives the opportunity to check the possibility to use the probabilistic calculations for:

- Drained and undrained soil,
- Phased analysis and interfaces (DIANA FEA options),
- Excavation and lowering the water level.

Figure 5.21: Overview of the sheet pile installation.

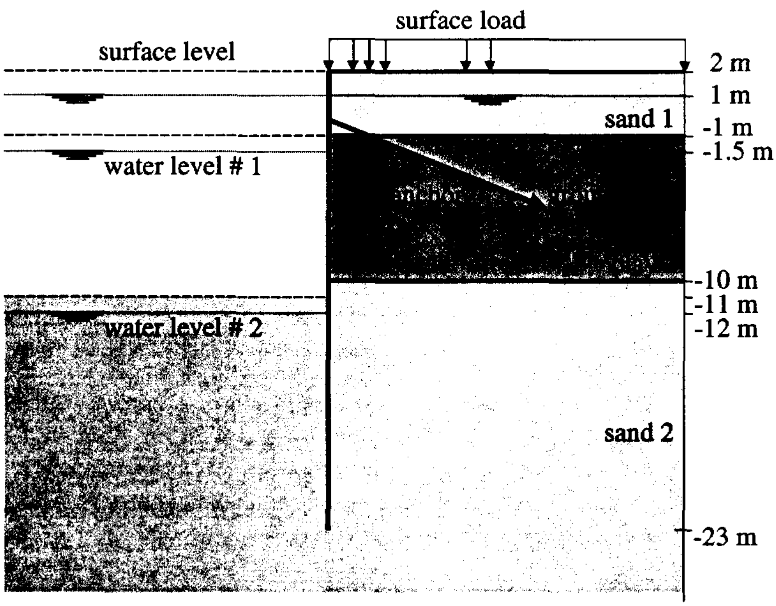

The main stochastic variables describe the soil behaviour. The soil is supposed to have a Mohr-Coulomb failure mechanism. Parameters of this mechanism are the cohesion c and friction angle φ. The Young's moduli and densities are random variables. The random variables are supposed to be fully correlated per layer. The friction between the soil and sheetpile is modelled with interface elements. The friction is described via a cohesion c and friction angle φ. There is no correlation between these friction parameters and Mohr-Coulomb parameters of the soil. The stochastic parameters are presented in Table 5.33.

Table 5.33: Stochastic parameters of the sheet pile installation model (n=19).

Material	Property	Unit	Mean	St.dev	Lower bound	Distribution type
Sand 1	c	N/m^2	1.0	0.2	0	Lognormal
	$\sin(\varphi)$	-	0.5	0.05	0	Lognormal
	γ	kg/m^3	18.0	0.9	-	Normal
	E	kN/m^2	17.5	2.0	1.9	Shifted lognormal
sand 1 interface	c	N/m^2	0.63	0.06	0.1	Shifted lognormal
	$\tan(\varphi)$	-	0.364	0.036	0.01	Shifted lognormal
clay	c	N/m^2	8.0	1.6	0	Lognormal
	$\sin(\varphi)$	-	0.342	0.0342	0	Lognormal
	γ	kg/m^3	16.0	0.8	0.1	Normal
	E	kN/m^2	3.0	2.0	1.9	Shifted lognormal
clay interface	c	N/m^2	3.876	0.4	0.1	Shifted lognormal
	$\tan(\varphi)$	-	0.176	0.01	0.01	Shifted lognormal
sand 2	c	N/m^2	1.0	0.2	-	Lognormal
	$\sin(\varphi)$	-	0.574	0.0574	-	Lognormal
	γ	kg/m^3	18.0	0.9	0.1	Truncated normal
	E	kN/m^2	35.0	2.0	1.9	Shifted lognormal
sand 2 interface	c	N/m^2	0.61	0.06	0.1	Shifted lognormal
	$\tan(\varphi)$	-	0.424	0.04	0.01	Shifted lognormal
Surface	Load	N/m^2	40.	10.	0	Lognormal

Table 5.34 shows the results of the full probabilistic analysis. The table shows a reasonably good result. The error in β in terms of percentage is rather high. DARS(3.0) leads to an error of 15 % in β. The error using $\lambda_{add} = 1.1$ is even higher. There is no clear explanation why these errors occur. In absolute sense there is only a small difference between DS and DARS.

As such, the reliability index is rather low. The main failure mechanism is collapse, because of a low density of the "sand 2" layer combined with a high surface load. The most likely failure mode is shown in Figure 5.22.

Table 5.34: Results of the sheet pile.

		ADI	DARS $\lambda_{add} = 1.1$	DARS $\lambda_{add} = 3.0$	DS
Results	$\mu(\beta)$	1.62	1.95	1.32	1.46
	β_{low}-β_{upper}	1.29 -	1.84 - 2.10	1.19-1.47	1.35 - 1.62
	λ_{min}	2.29	2.30	2.30	2.30
	$\beta_{RS,FORM}$	2.07	2.02	1.87	1.95
Samples	LSFE	75	75	193	600
	samples	38	400	182	212
Computer	hh:mm	00:11	11:30	26:41	67:16

Figure 5.22: Finite element mesh of the structure in the most likely failure mode.

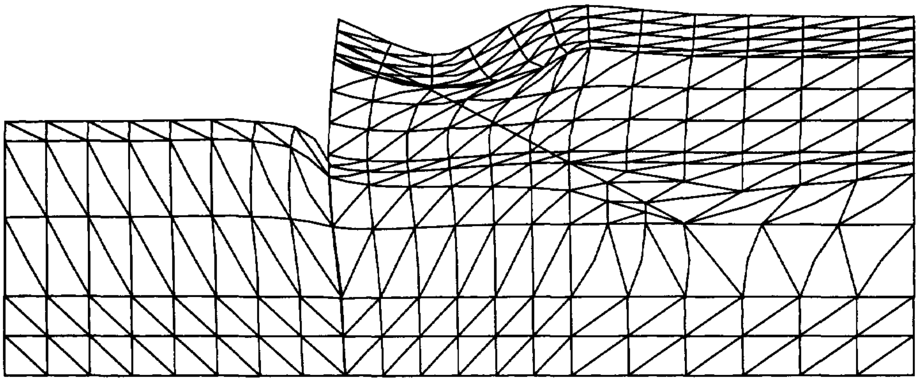

5.6 Summary of DARS applied to structural reliability

In the previous sections, the reliability of several structures has been calculated by means of the DARS procedure. The applications can be divided in:

- Beams: small structures with complex non-linear structural behaviour;
- Frames: small structures with system behaviour;
- Bridges: large structures with many stochastic variables and complex linear structural behaviour;
- Soil structures: large structures with complex non-linear structural behaviour, many stochastic variables and system behaviour.

Two versions of the DARS procedure have been used:

1. DARS(1.1): An additional distance $\lambda_{add} = 1.1$ is used. This leads to a fast version with lower accuracy
2. DARS(3.0): An additional distance $\lambda_{add} = 3.0$ is used, leading to more LSFE and therefore being slower. On the other hand a higher accuracy is expected.

Most cases, described in the previous sections, showed that an additional distance $\lambda_{add} = 1.1$ did not lead to a sufficient accurate result. Increasing the additional distance to $\lambda_{add} = 3.0$ improved the performance of DARS such that it does comply with the required accuracy.

The performance with respect to efficiency can be expressed by the number of LSFE. This number of LSFE is summarised in Table 5.35. Besides, for the sake of comparison with other reliability methods, the number of LSFE per variable (LSFE/n) is summarised. The number of LSFE is presented graphically in Figure 5.23 as a function of the number of random variables n. For the sake of completeness, the required number of LSFE according to section 2.3.5 (N = 160 n) is visualised in Figure 5.23 as well. It is supposed that, on average, 3 LSFE per sample are required. Consequently the number of LSFE equals 3 160 n = 480 n.

Figure 5.23: Number of LSFE as a function of the number of variables.

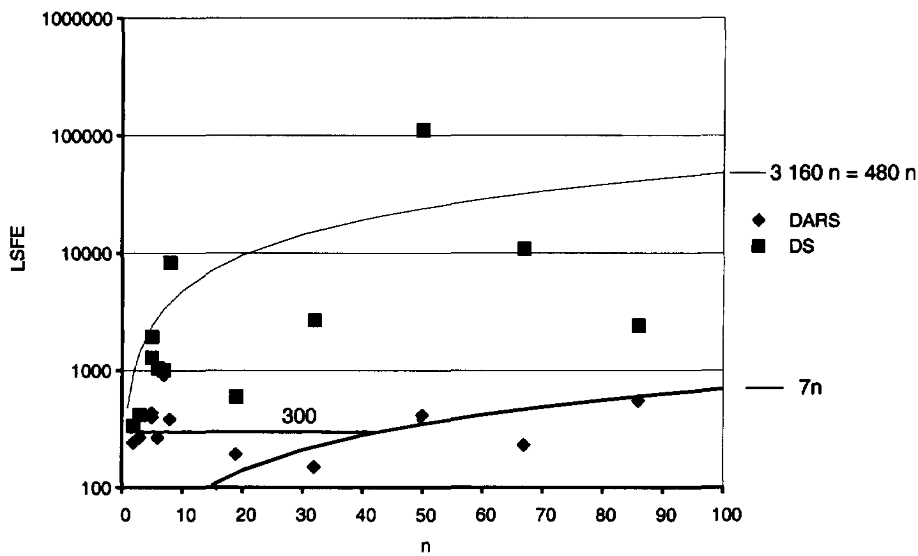

Figure 5.23 shows that the number of LSFE for DARS is hardly influenced by the number of variables. The required number of LSFE is approximately equal to LSFE = 300. For low dimensional problems, DARS has little advantage over crude directional sampling. This can simply be explained by the fact that nearly all directions have importance for low dimensional problems. For high dimensional problems only few directions are likely to have importance. For these problems, DARS performs much better than crude directional sampling.

The number of LSFE in the starting procedure (ADI) grows linear with the number of random variables. As a result it can be expected that the number of LSFE required by DARS grows with the number of random variables as well. Performing a straight line fit on the LSFE required by DARS ($n > 10$) leads to a mean number of LSFE equal to LSFE = 7 n.

Table 5.35: Summary of efficiency of DARS(3.0).

Structure	Case	type of analysis[1]	n	DS	DARS(3.0)	
				LSFE	LSFE	LSFE/n
Beams	Simply supported	F	5	1294	435	87
	Random Young	L	50	111299*	417	8
	Stüssi-Kollbrunner	F	5	1950	399	80
	Central buckling	GF	8	8315	385	48
Frames	1-storey, 1-bay	F	2	339	242	121
	1-storey, 2-bay	F	3	422	269	90
	2-storey, 2-bay	F	6	1053	267	45
Bridge	Deck	L	32	2701	150	5
	Cable stayed	L	67	10906	231	3
Soil	correlated	L	7	1015	917	131
	random base	L	86	2421	552	6
	Sheetpile	FP	19	600	193	10

* *Convergence not reached*

[1]: *type of analysis:* *L = Linear,*
G = Geometrically non-linear,
F = Physically non-linear,
P = Phased analysis

6. Retrospective view

The computation of the structural reliability with sufficient accuracy within a minimum of computational time is the main aim of this thesis. The evaluation of the limit state function by means of an FEA computation uses the most computational time. Emphasis is therefore laid on the minimisation of the number of Limit State Function Evaluations (LSFE). In this chapter it will be discussed how Directional Adaptive Response surface Sampling (DARS) performs in comparison with other reliability methods. Besides some thoughts will be given on how the performance of DARS can be improved. Finally some considerations are given how the results of the cases in chapter 5 impact other reliability methods.

6.1 FORM or DARS

Level II reliability methods like FORM are, in general, much more efficient than level III methods like Monte Carlo and Directional Sampling. Furthermore the level II FORM procedure is generally regarded as state-of-the-art. In chapter 4 it was concluded that FORM performs very well at component level. FORM is not fit to perform structural reliability studies if a system's reliability is to be computed that is not recognised by the user. For some cases FORM results in an incorrect answer without error message. FORM can therefore not be used when knowledge on the probabilistic behaviour of the structure is not present. The question arises whether FORM is to be preferred above the DARS procedure when preknowledge is available.

The advantage of a level III procedure is that a system's reliability is computed at once. The disadvantage of Monte Carlo sampling procedures is that never a final reliability index is computed but an expected reliability index with confidence intervals. Since DARS is a kind of Monte Carlo sampling, this means that repeating the DARS procedure might result in a slightly different answer.

The crucial question is whether FORM or DARS is the fastest for the computation of a system's reliability. The speed of the procedure in combination with FEA can be expressed in the number of LSFE. Supposing that a component reliability is to be computed, then FORM (numerical gradient) requires k(1+n) LSFE, where k is the number of iterations.

The examples in chapter 5 (summarised in Table 5.35) show that DARS (for high dimensional problems) uses a number of LSFE between 3 n and 8 n, with an average of 7 n. The examples in chapter 1 show that FORM uses approximately the same number of LSFE. DARS and FORM are therefore considered equally efficient on component level.

It may thus be concluded that DARS computes a systems reliability and FORM a component reliability in the same computational time. When a systems reliability is requested and carried out with FORM it has to be kept in mind that the number of LSFE increases considerably and bounds of the reliability index are computed instead of the 'exact' value.

A disadvantage of level III methods compared to FORM is that no design-point is computed. The design-point found in FORM gives insight in the influence of the various random variables on the limit state function. Level III methods only give a point where the minimum distance from origin to the limit state function is found. When using an infinite number of simulations, this 'minimum distance point' is the same as the FORM design-point. In practise, there are a limited number of simulations and as a result the 'minimum distance point' can differ from the FORM design-point. On the other hand, the usefulness of a FORM design-point is dubious where systems behaviour is at hand.

Most cases in chapter 5 show that the minimum distance point is found in the starting procedure (ADI). This way only the most important variable is identified. The influence of the other variables is less but unknown.

Carrying out the FORM procedure on the final response surface gives some insight into the important variables. Several examples in chapter 5 show a reliability index resulting from FORM on the response surface, which is not corresponding with the real probability of failure (found by DS). The influence factors can only be trusted when the FORM reliability index corresponds with the real probability of failure.

FORM uses far less LSFE for low dimensional cases compared to DARS. When a systems reliability is not at hand and the number of variables is less than 10 ($n < 10$), then FORM is to be preferred above DARS.

6.2 DARS compared to level I design procedures

The DARS procedure is of course less efficient in checking the structural reliability than code type level I procedures. It should however be pointed out that the case studies performed in chapter 5 show that the reliability of structures designed by a code type level I procedure is either higher or lower than required. The code type level I procedures can only be used to give an impression of the goodness of an average structure with respect to its reliability requirements.

It is expected that a full level I procedure makes it more likely that the structure meets its reliability requirements. The number of limit state function evaluations within the full level I procedure is approximately equal to three times the number of random variables. The DARS method approximately uses seven times the number of variables to compute the structural reliability. At approximately two times the computational effort of a full level I procedure, the DARS procedure computes an accurate structural systems reliability automatically.

Level I design methods can hardly take random fields into account. In chapter 5, in three cases, the influence of random fields instead of fully correlated variables is analysed. The results of these cases are summarised in Table 6.1 below.

Table 6.1: Summary of random field cases.

case	section	β	
		random field	fully correlated
I-Beam with random Young's modulus	5.2.2	2.3	3.9
Orthotrope bridge deck	5.4.1	2.4	2.8
Asphaltic pavement structure	5.5.1	2.1	2.3

The influence of taking the random fields into account on the reliability index largely depends on the correlation between the variables at two different locations. For the orthotrope bridge deck and asphaltic pavement structure, some best guess correlation functions were used. The effect of the correlation on the reliability index for these two cases is moderate. The effect is however such that the influence of the random fields should not be neglected.

The reliability of the "I-Beam with random Young's modulus" case was computed with an unrealistic low correlation between elements. As a result the influence of the random field on the reliability index is rather high. Contrary to the other two cases a parallel system (intersection) is at hand. The reliability index of the system of elements is higher than the fully correlated case. Forgetting the randomness in level I design procedures is therefore a conservative choice for this case.

6.3 Possible Improvements to the DARS procedure

In chapters 4 and 5 some improvements to the DARS methods were suggested, which are not implemented in the pilot version of the FEA software. In this section these suggestions are completed.

Response surface

The building of the initial response surface takes the main part of computational time. The quality of this response surface is essential for the quality of the directional sampling result. The examples shown in chapters 4 and 5 are based on a response surface fit in u-space. For some variables and distributions a response surface in x-space may perform better. Maybe the fit should be performed in both spaces separately and the minimum distances from both response surfaces should be used. Sometimes a linear response surface performs best, sometimes a quadratic or even higher polynomial function is better. An optimal response surface procedure is still to be found.

Non-linear FEA computations

The efficiency of the ADI (and DARS) can be improved by combining the iteration procedure in non-linear FEA and search for λ (section 3.2.4). This way one LSFE is required for every directional sample. This makes the number of LSFE equal to N. The computational time per LSFE will increase compared to the original time. The time needed depends on the iteration procedures in the FE code. It will however be far less than the computational time needed for the separate iterations of FEA and λ search.

Collapse is in most cases the essential ultimate limit state. This limit state can only be investigated when using (geometrically and) physically non-linear behaviour. Whether or not the structure collapses is investigated by means of convergence or divergence of the non-linear computations. This is a simple but costly (with respect to the computational time) method. The stability of the structure may be computed by means of eigenvalues as well.

Correlated fields

The calculation of the reliability where a correlated field is applicable gives problems in the use of a response surface. Chapter 3.2 showed the example of the asphalt structure where the DARS results for the partly correlated base did not compare well with the crude directional sampling results. This was probably due to the handling of the correlation. As discussed in section 5.5, the result of some reliability techniques (FORM and methods using Response Surfaces) may depend on the arrangement of the eigenvectors. When the arrangement is unfortunate with respect to the FE response, the ADI procedure will effect that only one variable is important, and the others relatively unimportant. The arrangement of eigenvectors should be improved in such a way that all variables get approximately the same importance in the ADI procedure.

ADI reliability estimate

Some examples in chapter 5 show that the ADI results differ very much from the final result. This is because the ADI procedure takes only a few samples. This difference ocuurs especially when only few of the random variables are really important to the limit state. An improvement may be to base the confidence levels of ADI only on the important variables

FORM performed on the response surface

The examples in chapter 5 show that a FORM procedure on the final response surface does not always lead to a good reliability index. This is due to the fact that samples in unimportant regions influence the response surface. Standard in DARS, all samples are given the same weight. For the purpose of a FORM analysis, the response surface can be improved by giving more weight to samples in important regions (samples with a low distance λ).

The FORM analysis on the response surface results in a direction, which leads to the minimum distance to the limit state (according to the response surface). After finishing the DARS procedure and the FORM analysis, the response surface may be improved by the FORM sample. Repeating the DARS procedure with this new response surface may lead to a better estimate of the probability of failure at cost of only a few extra computations.

ADI samples used in the DARS result

In chapter 3 (section 3.3.2) it was stated that, since every sample contributes, ADI samples are not to be excluded from the DARS result. In Annex I it was discussed that the ADI samples can be included in the reliability estimate calculation when all random variables are equally important to the limit state function. If the ADI results are added when only one variable is important and the other variables are totally unimportant to the limit state function, then the reliability index is underestimated.

The results in chapter 5 give the impression that often one of the u-space coordinate axis direction samples leads to the minimum observed distance from origin to limit state. When all other axis lead to an infinite distance λ, then an underestimated reliability estimate can be expected.

The cases presented in chapter 5 show that there is not just one important variable only, but also many less important variables too. In that case, it is expected that the error in the estimate is small.

Additional distance to be used in DARS

In this thesis, the additional distance λ_{add} is chosen to either 1.1 or 3.0. The additional distance should be higher when a relatively bad response surface is fit to the data (FEA response). The parameter ε_λ is a measure for the goodness of the fit and can be used to adjust the additional distance λ_{add} to be used.

6.4 Impact on other reliability methods

Impact on Level I and II applications

Most examples in chapter 5 show that the ADI procedure finds the minimum distance λ_{min}. After many more samples, DARS can not find a lower distance or finds only a slightly lower distance.

Since ADI nearly always leads to λ_{min}, level I methods can be performed in the u-space coordinate axis directions instead of the now used intermediate directions. The α values will be for instance $(0, 0, \ldots, \pm\beta, \ldots, 0)$ instead of $(\pm0.7\beta, \pm0.7\beta, \ldots\ldots, \pm0.7\beta)$.

In higher dimensional space, the search option in the coordinate axis directions requires 2 n LSFE as a maximum, instead of the approximate 3 n computations (see section 2.7).

Standard Response Surface approaches

The standard response surface approaches [Far89], [Buc88b] are mostly based on less LSFE than used in this thesis for the response surface (RS) in ADI. The resulting β_{RS} of ADI is, in most cases shown in chapter 5, inaccurate. The result of the standard response surface approaches has to be even worse.

Monte Carlo sampling

Section 2.3.1 concluded that crude Monte Carlo sampling is preferred above crude directional sampling for high dimensional cases ($n > 200$). The number of LSFE for Monte Carlo sampling is equal to the number of samples: $N = 3/ P_f$. For structural reliability, where $\beta \approx 4$, this means $N \approx 10^5$. The number of LSFE used by DARS is equal to approximately 7 n. Crude Monte Carlo sampling is preferred to DARS when $n > 10^5/7 \approx$ 14,000. In practise this means that Crude Monte Carlo analysis will never be preferred to DARS.

Improving Monte Carlo sampling with importance sampling suggested in section 2.4, leads to a required number of samples equal to approximately 300 n. The only requirement is that the outcome of the reliability index is approximately known. Since Monte Carlo sampling uses only one LSFE per sample, Monte Carlo importance sampling is preferred above crude directional sampling (using LSFE = 480 n).

Monte Carlo analysis may be improved with an (adaptive) sampling procedure (DARS alike) as well. The number of samples needed for this procedure is probably comparable with the number of LSFE needed for the DARS procedure. This idea is not elaborated in this thesis.

7. Conclusions

The computation of the structural reliability with sufficient accuracy within a minimum of computational time is the main aim of this thesis. Addionally, the effort of implementation in standard FE codes should be minimal and the method should be such that it can be used without prior knowledge of the probabilistic and system behaviour of the structure.

Using probabilistic method tools like DARS or FORM in combination with FEA has the intrinsic danger that they are used without knowledge of the physical behaviour of a structure as well. It is obvious that a probabilistic FEA will only find failure mechanisms that are potentially modelled with FEA. Other mechanisms will not be found nor will the probabilistic FEA show what failure mechanisms are missed. This warning seems superfluous but can, on the other hand, not be repeated enough.

The evaluation of the limit state function by means of an FEA computation uses the most computational time. Emphasis is therefore laid on the minimisation of the number of Limit State Function Evaluations (LSFE).

Three standard level III methods have been analysed with respect to efficiency under constraint of sufficient accuracy. It is concluded that the Numerical Integration (NI) method is preferred for reliability problems with very few stochastic variables ($n < 5$). Crude Monte Carlo sampling (MC) is preferred when the number of variables $n > 200$. For cases $5 < n < 200$ crude Directional Sampling (DS) is preferred. Besides it is concluded the adaptive MC sampling technique included in the COMREL software package may not result in the correct answer. A Monte Carlo importance sampling technique where the variance of variables is increased is to be preferred above crude Monte Carlo sampling and is equally efficient as crude directional sampling (when the resulting reliability index is approximately known on forehand). As a result there is no preference for either procedure.

Level II reliability methods (FORM/SORM) are, in general, much more efficient than level III methods. The disadvantage of level II methods is that they can only be applied directly when system effects are absent. If it is beyond doubt that system effects are absent then level II methods are highly preferred above level III methods because of efficiency.

The investigation into the system reliability can be carried out using, for instance, the Branch-and-Bound method. Much of the advantage of the level II methods with respect to efficiency is lost when using this method.

Two new reliability methods were proposed in this thesis, both based on an adaptive response surface: FORM-ARS (FORM on an adaptive response surface) and DARS (Directional Adaptive Response surface Sampling). Both reliability methods were first tested on artificial limit state functions.

FORM-ARS is in most cases performing better on efficiency than the standard FORM procedures. FORM has the disadvantage that it can not handle a limit state function in which system effects are included. In structural reliability it is likely that there are system effects. Since FORM can not recognise these, it is concluded that a level III method is more appropriate for the aims of this thesis. Based on the performance (accuracy and efficiency) on artificial limit state functions, the best performing of the level III methods is DARS.

The DARS procedure has been implemented in a pilot version of the existing FE code DIANA. Several structures, common in civil engineering practise have been analysed. The performance of DARS has been compared with crude directional sampling. Examples in chapter 5 showed that the method performs well for both structures with linear and non-linear behaviour. For low dimensional problems there is little advantage compared to crude directional samples (these problems take little time anyway). The benefit of the DARS method increases with increasing number of random variables.

As such the Directional Adaptive Response surface Sampling (DARS) method serves its purpose. The computation of the reliability index requires no prior knowledge of the probabilistic and system behaviour of the structure. The method can easily be implemented in standard FEA code since it uses only deterministic FEA computations.

The more random variables, the more samples are required in DARS. Although DARS reduces the number of limit state function evaluations (using FEA) considerably compared to crude directional sampling, an amount of about 7 times the number of random variables remains. The number of limit state function evaluations can be further reduced by the improvements mentioned in this thesis:

- combining the iteration procedure in non-linear FEA and search for λ (section 3.2.3);
- basing the additional distance λ_{add} on the parameter ε_λ (goodness of the response surface, see section 6.3);
- splitting the limit state into a linear-elastic and non-linear (plastic) part (section 3.2.4);

These improvements are expected to decrease the amount of FEA computations approximately to the number of random variables (so for 100 variables, approximately 100 FE computations are required). The time needed to perform these computations lies well below the target mentioned in the introduction of this thesis.

Referenced literature

[Abd90a] Abdo, T., R. Rackwitz, *A new beta-point algorithm for large time-invariant and time variant reliability problems*, 3rd WG 7.5 Working Conf. Berkely, 1990.

[Abd90b] Abdo, T., *Zur zuverlässigkeitsberechnung von statisch beanspruchten Tragwerken mit unsicheren Systemeigenschaften*, Berichte zur Zuverlässigkeitstheorie der Bauwerke, Heft 88/1990, TU München, 1990.

[Au99] Au, S.K., J.L. Beck, *A new adaptive importance sampling scheme for reliability calculations*, Struct. Saf., Vol. 21, No. 2, 1999.

[Bea81] Baecher, G.B., T.S. Ingra, *Stochastic FEM in settlement predictions*, J. Geotech. Eng. Div., ASCE, Vol. 107, No. GT4, 1981.

[Bje87] Bjerager, P., K. Karamchandani, C.A. Cornell, *Failure tree analysis in structural system reliability* in; N.C. Lind, International Conference on Applications of Statistics and Probability in Soil and Structural Engineering (ICASP5); 5th, Vancouver, May 1987.

[Bje88] Bjerager, P., *Probability integration by directional simulation*, J. of Eng. Mech., Vol. 114, No. 8, 1988.

[Bje91] Bjerager, P., *Course on reliability problems: General Principles and Applications in Mechanics of Solids and Structures*, CISM lecture notes, Springer Verlag, 1991.

[Boe99] Boer, A. de, P.H. Waarts, *Probabilistic FE analysis of a cable stayed bridge,* Proceedings of the IABSE conference on Cable Stayed Bridges, Malmö 1999.

[Bog92] Boggs, P.T., R.H. Byrd, J.E. Rogers, R.B. Schnabel, *User's Reference Guide for ODRPACK Version 2.01, Software for Weighted Orthogonal Distance Regression*, NISTR report 92-4834, 1992.

[Bor96] Borri, A., E. Speranzini, *Numerical procedure for optimal design with prefixed reliability level*, Proceedings of the 7th IFIP WG 7.5 Conference of Reliability and Optimisation of Structural Systems, Boulder, Colorado, 1996.

[Bor97] Borri, A., E. Speranzini, *Structural reliability analysis using a standard deterministic finite element code*, Structural Safety, Vol. 19, No. 4, 1997.

[Box78] Box, G.E.P., W.G. Hunter, J.S. Hunter, *Statistics for experimenters, An introduction to design data analysis and model building,* John Wiley & Sons, 1978.

[Bou95] Bouyssy, V., R. Rackwitz, *On conditional sampling to assess the reliability of dynamic offshore,* in: M. Lemaire et al. eds, International Conference on Applications of Statistics and Probability in Soil and Structural Engineering (ICASP7); 7th, Paris, July 1995.

[Bre84] Breitung, K., *Asymptotic approximation for multinormal integrals,* J. Eng. Mech. ASCE 110, 1984.

[Bri91] Brinkgreve, R.B.J., H.L. Bakker, *Non-linear finite element analysis of safety factors*, Proceedings of the seventh international conference on computer methods and advances in geomechanics, Vol. 2, 1991.

[Buc88a] Bucher, C.G., *Adaptive sampling – an iterative fast Monte Carlo procedure*, Struct. Saf, Vol. 5, No. 2, 1988.

[Buc88b] Bucher, G.C., Y.M. Chen, G.I. Schuëller, *Time variant reliability analysis utilising Response Surface approach*, Proceedings of the 2nd IFIP WG 7.5 Conference of Reliability and Optimisation of Structural Systems, 1988.

[Buc90] Bucher, C.G., U. Bourgund, *A fast and efficient Response Surface approach for structural reliability problems*, Struct. Saf, Vol. 7, 1990.

[Buc97] Bucher, G.C., *Some recent software developments for stochastic structural analysis Surface approach*, in: proceedings of ICOSSAR '97, Structural safety and reliability, Shiraisa, Shinozuka & Wen, Eds., November 1997, Balkema, Rotterdam, 1998.

[Col96] Colangelo, F., R. Giannini, P.E. Pinto, *Seismic reliability analysis of reinforced concrete structures with stochastic properties*, Struct. Saf., Vol. 18, No. 2/3, 1996.

[Cor69] Cornell, C.A., *A probability-based structural code,* J. of Am. Conc. Inst., Vol. 66, No. 12.

[Dea80] Deak, I, *Three digit accurate multiple normal probabilities*, Num. Math., 35 (1980), 369-380.

[Deo90] Deodatis, G., *Bounds on response variability of stochastic finite element systems,* J. Eng. Mech. Vol. 116, no. 3, 1990.

[Dey98] Dey, A., S. Mahadevan, *Ductile structural system reliability analysis using adaptive importance sampling*, Struct. Saf., Vol. 20, No. 2, 1998.

[DIA98] *Diana User's Manuals*, release 7.1, 1998.

[Dit79] Ditlevsen, O., *Generalized second order reliability index*, J. of Struct. Mech., Vol. 7, No. 4, 1979.

[Dit87] Ditlevsen, O., P. Bjerager, *plastic reliability analysis by directional simulation,* DCAMM report, Technical University of Denmark, Lyngby.

[Dit87] Ditlevsen, O., R. Olesen, G. Mohr, *Solution of a class of load combination problems by directional simulation*, Struct. Saf., No. 4, 1987.

[Dit88] Ditlevsen, O., P. Bjerager, R. Olesen, A.M. Hasofer, *Directional simulation in Gaussian process*, Prob. Eng. Mech., Vol. 3, No. 4, 1988.

[Dit90] Ditlevsen, O., R.E. Melchers, H. Gluver, *General multi-dimensional probability integration by directional simulation*, Comp. & Struct. Vol. 36, No. 2, 1990.

[Dol83] Dolinsky, K., *First-Order Second-Moment approximation in reliability of structural systems: critical review and alternative approach*, Struct. Saf. 1, 1983.

[Eng93] Engelund, S., R. Rackwitz, *A benchmark study on importance sampling techniques in structural reliability*, Struct. Saf., Vol. 12, 1993.

[ENV91] ENV 1991-1: Eurocode 1: Basis of design and actions on structures –Part 1: Basis of design, CEN 1994.

[Fab88] Faber, M., R. Rackwitz, *Excursion probabilities of non-homogeneous gaussian scalar fields based on maxima considerations,* Proceedings of the 2nd IFIP WG 7.5 Conference of Reliability and Optimisation of Structural Systems, 1988.

[Far89] Faravelli, L., *Response Surface Approach for Reliability analysis*, J. Eng. Mech. ASCE, 1150(12), 1989.

[Fra96b] Frangopol, D.M., Y-H. Lee, K.J. Willam, *Nonlinear Finite Element Reliability analysis of concrete*, J. Eng. Mech., dec. 1996.

[Fra96a] Frangopol, D.M., Y. Ide, E. Spacone, I. Iwake, *A new look at reliability of reinforced concrete columns*, Struct. Saf., Vol. 18, No. 2/3, 1996.

[Gha91] Ghanem, R.G., P.D. Spanos, *Stochastic finite elements: A spectral approach,* Springer Verlag, New York, 1991.

[Gie92] Gierlinsky, J.T., J. Holnicki-Szulz, J.D. Sorensen, *Sensitivity analysis of structures by virtual distortion method*, Proceedings of the 3rd IFIP WG 7.5 Conference of Reliability and Optimisation of Structural Systems, 1992.

[Gra98] Graham, L., G. Deodatis, *Variability response functions for stochastic plate bending problems*, Struct. Saf. Vol. 20, No. 2, 1998.

[Gua97] Guan, X.L., R.E. Melchers, *A load space formulation for probabilistic finite elements of structural reliability*, J. Prob. Eng. Mech., Vol. 14, 1998.

[Gua97] Guan, X.L., R.E. Melchers, *Multitangent-plane surface method for reliability calculation*, J. Eng. Mech. Vol. 123, No. 10. 1997.

[Gut94] Gutiérrez, M.A., J. Carmeliet, R. de Borst, *Implementation of finite element reliability methods in DIANA*, DIANA Computational Mechanics '94, (eds. G.M.A. Kusters and M.A.N. Hendriks) Kluwer, Dordrecht, 1994.

[Gut99] Gutiérrez, M.A., *Objective simulation of failure in heterogeneous softening solids,* Dissertation Delft University of Technology, The Netherlands, May 1999.

[Haf85] Haftka, R.T., H.P. Kamat, *Elements of Structural Optimisation*, Martinus Nijhoff Publicers, Dordrecht, 1985.

[Har86] Harbitz, A., *An efficient sampling method for probability of failure calculations*, Struct. Saf. Vol. 3, 1986.

[Has74] Hasofer, A.M., N.C. Lind, *An exact and invariant first order reliability format*, J. Eng. Mech. Div., ASCE, Vol. 100, 1974, p. 111-121.

[Him72] Himmelblau, D.M., *Applied Nonlinear Programming,* McGraw-Hill, New York, 1972.

[His81] Hisida, T., S. Nakagari, *Stochastic finite element method developed for structural safety and reliability,* Proc. 3rd int. conf. on structural safety and reliability, Trondheim, Norway, 1981.

[Hoh82] Hohenbichler, M., *An approximation to the multivariate normal distribution function*, Reliability of structural systems, SFB96, TU München, 1982.

[Hoh87] Hohenbichler, M., S. Gollwitzer, W. Kruze, R. Rackwitz, *New light on First- and second-order reliability methods,* Struct. Saf., Vol. 4, 1987.

[Hoh88] Hohenbichler, M., R. Rackwitz, *Improvement of second-order reliability estimates by importance sampling,* J. Eng. Mech., Vol. 114, 1988.

[ISO98] ISO 2394, *General principles on reliability of structures*, 1998.

[JCSS81] Joint Committee on Structural Safety, *General principles on reliability for structural design*, IABSE, 1981.

[Joh72] Johnson, N.L., S. Kotz, *Continuous multivariate distribitions*, John Wiley & Sons, New York, 1972.

[Jud80] Judge, G.J., W.E. Griffits, R. Carter Hill, T-C. Lee, *The theory and practise of econometrics,* John Wiley, New York, 1980.

[Kar87] Karamchandani, K., *Structural System Reliability Analysis Methods*, Report 83, John A. Blume Earthquake Engineering Center, Stanford University, 1987.

[Kat98] Katsuki, S., D.M. Frangopol, *Advanced hyperspace division method for structural reliability*, in: proceedings of ICOSSAR '97, Structural safety and reliability, Shiraisa, Shinozuka & Wen, Eds., november 1997, Balkema, Rotterdam, 1998.

[Kija92] Kijawatworawet, W., *An efficient adaptive importance directional sampling for nonlinear reliability problems*, Universität Innsbruck, 1992.

[Kiu98] Kiureghian, A. Der, T. Dakessian, *Multiple design points in first and second-order reliability*, Struct. Saf., Vol. 20, No. 1, 1998.

[Kim97] Kim, S-H., S-W. Na, *Response surface method using vector projected sampling points*, Struct. Saf, Vol. 19, No. 1, 1997.

[Kus99] Kuschel, N. R. Rackwitz, A. Pieracci, *Multiple β-points in structural reliability,* in: Computational Stochastic Mechanics, Balkema, Rotterdam, 1999.

[Law87] Lawrence, M., *An introduction into reliability methods,* Computational mechanics of probabilistic and relaibility analysis, Elmepress International, Lausanne, 1989.

[Lem96] Lemaire, M., A. Mohamed, O. Flores-macias, *The use of finite element codes for the reliability of structural system*, Proceedings of the 7th IFIP WG 7.5 Conference of Reliability and Optimisation of Structural Systems, Boulder, Colorado, 1996.

[Lin87] Lin, H-Z., A. Der Kiureghian, *Second-order system reliability using directional simulation*, in: N.C. Lind, International Conference on

Applications of Statistics and Probability in Soil and Structural Engineering (ICASP5); 5th, Vancouver, May 1987.

[Liu86] Liu, W.K., T. Belytschko, A. Mani, *Random field finite elements*, Int. J. Num. Meth. in Eng., Vol. 23, 1986.

[Liu87] Liu, W.K., A.Mani, T. Belytschko, *Finite element methods in probabilistic mechanics*, Prob. Eng. Mech, Vol. 2, No. 4, 1987.

[Liu91] Liu, P-L, A. Der Kiureghian, *Finite Element Reliability of Geometrical Non-linear Uncertain Structures*, J. Eng. Mech. 117(8), 1991.

[Mad86] Madsen, H.O., S. Krenk, N.C. Lind, *Methods of Structural Safety*, Prentice-Hall, 1986.

[Mar98] Marckzyk, J., *Computative stochastic mechanics in a meta-computing perspective*, CIMNE, Barcelona, Spain.

[Mit98] Mitteau, J.C., *Error evaluations for the computation of failure probability in static analysis of structural reliability,* J. Prob. Eng. Mech., Vol. 14, No. 1-2, 1998.

[Moa96] Moarefzadeh, M.R., R.E. Melchers, *Directional Simulation applied to idealized off-shore structures,* Proceedings of the 7th IFIP WG 7.5 Conference of Reliability and Optimisation of Structural Systems, Boulder, Colorado, 1996.

[Moh96] Mohamed, A., F. Suau, M. Lemaire, '*A new tool for reliability based design with ANSYS FEA*, proceedings of the 12th ANSYS Conference, May 1996.

[Nat62] Nataf, A., *Détermination des distribution don't les marges sont donées*, Comptes rendus de l'academie des sciences, vol. 225, pp 42-43 , 1962.

[Nea77] Neal, B.G., *The plastic methods of structural analysis,* Chapman and Hall, London, 1977.

[Ouy87] Ouybornprasert, W., *Adaptive numerical integration for reliability analysis*, Universität Innsbruck.

[Ped96] Redersen, C., *Interactive reliability based optimazation of structural systems*, Ph.D. Thesis, Aalborg University, Danmark, 1996.

[Pow82] Powell, M.J.D. (1982*), VMCWD: A FORTRAN Subroutine for constrained Optimisation*, Report DAMTP 1982/NA4, Cambridge University, United Kingdom.

[Rac78] Rackwitz, R., B. Fiessler, *Structural Reliability under combined Random Load Sequences*, Comp. & Struct., Vol. 9, 1978.

[Rac82] Rackwitz, R., *Response surfaces in structural reliability* Berichte zur Zuverlässigkeitstheorie der Bauwerke, Heft 67/1982, TU München, 1982.

[RCP97] STRUREL users manual, RCP, Munchen, 1997.

[Reh91] Reh, S., F. Bohm, A. Bruekner-Foit, H. Riesch-Opperman, *First Order Reliability Analysis Using Stochastic Finite Element Methods,* in Computable Stochastic Mechanics '91, Eds P.D. Spanos and C.A. Brebbia.

[Ros52] Rosenblatt, M., *Remarks on a Multivariate Transformation*, The annals of Mathematical Statistics, Vol. 23, pp 470-472, 1952.

[Rub81] Rubinstein, R.Y., *Simulation and the Monte Carlo method,* John Wiley and Sons, New York, 1981.

[Sch85] Schittkowski, K., *A Fortran subroutine solving constrained nonlinear programming problems'*, Ann. Operations Research 5, 1985.

[Sch97] Schuëller, G.I., *IASSAR report on computational stochastic mechanics*, J. Eng. Mech., Vol. 12, No. 4, 1997.

[Sha98] Shao, S., Y. Morotsu, *Approach of failure mode analysis of large structures,* J. Prob. Eng. Mech., Vol. 14, No. 1-2, 1998.

[Shi98] Shiao, M.C., C.C. Chamis, *Probabilistic evaluation of fuselage-type composite structures,* J. Prob. Eng. Mech., Vol. 14, No. 1-2, 1998.

[Soe79] Soest, J. van, *Elementaire statistiek,* DUM, the Netherlands, 1979.

[Sta71] Stange, K. *Angewandte Statistik -Zweiter Teil, Mehrdimensionale Probleme,* Springer-Verlag, 1971 (290-295).

[Stu35] Stüssi, F., C.F. Kollbrunner, *Beitrag zum Traglastverfahren*, Die Bautechnik, 13, heft 21, 1935.

[Tho85] Thoft-Christensen, P., P.T.Y. Murotsu, *Application of Structural systems Reliability Theory*, Springer, Berlin, 1985.

[Tho98] Thoft-Christensen, P., *Industrial Application of Structural Reliability Theory,* ESReDA, DNV, Berlin, 1998.

[Tve90] Tvedt, L., *Distribution of quadratic forms in the normal space - Application to structural reliability,* J. Eng. Mech. ASCE, 1990.

[Val97] Val, D., F. Bljuger, D. Yankelevsky, *Reliability evaluation in non-linear analysis of reinforced concrete structures*, Struc. Saf., Vol. 19, No. 2, 1997.

[Van83] Vanmarcke, E.H., M. Grigoriu, *Stochastic finite elements analysis of simple beams,* J. Mech. Eng., Vol. 109, No. 5, 1983.

[Van94] Vanmarcke, E.H., *Stochastic finite elements and experimental measures,* J. Prob. Eng. Mech., No. 9, 1994.

[Vro87] Vrouwenvelder, A.C.W.M., A.J.M. Siemes, *Probabilistic calibration procedure for the derivation of partial safety factors for the Netherlands building codes*, Heron, Vol. 32, No. 4., 1987.

[Vro87a] Vrouwenvelder, A.C.W.M., A.J. Wubs, *Vergelijking Nivo II programma's,* TNO report B-87-326, October 1987.

[Vro84] Vrouwenvelder, A.C.W.M., J.K. Vrijling, *Probabilistisch ontwerpen,* Lecture nodes b3, TU Delft, The Netherlands, 1984.

[Vro93] Vrouwenvelder, A.C.W.M, P.H. Waarts, *Traffic loads on bridges*, Structural Engineering International, IABSE, Vol. 3, No. 3, 1993.

[Vro99] Vrouwenvelder, A.C.W.M, *COB L550 Betrouwbaarheidsaspecten boortunnels*, TNO report 99-CON-DYN-R0089, October 1999.

[Waa96] Waarts, P.H., A.C.W.M. Vrouwenvelder, *Probabilistic Finite Element Analysis of High strength structures*, Proceedings of the 7th IFIP WG 7.5 Conference of Reliability and Optimisation of Structural Systems, Boulder, Colorado, 1996.

[Waa97] Waarts, P., A. Vrouwenvelder, *Probabilistic analysis of the Stussi-Kollbrunner Paradox*, Heron, Vol. 42, No. 3, 1997.

[Waa98] Waarts, P.H., A.C.W.M. Vrouwenvelder, *The use of directional sampling in structural reliability*, 8th IFIP WG 7.5 Conference on reliability and optimisation of structural systems, Krakow, Poland, 1998.

[Win88] Winterstein, S.R., *Nonlinear vibration models for extremes and fatique,* j. Eng. Mech. Vol. 114, no. 10, 1998.

[Yam88] Yamazaki, F., M Shinozuka, G. Dasgupta, *Neumen expansion for stochastic finite element analysis,* J. Eng. Mech. Vol. 114, No 8, August 1988.

[Yon98] Yonezawa, M., S. Okuda, *Directional vectors approximation for assessment of structural failure probability*, in: proceedings of ICOSSAR '97, Structural safety and reliability, Shiraisa, Shinozuka & Wen, Eds., November 1997, Balkema, Rotterdam, 1998.

[Xia94a] Xiao, Q., Mahadevan S., *Plastic effects on frame member reliability,* Struct. Saf., Vol. 16, No. 3, 1994.

[Xia94b] Xiao, Q., Mahadevan S., *Fast failure mode identification for ductile structural system reliability*, Struct. Saf., Vol. 13, No. 4, 1994.

[Zha94] Zhang, Y., A. Der Kiureghian, *First excursion probability of uncertain structures*, J. Prob. Eng., No. 9, 1994.

Annex A: Procedures of directional sampling

Annex A.1: Procedure to find the distance λ from origin to limit state

The first sampling points in u-space are located at 0 and f. Initially f is set equal to the expected reliability index β. In case of DARS, f is set equal to the estimated λ according to the Response Surface. In case of a perfect forecast by the Response Surface, the distance λ is found instantly.

First a straight line is fitted through the above mentioned two points. A new sampling point is chosen where the limit state function is supposed to be zero according to the straight line fit. The procedure is stopped if the distance is negative. The next estimate of λ is limited to the old estimate of λ plus 3.

Next a quadratic function $g^* = a + bf + cf^2$ is fitted to three points (see Figure A-1) and an estimate of λ is found in the zero point of the quadratic function. Next a quadratic function is fitted to four data points. This continues until the response is sufficiently low ($g^*(0,\dots f,\dots\dots,0) \approx 0$). The iteration also stops when the maximum f with positive g value and minimum f with negative g-value is nearly coinciding. Sometimes the fitted line is such that no positive 'zero point' is found. A refit is carried out with one data point less. The data point that is most remote from the last estimate λ is left out.

For structures with a linear behaviour, examples show that on average 4 data points are sufficient to find the distance λ.

The value of g can be negative and not quantified in case of structures with a non-linear behaviour with collapse as limit state. In this case only positive g-values are known. In case of collapse the value of g is set to minus the minimum found positive value of g. The value is set to 0.9 times the previous negative g-value if in a next iteration the value of f is less than the previous and g is negative. For higher values of f and negative g, the value of g is set to the previous g-value divided by 0.9. The procedure is visualised in Figure A-2.

Figure A-1: Procedure to find λ.

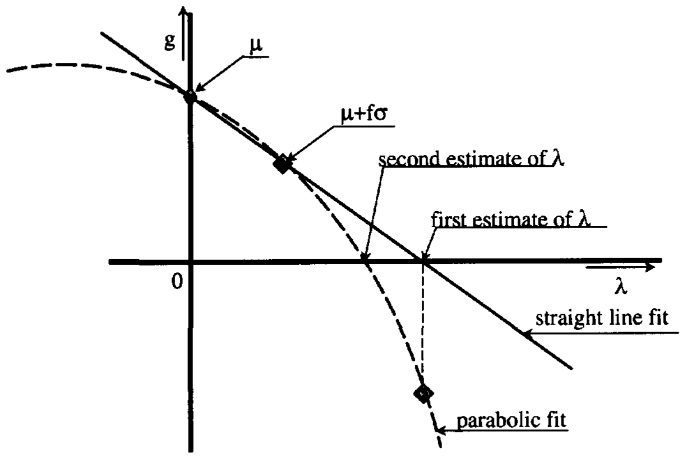

Figure A-2: Procedure to find λ in case of collapse as limit state (λ=9.9).

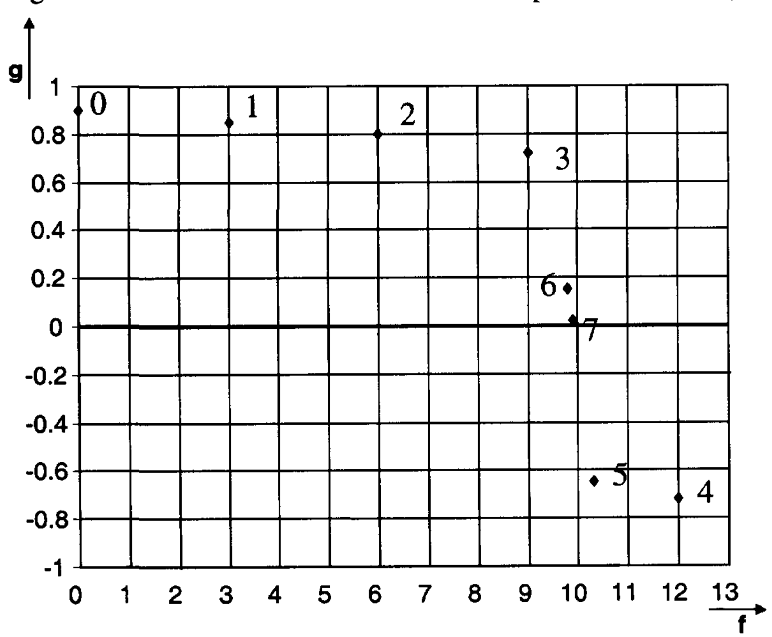

Annex A.2: Directional Integration

The directional integration method is explained for a case with two standard normal variables. The joint probability density function of two variables x_i and x_j equals:

$$f_{x_{i,j}} = \frac{1}{2\pi}\exp[-\frac{1}{2}(x_i^2 + x_j^2)] \tag{A.1}$$

In the directional integration procedure, equation (A.1) can be seen as a probability of a direction of $P_\Phi = 1/\pi$ and a probability density given the direction of:

$$f_r = \frac{1}{2}\exp[-\frac{1}{2}r_i^2] \tag{A.2}$$

The probability of failure given a certain direction and limit state $g = r - \lambda$ is equal to:

$$F_{r>\lambda} = \int_\lambda^\infty \frac{1}{2}\exp[-\frac{1}{2}r_i^2]dv \tag{A.3}$$

As shown, the main interest lies in the sum of the squares of the variables. The χ^2 distribution describes the sum of squares of n independent normal variables. The density function is described as:

$$f_y = \frac{\frac{1}{2}(y/2)^{(n/2)-1}\exp(-y/2)}{\Gamma(n/2)} \tag{A.4}$$

Here y is the sum of the squires of independent standard normal variables χ^2, Γ is the gamma function and n is the number of variables.

For 2 variables equation (A.4) becomes: $f_y = \frac{1}{2}\exp(-y/2)$. Since y equals r^2, equation (A.4) and (A.2) are the same.

The directional integration method integrates over the directions $\underline{\theta}$:

$$P_f = \int \chi_n^2(\lambda^2(\underline{\theta}))d\theta \tag{A.5}$$

Annex B: System analysis

Annex B.1: Branch-and-Bound method

One of the methods described in literature [Tho85] to investigate the failure path is the Branch-and-Bound method: The Branch-and-Bound method is especially useful in case of frame structures. First of all (before the first exceedance of a limit state (yielding)) the reliability indices of all limit state functions are computed. Per limit state function j a reliability index β_{1j} (1st level) results. The limit state function j with the lowest β (β_{low}) is branched. Given the exceedance of the limit state function in level 1 the reliability indices are computed for the next limit state to fail. When the number of limit state functions in the first level equals k, in the second level k-1 reliability indices are found. Again, the limit state function with the lowest β is branched. This continues until total failure.

The parallel system (intersection) of the complete branch of all exceeded limit state functions with $\beta_{j,low}$ are combined into an overall $\beta_{T,low}$. The next step is researching the possibilities of branches with higher reliability indices in the first lower level, finally ending in a lower total reliability. Therefore the next to lowest β limit state function in the next to final level is investigated and further branched until total collapse occurs. Of course this will only be carried out when $\beta_{j,low-1} < \beta_{T,low}$ and the branching will be stopped (bounded) when $\beta_{Tmom} > \beta_{T,low,}$ where β_{Tmom} is the reliability of a failure set limit state functions not having total collapse.

This scheme is performed at each level of failed elements, and is therefore also analysed for the next to lowest β in level i. After this, the next to i level is analysed with the next to lowest β in this level. This continues backwards until level 1.

Bounding is carried out by means of the lower bound system reliability. At first this reliability is computed using the lowest β in the failure tree. The system reliability index β_{sys} is updated every time a new (lower) β is found in the tree.

In branching there are two options: After the lower bound system reliability is found as a system of lowest β in the failure tree, the next to failure level is branched (those elements with $\beta < \beta_{sys}$). The other option is to branch from level 1 and bound when $\beta > \beta_{sys}$.

Annex B.2: System reliability calculation

A series system (union) of m components is considered to have failed if any of the components fails. When the event that component j has failed is denoted E_{fj} the probability of the union can be determined as:

$$P_f = P\left(\bigcup_{j=1}^{m} E_{fj}\right) \tag{B.1}$$

The Ditlevsen bounds are upper and lower bound approximations of the failure probability:

$$\begin{aligned} P_f &\geq P_{f1} + \sum_{j=2}^{m} \max\{P_{fj} - \sum_{i=1}^{j-1} P_{f(i\cap j)}, 0\} \\ P_f &\leq \sum_{j=1}^{m} P_{fj} - \sum_{j=2}^{m} \max\{P_{f(i\cap j)}\} \forall i < j \end{aligned} \tag{B.2}$$

A parallel system (intersection) of m components is considered to have failed when all of the components fail. When the event that component j has failed is denoted E_{fj}, the probability of failure of the intersection can be determined as:

$$P_f = P\left(\bigcap_{j=1}^{m} E_{fj}\right) \tag{B.3}$$

The Hohenbichler approximation [Hoh82] replaces the probability $P_f = P(g_1 < 0 \text{ and } g_2 < 0)$ by the probability:

$$P_f = P\{\beta_2 - \rho u' - w\sqrt{(1-\rho^2)} < 0\} \tag{B.4}$$

The approximation is based on the transformation of g_1 into $g_1 = \beta_1 - u$ and g_2 into $g_2 = \beta_2 - v$. The parameters u and v are (dependent) standard normal variables. The dependent variables u and v replace the independent variables u and w standard normal variables according to:

$$g_2 = \beta_2 - \rho u - w\sqrt{(1-\rho^2)} \tag{B.5}$$

The variable u′ in equation (B.4) is the truncated standard normal variable. The truncation parameter is equal to β_1:

$$u' = \Phi^{-1}\{1 - P(u > \beta_1)\Phi(u)\} \tag{B.6}$$

The probability of failure of the combination of limit state functions g_1 and g_2 can be analysed within the FORM procedure using the following limit state function:

$$g = \beta_2 - \rho\Phi^{-1}\{1 - P(u > \beta_1)\Phi(u)\} - w\sqrt{1-\rho^2} \tag{B.7}$$

Subsequently, the intersection probability (system reliability) is computed by a level II approximation.

Annex C: Reducing the required number of directional samples by truncating

One of the methods to reduce the required number of samples is truncating the distribution function of the random variables. This is effective when it is known whether a variable has only positive or negative influence on the limit state function. For example, only positive parts of the standardised distribution function of the variable describing the loads can be used. In most cases the important direction of only part of the variables is known. Equation (2.24) can not be used directly because a part of the importance sampling distribution is zero. For one truncated standard normal distribution function $f(\underline{\kappa})/h(\underline{\kappa}) = 0.5$. For υ truncated variables, $f(\underline{\kappa})/h(\underline{\kappa}) = 1./2^{\upsilon}$ results. So P_i in equation (2.18) becomes:

$$P_i = \chi^2(\lambda_{ij}, n)/2^{\upsilon} \tag{C.1}$$

This method assumes that samples in the directions other then the important directions have a probability P_i equal to zero. In the case of one truncated variable this is correct. This assumption can only be justified for a small number of truncated variables.

The more variables are truncated, the smaller the sampling area gets. In consequence, the probabilities P_i that are assumed to be zero, might not be significantly different from the P_i inside the sampling area.

Figure C-1 shows the error in the reliability index β due to truncating. The results are computed for the case where all variables have equal importance on the limit state function and some of the variables are truncated:

$$g = \beta - \sum_{i=1}^{10} u_i / \sqrt{10} \qquad \text{(C.2).}$$

Up to 5 truncated variables seems uncomplicated. The error does not exist when equation (2.26) instead of (C.1) is used in the computation. This is however more time consuming.

Figure C-2 shows the required amount of samples when all variables have equal importance and for some variables the important direction is known. The limit state function equals:

$$g = \beta - \sum_{i=1}^{n} u_i / \sqrt{n} \tag{C.3}$$

Figure C-3 gives the required number of samples when the important direction is known of all q dominant variables and when the other (n-q) variables are totally unimportant:

$$g = \beta - \sum_{i=1}^{q} u_i/\sqrt{q}\,,\; q \le n \tag{C.4}$$

Figure C-2 gives, compared to Figure C-3, a larger required number of samples N. The number of samples decreases however quickly when of some of the variables the important direction is known. The number of samples N in Figure C-3 can be estimated empirically from:

$$N = \max(20, n \cdot 10^{\frac{1}{6}(9-q)}) \tag{C.5}$$

where q is the number of the important variables (with known important part).

For the example with $\mu(\beta) = 4$ using 100 variables the needed number of samples according to paragraph 2.3.1 equals 16000. When of 12 out of 100 variables the direction is known and the rest of the variables is unimportant the number of samples needed decreases to max(20,100 $10^{(9-12)/6}$)= 31. This number is very acceptable for use in structural reliability cases. If the direction of all variables is known, only 20 samples will be needed to get a result with sufficiently low $V(\beta)$. This number of samples is independent of the number of variables.

Figure C-1: Error in β as function of the number of truncated variables.

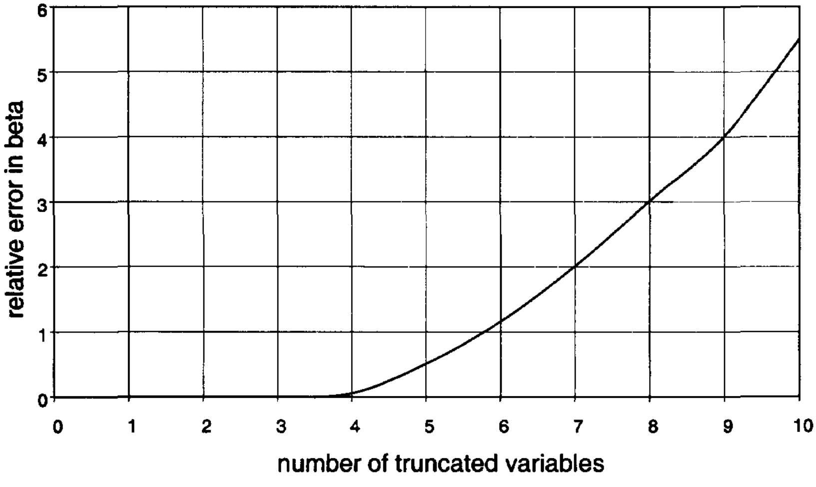

Figure C-2: Required number of samples N, in case the important influence of some variables is known; all variables have equal importance, $V(\beta) = 0.05$.

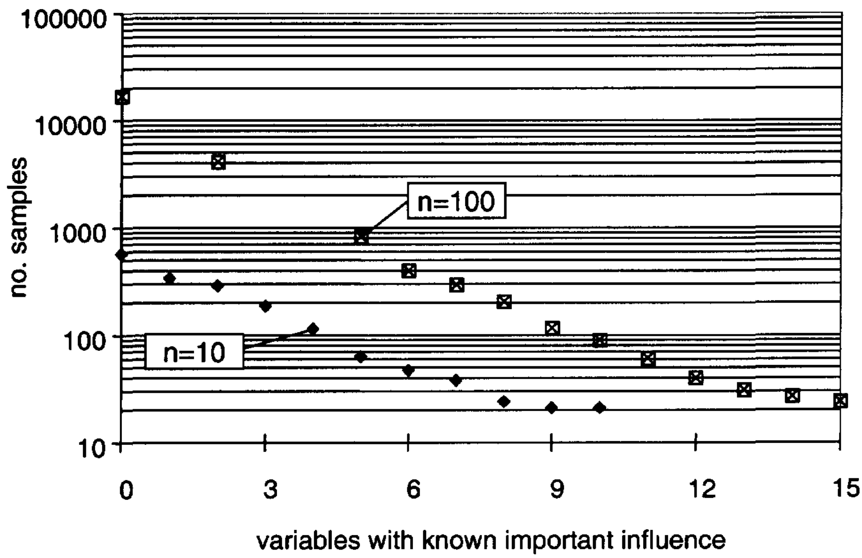

Figure C-3: Important directions of all important variables are known; other variables have no influence, $V(\beta)=0.05$.

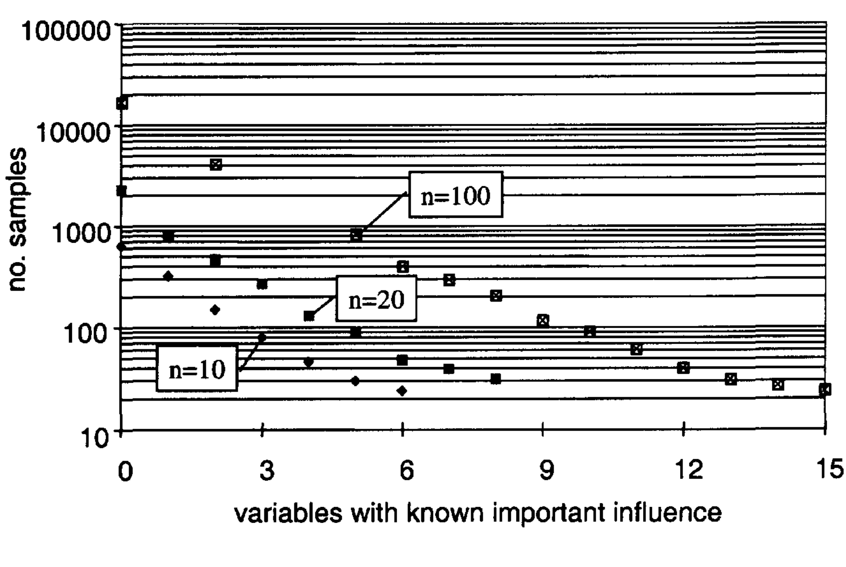

Incorrect assumption for important direction of the distribution
The important part of a variable might be assessed in an incorrect way. In general it is advisable not to truncate the complete positive or negative part of a variable. Better use some (but few) samples in the part which is assumed to be non-important. This way a possible prior incorrect assumption will be recognised and corrected. Table C-1 shows the number of samples needed for analysis of a limit state function with 10 variables in which one is important (only the positive part).

Table C-1: Number of samples needed with incomplete truncation of (assumed) unimportant part.

% of samples in assumed incorrect direction	no samples
0 (all samples are in the correct direction)	270
10	300
50 (no importance sampling)	600
90	3300

When no importance sampling is performed, a total of 600 samples is needed. This agrees with Figure 2.5 (β=4). Merely 270 samples are to be used when only the positive part of the variable (0 % in Table C-1) is used (factor 2 less). 300 samples (10 % increase) are to be used when 10 % of the samples are based on the negative part of the variable. When the incorrect direction is chosen, only 10 % of the samples lead to the right result. The number of samples increases to 3300. The incorrect assumption will cause many extra computations. The presumption can be changed when the process shows that the direction was chosen erroneously. If the design-point (i.e. the point with lowest distance to the origin) is in a certain direction then another assumption can be made (adaptive sampling).

Reduction of the number of directional samples by means of precluding non-dominating variables
Non-dominating variables count in the necessary number of samples. It is of course possible to truncate the tails of the distributions, see Figure C-4. This is in fact the same as truncating important variables. It can be seen as rotating the g-function. Truncating the directions leads to the same error as shown in Figure C-1. In most cases there are plenty of non-dominant variables and only a few dominant variables. The high number of non-dominant variables leads to a large error. Truncating non-dominant variables this way is therefore useless. Decreasing the variance of the non-dominant variables is far better because of the correction $f(\underline{\kappa})/h(\underline{\kappa})$.

Since the non-dominating variables do influence the result (β), it would be best to omit these variables. A method to recognise these non-dominating variables is still to be found.

Figure C-4: Truncating the tail of the distribution functions of non-dominating variables.

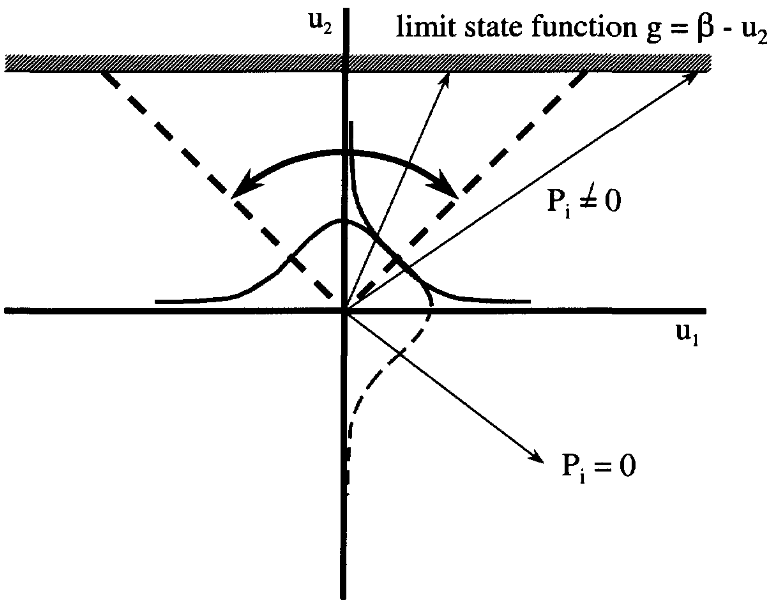

Annex D: Directional Importance Sampling

Chapter 2.4 showed the possibility of directional importance sampling. Importance sampling may be directed by the results of an FORM analysis. Parameters with an influence factor α nearly equal to zero can be given a decreased standard deviation, i.e. given less importance. Variables with $\alpha > 0.5$ are surely important and can be used for importance sampling.

The difficulties of this method are explained by the example in section 4.5: Series system with 4 branches (a copy of the limit state function is given in Figure D-1. Section 4.5 showed the result of directional sampling: $\beta = 2.8$. First importance sampling is performed in an (incorrect) design-point (2.12, 2.12). Performing directional sampling with a decreased standard deviation $\sigma = (0.5,0.5)$ leads to (40 samples) $\beta = 3.0$. Secondly, another design-point is focussed on (-2.5,2.5). Using $\sigma = (0.5,0.5)$ leads to $\beta = 3.5$ (200 samples). Without decreasing the standard deviation, concentrating on (-2.5,2.5) with $\sigma = (1,1)$, a reliability index $\beta = 3.0$ is found (85 samples $V(\beta) = 0.05$).

Figure D-1: Series system with 4 branches (equal to Figure 4.4)

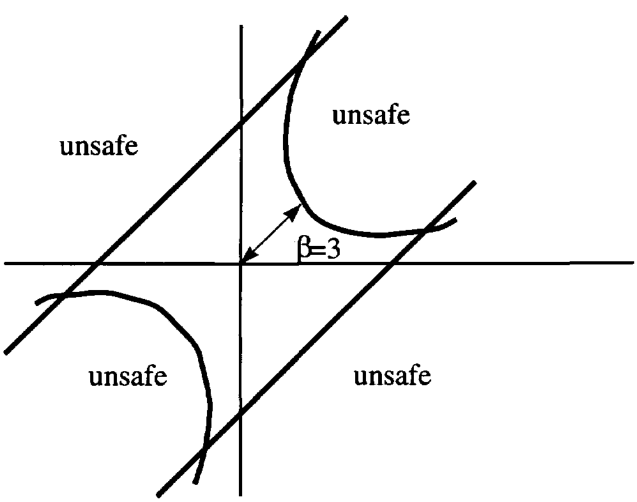

Clearly focussing on a certain point may lead to wrong answers. In fact, this example is a bit academic. Most structural reliability limit state functions are non-symmetric. The lesson however is that the sampling density should not be made too directed. An erroneous answer is not recognised.

The series system shows that importance directional sampling in a design-point does not always leads to a correct result. Focussing too much on a certain point of the limit state function leads to an answer that has left out a region that might have been of importance. For example in multiple mode failure criteria, a FORM answer could be found as (one) design-point at minimum distance. Focussing on this design-point and decreasing σ from 1 to 0.5, will lead to never finding the other minima. The directional sampling answer is by definition the same as the FORM answer.

Applying importance Directional Sampling around the design-point in a 2-dimensional u-space leads to approximately a factor 2 error in P_f (and is equal to the component FORM result).

Annex E: Input and output of the Artificial Limit State function

Annex E.1: Standard linear Resistance-Solicitation problem

Limit state function:

$$g = R - S$$

Table: Input variables

Variable	μ	σ	
R	7.0	1.0	N
S	2.0	1.0	N

Table: Results

Method	β	LSFE	$V(P_f)$
Exact	3.54		-
FORM basic	3.54	6	-
FORM NLPQL	3.54	7	-
FORM RFLS	3.54	9	-
FORM RFLS imp. samp	3.54	309	-
FORM-ARS (u-space)	3.54	6	-
FORM-ARS (x-space)	3.54	6	-
SORM	3.54	12	-
SORM imp. samp.	3.54	314	-
MC (adsamp)	3.54	10000	0.02
MCI(σ_h=3)	3.57	122	0.49
DS	3.55	100	0.49
DARS	3.55	18	0.49

Table: Intermediate results from DARS

Method	ADI	DARS
β	4.62	3.55
λ_{min}	5.00	3.54
$\beta_{RS,FORM}$	3.53	3.54

Annex E.2: Noisy limit state function

Limit state function:

$$g = x_1 + 2x_2 + 2x_3 + x_4 - 5x_5 - 5x_6 + 0.001\sum_{i=1}^{6}\sin(100x_i)$$

Table: Input variables

Variable	μ	σ	
x_1	120	12	LN
x_2	120	12	LN
x_3	120	12	LN
x_4	120	12	LN
x_5	50	15	LN
x_6	40	12	LN

Table: Results

Method	β	LSFE	$V(P_f)$
Exact [Eng93]	2.25		-
FORM basic	2.35	40	-
FORM NLPQL	2.35	44	-
FORM RFLS	2.35	452	-
FORM RFLS imp. samp.	2.23	1010	-
FORM-ARS (u-space)	2.35	37	-
FORM-ARS (x-space)	2.35	15	-
SORM	2.25	71	-
SORM imp. samp.	2.26	973	-
MC (adsamp)	2.24	10000	0.01
MCI(σ_h=2)	2.24	1225	0.25
DS	2.24	925	0.25
DARS	2.24	271	0.25

Table: Intermediate results from DARS

Method	ADI	DARS
β	1.75	2.24
λ_{min}	2.67	2.54
$\beta_{RS,FORM}$	2.09	2.19

Annex E.3: A Resistance-Solicitation problem with one quadratic term

Limit state function:

$$g = R\text{-}S^2$$

Table: Input variables

Variable	μ	σ	
R	11.0	1.0	N
S	1.5	0.5	N

Table: Results

Method	β	LSFE	$V(P_f)$
Exact	3.46		-
FORM basic	3.47	12	-
FORM NLPQL	3.47	19	-
FORM RFLS	3.47	14	-
FORM RFLS imp.samp	3.47	346	-
FORM-ARS (u-space)	3.47	7	-
FORM-ARS (x-space)	3.47	6	-
SORM	3.46	24	-
SORM imp.samp	3.47	319	-
MC (adsamp)	3.47	10000	0.02
MCI(σ_h=3)	3.50	267	0.49
DS	3.43	60	0.49
DARS	3.43	38	0.49

Table: Intermediate results from DARS

Method	ADI	DARS
β	3.40	3.43
λ_{min}	3.63	3.48
$\beta_{RS,FORM}$	3.53	3.76

Annex E.4: Limit state function with 10 quadratic terms

Limit state function:

$$g = R - \sum_{i=1}^{10} S_i^2 / i$$

Table: Input variables

Variable	μ	σ	
R	0.5	0.1	N
S_i	0.2	0.1	N

Table: Results

Method	β	LSFE	$V(P_f)$
Exact	2.98	-	-
FORM basic	3.20	65	-
FORM NLPQL	3.20	61	-
FORM RFLS	3.20	74	-
FORM RFLS imp. samp	2.98	574	-
FORM-ARS (u-space)	3.20	14	-
FORM-ARS (x-space)	3.20	16	-
SORM	2.97	151	-
SORM imp. samp.	2.96	637	-
MC (adsamp)	2.98	10000	0.11
MCI(σ_h=2)	3.08	2868	0.39
DS	2.90	1132	0.39
DARS	2.90	221	0.39

Table: Intermediate results from DARS

Method	ADI	DARS
β	2.29	2.90
λ_{min}	3.82	3.64
$\beta_{RS,FORM}$	2.67	3.52

Annex E.5: Limit state function with 25 quadratic terms

Limit state function:

$$g = R - \sum_{i=1}^{25} S_i^2/i$$

Table: Input variables

Variable	μ	σ	
R	0.5	0.1	N
S_i	0.2	0.1	N

Table: Results

Method	β	LSFE	$V(P_f)$
Exact	2.63	-	-
FORM basic	2.92	84	-
FORM NLPQL	2.84	136	-
FORM RFLS	2.84	164	-
FORM RFLS imp. samp.	2.52	674	-
FORM-ARS (u-space)	2.94	57	-
FORM-ARS (x-space)	2.94	57	-
SORM	2.52	541	-
SORM imp. samp.	2.63	314	-
MC (adsamp)	2.98	10000	0.27
MC (crude)	2.63	100000	-
MCI(σ_h=1.5)	2.74	6501	0.31
DS	2.65	2540	0.31
DARS	2.65	188	0.31

Table: Intermediate results from DARS

Method	ADI	DARS
β	1.79	2.65
λ_{min}	3.47	3.47
$\beta_{RS,FORM}$	2.33	3.17

Annex E.6: Convex failure domain

Limit state function:

$$g = 0.1(u_1 - u_2)^2 - (u_1 + u_2)/\sqrt{2} + 2.5$$

Both variables u_1 and u_2 have a standard normal distribution.

Table: Results

Method	β	LSFE	$V(P_f)$
Exact	2.63	-	-
FORM standard	2.50	8	-
FORM NLPQL	2.50	7	-
FORM RFLS	2.50	9	-
FORM RFLS imp. samp.	2.61	484	
FORM-ARS	2.50	7	-
SORM	2.63	14	-
SORM imp. samp.	2.63	314	-
MC (adsamp)	2.63	10000	0.02
MCI(σ_h=1.5)	2.63	513	0.32
DS	2.63	208	0.32
DARS	2.61	47	0.32

Table: Intermediate results from DARS

Method	ADI	DARS
β	∞	2.61
λ_{min}	∞	2.50
$\beta_{RS,FORM}$	2.88	2.50

Annex E.7: Oblate spheroid

Limit state function:

$$g = R - \sum_{i=1}^{10} S_i^2/(1+i/10)$$

with R = 10 and S_i is standard normal distributed.

Table: Results

Method	β	LSFE	$V(P_f)$
Exact	1.10	-	-
FORM standard	3.33	204	-
FORM NLPQL	3.31	187	-
FORM RFLS	3.31	482	-
FORM RFLS imp. samp.	1.93	1319	-
FORM-ARS	3.21	22	-
SORM	*	-	-
SORM imp. samp.**	0.97	191613	-
MC (adsamp)	1.26	100000	0.15
MC (crude)	1.10	100000	-
MCI(σ_h=2)	1.10	1682	0.09
DS	1.07	170	0.09
DARS	1.06	160	0.09

* *error message*
** *10.000 imp. samp used for convergence to $V(P_f) < 0.08$*

Error message of SORM

Warning from 2nd-order improvement:
There are very large curvatures at u-.*
2nd-order improvement might be biased !
1st-order result is likely to have a large error !

Table: Intermediate results from DARS

Method	ADI	DARS
β	1.05	1.06
λ_{min}	3.32	3.32
$\beta_{RS,FORM}$	46.4	46.4

Annex E.8: Saddle surface

Limit state function:

$$g = 3 - u_1 u_2$$

Both variables are standard normal distributed.

Table: Results

Method	β	LSFE	$V(P_f)$
Exact	2.34	-	-
FORM standard*	2.86	16	-
FORM NLPQL*	2.45	47	-
FORM RFLS*	2.45	36	-
FORM RFLS imp. samp.*	2.56	620	-
FORM-ARS*	2.50	33	-
SORM*	2.58	41	-
SORM imp. samp.*	2.58	409	-
MC (adsamp)	2.58	10000	-
MC (crude)	2.32	100000	-
MCI(σ_h=3)	2.34	385	-
DS	2.26	299	0.25
DARS	2.35	225	0.25

**FORM/SORM starting in point (0,0) results in an error message*

Table: Intermediate results from DARS

Method	ADI	DARS
β	∞	2.35
λ_{min}	∞	2.45
$\beta_{RS,FORM}$	∞	0.0

Annex E.9: Discontinuous limit state function

Limit state function:

$$g = -0.5 + \sqrt{R - S} \cdots \forall R \geq S$$
$$g = -0.5 \cdots\cdots\cdots\cdots \forall R < S$$

Table: Input variables

Variable	μ	σ	
R	15.0	2.5	N
S	5.0	0.5	N

Table: Results

Method	β	LSFE	$V(P_f)$
Exact	3.83	-	-
FORM standard	*	-	-
FORM NLPQL	6.60	7	-
FORM RFLS	*	-	-
FORM RFLS imp. samp.	*		
FORM-ARS (u-space)	3.85	11	-
FORM-ARS (x-space)	3.84	13	-
SORM	6.60	12	-
SORM imp. samp.	*		
MC (adsamp)	3.82	10000	0.02
MC (crude)	3.83	1000000	-
MCI(σ_h=2)	3.84	325	0.54
DS	3.94	333	0.54
DARS	3.84	55	0.54

* *error message*

Table: Intermediate results from DARS

Method	ADI	DARS
β	3.66	3.84
λ_{min}	3.90	3.83
$\beta_{RS,FORM}$	3.83	3.82

Annex E.10: Two branches

Limit state function:

$$g = x_1 - x_2 - x_3 \cdot\cdot \forall x_3 \leq 5$$
$$g = x_3 - x_2 \cdots\cdots\cdot \forall x_3 > 5$$

Table: Input variables

Variable	μ	σ	
x_1	10.0	0.5	N
x_2	0.0	1.0	N
x_3	4.0	1.0	N

Table: Results

Method	β	LSFE	$V(P_f)$
Exact	5.03	-	-
FORM standard	-	-	-
FORM NLPQL	4.00	244	-
FORM RFLS	2.21*	769	-
FORM RFLS imp. samp.	*		
FORM-ARS (u-space)	*	-	-
FORM-ARS (x-space)	4.84	29	-
SORM	4.51	253	-
SORM imp. samp.	*		
MC (adsamp)	5.03	10000	0.06
MCI(σ_h=3)	5.15	2787	0.57
DS	5.01	728	0.57
DARS	5.00	135	0.57

** error message*

Table: Intermediate results from DARS

Method	ADI	DARS
β	5.57	5.00
λ_{min}	6.00	4.70
$\beta_{RS,FORM}$	5.37	4.71

Annex E.11: Concave failure domain

Limit state function:

$$g = -0.5(u_1^2 + u_2^2 - 2u_1u_2) - (u_1 + u_2)/\sqrt{2} + 3.0$$

Both variables have a standard normal distribution.

Table: Results

Method	β	LSFE	$V(P_f)$
Exact	1.26	-	-
FORM standard	1.66	8	-
FORM NLPQL	1.66*	7	-
FORM RFLS	1.66*	9	-
FORM RFLS imp. samp.	1.64	407	-
FORM-ARS	2.06	18	-
SORM	1.66*	12	-
SORM imp. samp.	1.52	494	-
MC (adsamp)	1.12	10000	0.19
MC (crude)	1.26	100000	-
MCI(σ_h=3)	1.25	1172	0.10
DS	1.27	260	0.10
DARS	1.27	240	0.10

**FORM/SORM starting in point (0,0) results in* $\beta = 3.00$

Table: Intermediate results from DARS

Method	ADI	DARS
β	1.31	1.27
λ_{min}	1.84	1.66
$\beta_{RS,FORM}$	1.71	1.80

Annex E.12: Series system

Limit state function:

$$g_1 = 0.1(u_1 - u_2)^2 - (u_1 + u_2)/\sqrt{2} + 3.0$$
$$g_2 = 0.1(u_1 - u_2)^2 + (u_1 + u_2)/\sqrt{2} + 3.0$$
$$g_3 = u_1 - u_2 + 3.5\sqrt{2}$$
$$g_4 = -u_1 + u_2 + 3.5\sqrt{2}$$
$$g = \min\{g_1, g_2, g_3, g_4\}$$

Both variables have a standard normal distribution.

Table: Results

Method	β	LSFE	$V(P_f)$
Exact	2.85	-	-
FORM standard	3.50	32	-
FORM NLPQL	3.00	7	-
FORM RFLS	3.00	8	-
FORM RFLS imp. samp.	3.11	494	-
FORM-ARS	3.01	8	-
SORM	3.13	12	-
SORM imp. samp.	3.13	313	-
MC (adsamp)	3.04	10000	0.23
MC (crude)	2.85	100000	-
MCI(σ_h=3)	2.87	166	0.37
DS	2.84	227	0.37
DARS	2.92	175	0.37

Table: Intermediate results from DARS

Method	ADI	DARS
β	4.28	2.92
λ_{min}	4.81	3.00
$\beta_{RS,FORM}$	14.5	5.03

Annex E.13: Parallel system

Limit state function:

$$g_1 = 2.677 - u_1 - u_2$$
$$g_2 = 2.500 - u_2 - u_3$$
$$g_3 = 2.323 - u_3 - u_4$$
$$g_4 = 2.250 - u_4 - u_5$$
$$g = \max(g_i)$$

All variables have a standard normal distribution.

Table: Results

Method	β	LSFE	$V(P_f)$
exact	3.52		-
FORM standard	*		-
FORM NLPQ	1.85	1086	-
FORM RFLS	*		-
FORM RFLS imp. samp.	*		-
FORM-ARS	*		-
SORM	3.73	523	-
SORM imp. samp.	*		-
MC (adsamp)	3.52	10000	0.05
MC (crude)	3.55	100000	-
MCI(σ_h=3)	3.58	2778	0.49
DS	3.52	581	0.49
DARS	3.52	127	0.49

* *error message*

Table: Intermediate results from DARS

Method	ADI	DARS
β	∞	3.52
λ_{min}	∞	3.49
$\beta_{RS,FORM}$	3.25	3.86

Annex F: Fitting a response surface in x-space or u-space

This annex gives an example of the problems of fitting a response surface in x-space when using bobtailed distributions. Suppose a limit state function depending on one beta-distributed random variable:

$$g = 100 - 10\,x$$

The variable x is beta distributed with the following parameters:

- Mean: 0.5;
- St. dev: 0.14;
- Lower bound: 0.0;
- Upper bound: 0.5.

The procedure in ADI is explained in Annex A. Figure F.1 gives the response data when using this procedure in u-space. Besides the response data, the fitted response surface is shown in the figure. The figure clearly shows that a root is never reached when fitting in u-space. There seems little influence of u on the response for higher u.

Figure F.2 shows the result of fitting in x-space. The data points that belong to higher u all lay very near to each other. The response surface shows a linear relation between x and g (which is correct). The consequence of the iteration procedure is that a higher value of x will be tried (aiming to reach the limit state). Of course the root will never be found. It will however take much more samples (and consequently computational time) before the iteration procedure is stopped. In such cases fitting in u-space is better than in x-space. On the other hand, for long tailed (sides of) distributions fitting in x-space will be better than in u-space.

Figure F.1: Response in u-space and x-space

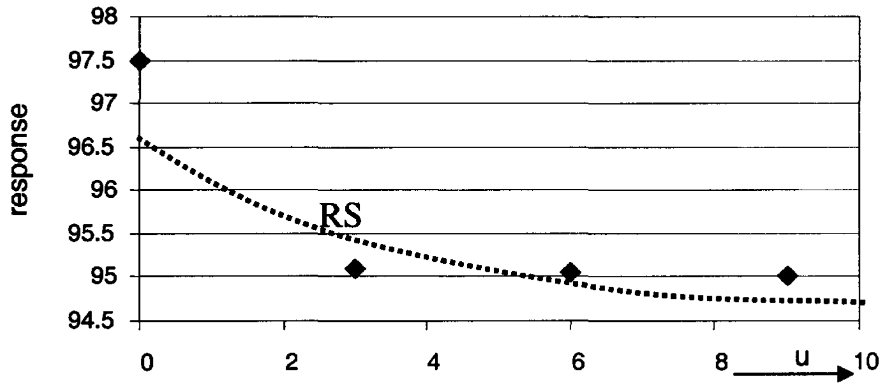

Figure F.2: Response in u-space and x-space

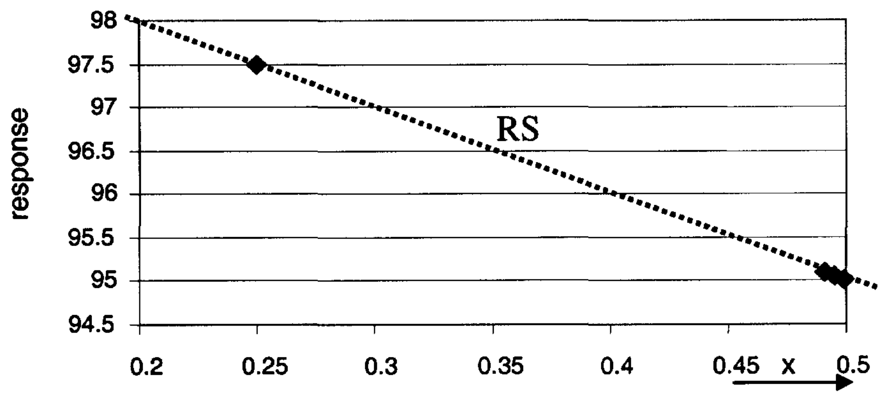

Annex G: DIANA module PROBAB

Annex G.1: Flow diagram of DIANA module PROBAB

The PROBAB module in DIANA computes the probability of failure of the structure. Stochastic properties can be given to each input item of DIANA ('PROBAB'). The ultimate state has to be defined with 'LIMITS'. Correlation is possible between each (stochastic) item and is described in 'CORREL'. The probability of failure is calculated by means of the directional sampling (DS) method.

The database is initially filled with results of the initial main directions: the zero point and intermediate points. While performing crude directional sampling only the zero points are stored.

Flow diagram:

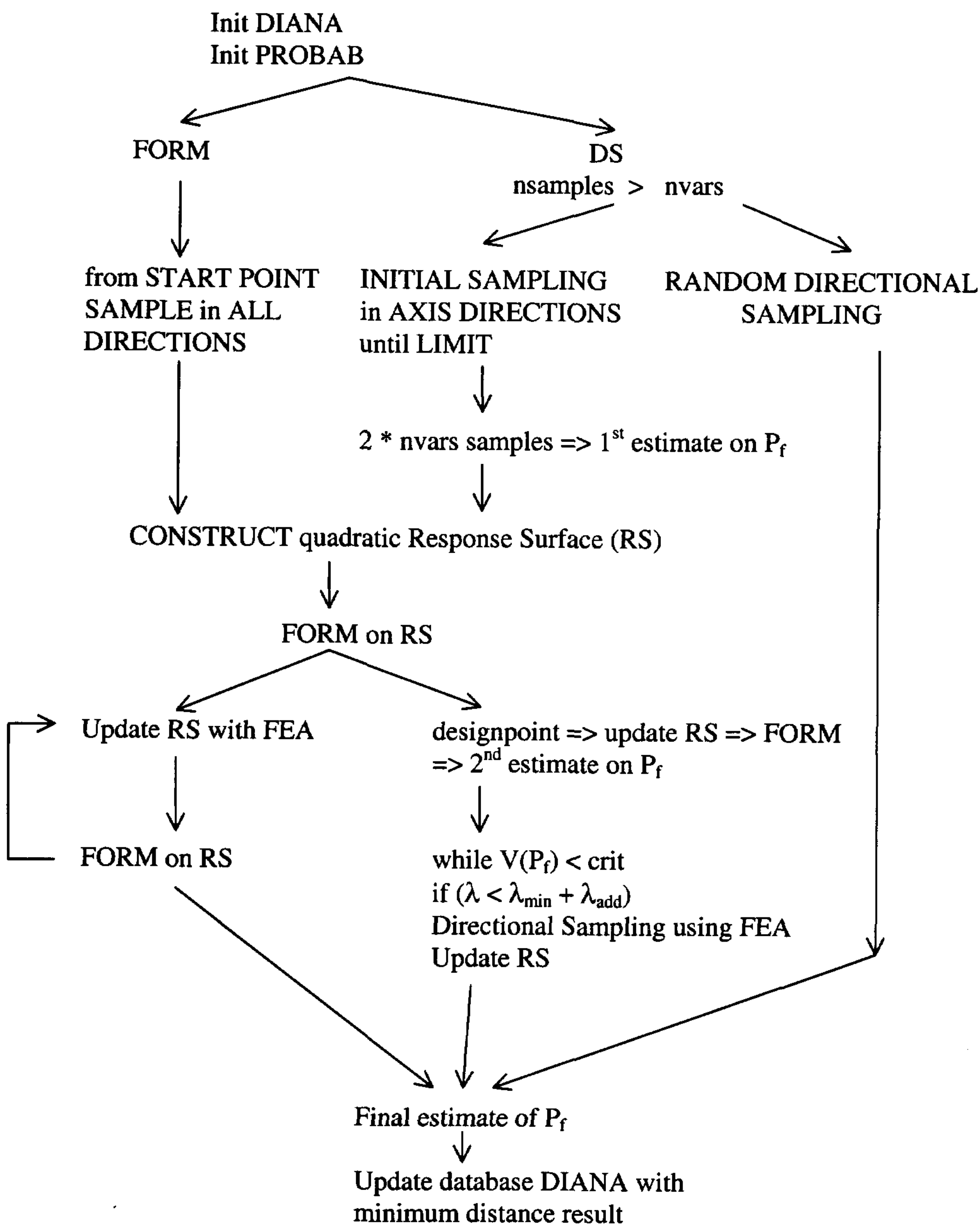

Annex G.2: Input tables for DIANA module PROBAB

Two tables have to be added to the data file: 'PROBAB' and 'LIMITS'. The table 'CORREL' describing the correlation between random variables is optional. PROBAB describes which input is stochastic instead of deterministic. The table LIMITS describes the limit states. Standard the limit state is collapse of the structure (in case of non-linear analysis). Limit states might be maximum displacement, stress or strain.

'PROBAB'
It is possible to make all input data stochastic. This includes coordinates, material behaviour, geometric properties and loads. Making a variable stochastic is done by repeating the item word (MATERI, LOAD, COORDI, GEOMET).

Syntax

'PROBAB'
GEOMET
$\mathtt{geonr}_n$ $\mathtt{geonm}_w$ $\mathtt{geodat}_?$

geonr
is the number for reference from subtable GEOMET of table 'ELEMEN'.

geonm
indicates the items property name and is followed by geodat, with 5 values (see table G-1 and G-2).

```
GEOMET
   1  THICK 0.1 0.1 0.09 1. 0.
   2  THICK 0.1 0.1 0.09 1. 0.
```

MATERI
$\mathtt{matnr}_n$ $\mathtt{matnm}_w$ $\mathtt{matdat}_?$

matnr
is the number for reference from subtable MATERI of table 'ELEMEN'.

matnm
indicates the items property name and is followed by matdat, with 5 values (see table G-1).

```
MATERI
   1  YOUNG   2.1e11  8.4e9  0.0     2.  0.
   2  YOUNG   2.1e11  8.4e9  0.0     2.  0.
   2  POISON 0.2      0.1    0.01    1.  0.
```

```
COORDI
coonr_n   dirnm   coodat
```

coonr

is the number for reference from table 'COORDI'.

coonm

indicates the direction name and is followed by coodat, with 5 values (see table G-1 and G-2).

```
COORDI
   1  X      0. 0.  0   2  0
   2  Y      1. 1.  0   1  0
```

```
LOADS (loanr_n)
NODAL
/ nos /    type  dirnr   loadat
```

nos

is a single or series of node number(s), it must be specified between slashes and may comprise either numbers or groups or both.

type is the load type: FORCE for force or MOMENT for moment. The direction number dirnr refers to table 'DIRECT': a force in, or a moment around the specified direction.

Loadat gives the 5 stochastic load parameters (see table G-1 and G-2).

```
LOADS (1)
 NODAL
 /  7 / F 1 50.e3  12.50e3   0.   1.   1.
 / 13 / F 1 56.e3  14.0e3    0.   1.   1.
 / 19 / F 1 58.e3  14.50e3   0.   1.   1.
 / 25 / F 1 60.e3  15.0e3    0.   1.   1.
 / 31 / F 1 62.e3  15.50e3   0.   1.   1.
```

```
 / 37 / F 1 64.e3  16.0e3    0.    1.    1.

LOADS (loanr_n)
ELEMEN
/ nos /   lodnam loddat
```

The input of element load depends on the element type.

The loddat can be made stochastic using 5 values see table G-1 and G-2.

```
ELEMEN
 / 37 /
      LINE
      DIRECT 2
      FORCE  3.e3  3.e2 0. 1. 0.
 / 14 /
      EDGE ETA2
      DIRELM NORMAL
      FORCE  1000. 100. 0. 1. 0.
```

'LIMITS'

The 'LIMITS' input describes the ultimate or serviceability limit state. Limit can be: stress, strain, force and/or displacement. The limits can be stochastic or deterministic.

Syntax

```
'LIMITS'
ELEMEN
  elnrs   itnam limdat
NODES
  nodnr   itnam limdat
```

itnam refers to the output name see output tables in *POST.
The limit is deterministic when one value is submitted in limdat. Giving 5 extra values (see table G-1 and G-2) makes the limit a random variable.

```
'LIMITS'
ELEMEN
 / 25 /  Sxx     240e6   268.e6 22.e6 227. 22. -1.
 / 23 /  Seq     240.e6
NODES
 / 1-3 /  DTZL     5.
 /  4 /   DTXL     4.
```

Table G-1: Probabilistic parameters

parameter	
1	mean
2	standard deviation
3	shift/upper boundary
4	statistical distribution
5	important direction

Table G-2: Implemented distributions

Distribution	Par. 1	Par. 2	Par. 3	Par. 4
normal	Mean	st dev	0	1
lognormal	Mean	st dev.	0	2
Exponential	Mean	st dev	0	4
Beta (lower bound = 0)	Mean	st. dev	upper boundary	6
Gumbel	Mean	st dev	0	7
Deterministic	Value	0	0	20
Lower truncated normal	Mean*	st dev*	lower truncation	21
Shifted lognormal	Mean	st dev	shift	22

**mean and standard deviation of the untruncated distribution*

Special attention is needed on the correctness of the input with respect to the boundaries. For several input parameters, a negative input is erroneous. Using a truncated normal instead of a normal distribution for such parameters is advised. Other parameters such as Poison ratio have an upper limit as well. For this parameter a beta distribution could be applied.

'CORREL'

The correlation between random variables is entered in table CORREL. The correlation value should be between -1 and 1 ($-1 < \rho < 1$).

Syntax

```
'CORREL'
  corrnr  itnam  itnr
          itsub
 ,corrnr  COHVAL corval
```

corrnr is the subsequent numbering of the CORREL table. Itnam refers to the random variable, itsub to the subitem. The item ,corrnr can only be added for ,corrnr < corrnr and gives the correlation between item corrnr and ,corrnr ($-1 < \rho < 1$).

```
'CORREL'
  1    MATERI 1
       YOUNG
  2    MATERI 2
       YOUNG
 ,1    COHVAL 0.9
  3    GEOMET  5
       THICK
 ,1    COHVAL  0.1
 ,2    COHVAL  0.7
```

EXAMPLE

```
'PROBAB'
MATERI
   1  YOUNG  2.1e11  8.4e9  0.0     2.  0.
   2  YOUNG  2.1e11  8.4e9  0.0     2.  0.
LOADS (1)
 NODAL
 /  7 / F 1 50.e3  12.50e3   0.   1.   1.
 / 13 / F 1 56.e3  14.0e3    0.   1.   1.
 / 19 / F 1 58.e3  14.50e3   0.   1.   1.
 / 25 / F 1 60.e3  15.0e3    0.   1.   1.
 / 31 / F 1 62.e3  15.50e3   0.   1.   1.
 / 37 / F 1 64.e3  16.0e3    0.   1.   1.
 ELEMEN
 / 37 /
      LINE
      DIRECT 2
      FORCE 3.e3  3.e2 0. 1. 0.
'LIMITS'
ELEMEN
 / 2-10 / Sxx     120e5  120e5 10e5 0. 1. 1.
 / 1 /    Seq     240e6   268.e6 22.e6 227. 22. 0.
 / 13 /   Sxx     240e6   268.e6 22.e6 217. 22. 0.
 / 25 /   Sxx     240e6   268.e6 22.e6 237. 22. -1.
NODES
/ 1-3 / DTYL   1.0
'COHER'
  1   MATERI 1
```

```
       YOUNG
  2    MATERI 2
       YOUNG
 ,1    COHVAL 0.9
'END'
```

command file

Four probabilistic methods are implemented in PROBAB

- Crude Directional Sampling (DS)
- Directional Adaptive Response surface Sampling (DARS)
- First Order Reliability method (FORM)
- Adapted Response Surface FORM (FORM-ARS)

DS requires input:

nsamp	maximum number of (directional) samples (100)
norm	convergence criterion for limit state (0.01)
variat	required coefficient of variation of the probability of failure (0.30)

After every sample, the output of DS is the expectation and coefficient of variation of the probability of failure. The sampling stops on either the maximum number of samples or when the required coefficient of variation V has been reached.

DARS

input:

nsamp	maximum number of (directional) samples (100)
norm	convergence criterion for limit state (0.01)
maxiter	maximum number of iterations in finding the limit state (15)
nfit	maximum number of terms to be used in the fitted Response Surface (min = 2*number of random variables + 1)
pcond	factor λ_{add} on minimum distance to fulfil the condition for directional sampling ($\lambda_{RS} < \lambda_{min} + \lambda_{add}$ (3.0)
pvari	required coefficient of variation of the probability of failure (0.30)

In DARS the sample response is calculated by means of a Response Surface (RS). A DIANA analysis is only performed if (according to the RS) the sample is of worth to the directional sampling. The criterion is whether the RS distance is less than *pcond* plus the minimum found distance.

DARS can be performed only if maxsam > 2 times the number of random variables. If maxsam < 2 *nvars, DS is performed automatically.

FORM
input:

maxiter	maximum number of iterations (10)
norm	convergence criterion for limit state (0.01)

FORM-ARS
input:

maxiter	maximum number of iterations per direction to find λ (10)
norm	convergence criterion for limit state (0.01)
nfit	maximum number of terms to be used in the fitted Response Surface (min = 2*number of random variables + 1)

example linear elastic

```
*filos
  .........
*INPUT
*PROBAB
  begin DS
      nsamp = 100
      maxiter = 15
      cond  2.
      Variat 0.5
      norm 0.01
  end cds
 *END
```

example non-linear

```
*filos
  .........
*INPUT
*PROBAB
  begin nonlin
  begin initia
    analys  geomet total
  end initia
  begin loadin
    begin LOAD
     case 1
     factor 1.
```

```
     end load
  end loadin
  begin execut
   LOADNR 1
   begin size
     SIZES 0.5 0.5
   end size
   begin perfor
:     newton modify on
:     maxite 20
   end perfor
   norm energy
 end execut
 end nonlin
 nsteps = 90
*end
```

Annex H: Intermediate results of the simply supported beam case

In Section 5.2.1, after ADI, a difference between β_{RS} and λ_{min} is noticed. The reliability index $\beta_{RS} = 7.63$ is much higher than λ_{min} (= 4.69). The intermediate results of the ADI procedure are given in the table H-1. The minimum distance from the origin to the limit state equals $\lambda_{min} = 4.689$. A linear Response Surface is fitted to the data shown in Table H-1. The parameters of this function are given in Table H-2. Table H-1 shows clearly two important variables (u_4 and u_5). As a result a reliability index less than 4.7 would be expected. The RS fitted to the data gives the same weight to all data.

Figure H-1 gives the value of the limit state function g as a function of variable u_5 and the fitted response surface g*. The RS crosses the zero axis at approximately $u_5 = -11.6$. An another zero point (according to the response surface) is $u_4 = 10.6$. Given these two results and a linear RS leads to $\beta_{RS} = 7.63$. For sake of completeness, in table H-3 the parameters of the final response surface are given.

Table H-1: Results of ADI used to fit a RS.

u_1	u_2	u_3	u_4	u_5	g(u)
0	0	0	0	0	0.9988
-3	0	0	0	0	0.9988
0	-3	0	0	0	0.9988
0	0	-3	0	0	0.9986
0	0	0	0	-3	0.9952
0	0	0	0	-4.689	0
3	0	0	0	0	0.9988
0	0	3	0	0	0.9989
0	0	0	3	0	0.9981
0	0	0	5.998	0	0

Table H-2: Parameters of the response surface after ADI: $g^* = a_1 + \sum_{i=2}^{n+1} a_i u_i$.

i	a_i
1	+0.9957
2	-2.6168E-17
3	-3.1390E-02
4	+1.6284E-05
5	-9.3446E-02
6	+8.5510E-02

Figure H-1: g and g* as a function of u_5.

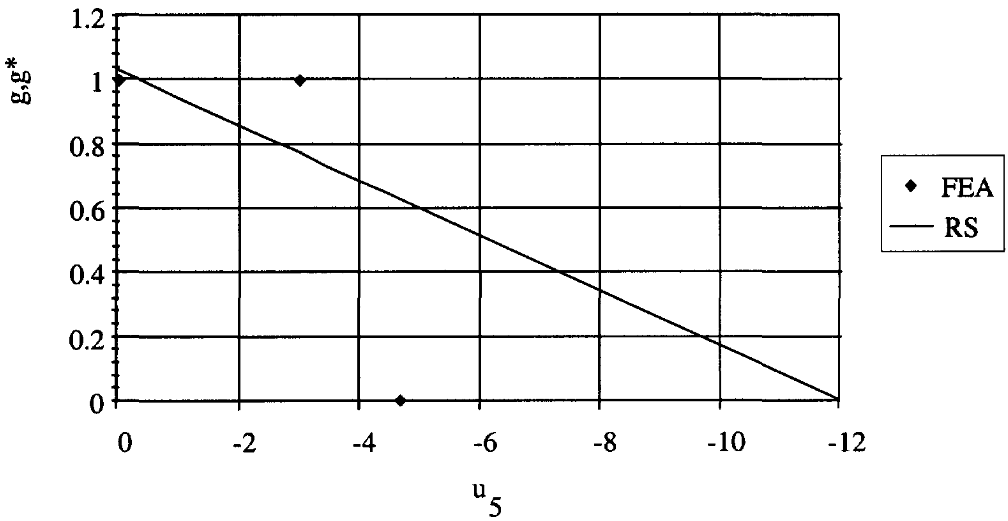

Table H-3: Parameters of the response surface after crude directional sampling:

$$g^* = a_1 + \sum_{i=2}^{n+1} a_i u_{i-1} + \sum_{i=7}^{n+6} a_i u_{i-6}^2$$

i	a_i
1	+0.3366
2	-1.1607E-02
3	+9.3701E-03
4	+1.5944E-03
5	-3.4465E-02
6	+2.0478E-02
7	-1.4069E-03
8	-1.1207E-04
9	-3.2256E-04
10	-2.2876E-03
11	-6.1486E-03

Annex I: Convergence of directional sampling in structural reliability

The examples of structural reliability in chapter 5 show that the minimum distance λ_{min} is most of the times found in the u-space coordinate axis directions. When performing crude directional sampling it is unlikely that this minimum is found in the first samples. Suppose a limit state function with 10 random variables, where only one is important to the limit state function:

$$g = 4 - u_1 \tag{I.1}$$

For crude directional sampling this limit state function performs the same as limit state function (2-9) where all variables are equally important. The only difference is that the axes are rotated:

$$g = 4 - \sum_{i=1}^{10} u_i / \sqrt{10} \tag{I.2}$$

Figure I.1: reliability index β as a function of the number of samples.

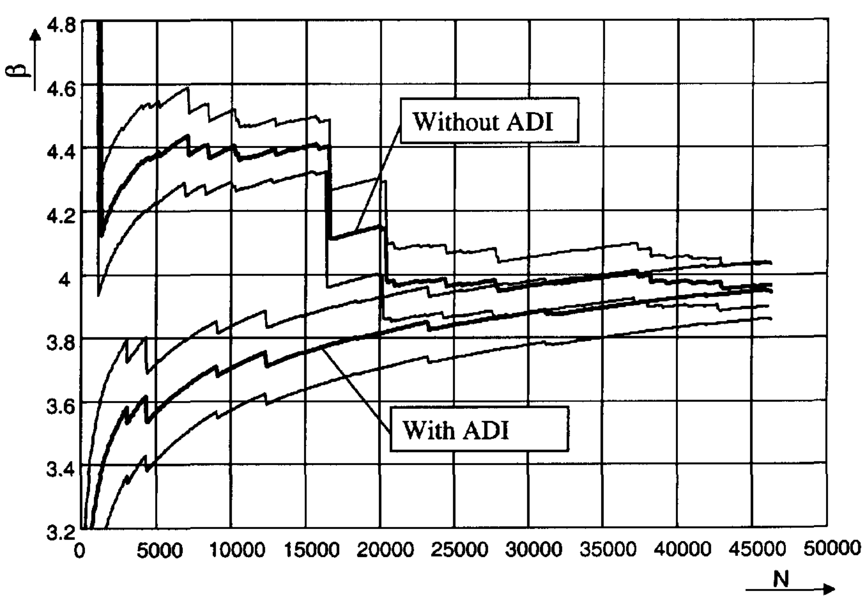

Figure I.1 shows the expected reliability index β as a function of the number of samples with its confidence intervals. The convergence of the crude directional sampling procedure is shown as "Without ADI". For a low number of samples, the figure shows a too high reliability index. The real reliability index is not even between the interval bounds. The high reliability index is found because of the fact that samples near the minimum distance are still to be found and $V(\beta)$ is underestimated. The error however is small. Using equation (I.2) instead of (I.1) makes no difference in this case.

A far too low value of β is found however when using the ADI data in the directional sampling procedures. In the ADI procedure, λ_{min} is found instantly. As a result the consequent random sampling only finds higher values of λ. This is the reason for the low start of β in figure I.1 "With ADI". After the ADI procedure, the coefficient of variance of P_f is relatively high. The confidence interval is however not large enough, to have the real reliability index within the interval bounds.

For the procedure "With ADI", equation (2.9) leads a result "Without ADI" alike. All u-space coordinate axis directions lead to the same distance λ. Consequently a good estimate of β is found instantly.

Annex J: Required computer time

For comparison of computational speed, the CPU seconds, File Access (FA), and Input-Output (IO) seconds needed to perform the case studies presented in chapter 5 are given below. The computations are performed on a HP 9000, 160 MHz UNIX machine.

Simply supported beam

	ADI	DARS $\lambda_{add}=1.1$	DARS $\lambda_{add}=3.0$	DS
CPU	214	3553	4856	14216
IO	25	465	598	1610
FA	150226	2301574	3546724	10649517

Beam with random Young's modulus

CPU	242	497	1770	142459
IO	56	65	151	16016
FA	119613	120160	127827	33902871

Stüssi-Kollbrunner beam

CPU	1438	15746	26346	127114
IO	43	437	722	3522
FA	268326	2939392	4889710	23369246

Central elastic plastic buckling

CPU	4649	6262	33312	698867
IO	97	133	928	23478
FA	526676	690687	4057968	87666970

One-storey, one-bay frame structure

CPU	42	169	987	1340
IO	4	69	101	124
FA	16976	311566	443328	609220

One-storey two-bay frame structure

CPU	64	601	1418	2361
IO	6	47	116	184
FA	22112	216324	509778	86137

Two-story, two-bay frame structure

CPU	301	875	2663	10432
IO	11	35	106	396
FA	56051	160801	487563	1875117

Bridge deck

CPU	7467	7722	12556	216640
IO	1070	1074	2259	33125
FA	646785	662198	777168	13449686

Cable-stayed bridge

CPU	9419	11114	13201	522308
IO	1312	1459	1512	67050
FA	784607	799233	861247	39768954

Road structure, fully correlated Young's modules

CPU	10131	164486	206229	225780
IO	562	8490	12327	12810
FA	315331	3765781	7166392	7914286

Road structure, partly correlated random field Young's modules

CPU	132595	158967	191665	853565
IO	7180	9557	9778	42648
FA	4145906	4723278	4326490	8856655

Sheet pile installation

CPU	39107	37804	89947	224682
IO	2338	2804	6086	17461
FA	35662266	3721473	9240899	28608160

Summary

The structural behaviour of a complex structure is often calculated using a Finite Element Analysis (FEA). Stresses and deformations of the structure can be computed given the (deterministic) parameters of loads, geometry and material behaviour.

Structural codes require a certain level of structural reliability. This structural reliability is ideally translated into partial safety factors by which variables like strength and load have to be divided or multiplied to find the so-called design values. These design values are to be used as input for a Finite Element Analysis. The outcome of the calculations is compared with the limit states (for example collapse or maximum deformation). The structure is supposed to have met the reliability requirements when the limit states are not exceeded.

In particular for small structures or components of structures with a well-known material behaviour this so-called code type level I method makes it plausible that the reliability requirements are met. For other types of structures the code type level I method may lead to an under or overestimate of the structural reliability.

The main aim of this thesis is the development of a method to compute the structural reliability using a finite element analysis. This structural reliability is to be computed with sufficient accuracy and with minimal computational time. Besides, the method should be such that no detailed prior knowledge of the probabilistic and system behaviour of the structure is required.

First of all standard reliability methods are analysed with respect to their feasibility to compute the structural reliability. Well-known reliability methods such as Numerical Integration (NI), Monte Carlo sampling (MC), Monte Carlo Importance sampling (MCI), Directional Sampling (DS) and the First and Second Order Reliability Methods (FORM and SORM) are described in chapter 2. For all reliability methods, the repeated evaluation of the limit state function by means of a finite element computation takes the main computational effort. Since the computational time is to be minimised, emphasis is laid on the minimisation of the number of limit state function evaluations.

With respect to reliability computations, large and complex structures can be characterised by many random variables and many failure mechanisms. In chapter 2 it is concluded that Monte Carlo importance sampling (with increased variance), Directional

sampling and FORM are the best performing methods with respect to efficiency. These methods, however, use too many limit state function evaluations to match with the aims of the thesis.

Chapter 3 goes into possibilities to increase the efficiency of the reliability methods. Two existing methods (FORM and Directional Sampling), are adapted with an interactive response surface technique, leading to two new methods: FORM-ARS and DARS. Both are supposed to give a substantial decrease of the needed amount of exact limit state function evaluations.

In FORM-ARS, a response surface instead of the exact limit state function is evaluated. The response surface is adapted, every time FORM has found a design-point (on the response surface). The FORM-ARS method is in particular useful for non-smooth limit state functions and when many limit state functions are to be evaluated simultaneously.

When applying DARS, the directional sampling is carried out using finite element limit state function evaluations only under the condition that an important region is expected. The sampling is first performed on a response surface and no finite element analyses are carried out for (expected) non-important regions. Every time a finite element analysis is performed, the response surface is adapted and it is checked whether or not erroneously the response surface has been used instead of an exact finite element analysis for previous samples.

The efficiency and accuracy of both adaptive methods are first examined on artificial (non-structural) limit state functions. Chapter 4 compares the various reliability methods. The efficiency on component level of the FORM methods is best. With unknown system behaviour however, mistakes may occur while using FORM. The level III methods MC, MCI, DS and DARS always come up with a sufficient accurate answer, but are less efficient than FORM. Since an accurate answer is more useful than a fast but untrustworthy answer, the DARS procedure is chosen to be best for the aims in this thesis because it is the most efficient method.

The DARS method has been implemented in a pilot version of the existing finite element code DIANA. The structural reliability of a number of structures that are typical for civil engineering practice has been researched in chapter 5. In particular structures that have outspoken system behaviour, such as steel frames, and structures made out of material with a high uncertain behaviour such as ground and road structures are analysed. Furthermore large and small structures have been chosen and structures with a geometrically and physically non-linear behaviour and a structure for which a phased analysis is useful. This way, it is supposed to have a representative mixture of the civil engineering practise where a probabilistic finite element analysis might be used. The examples show overall that the DARS method is a sufficiently accurate tool to compute the structural reliability.

Procedures are evaluated and consequences to other fields of applications are discussed in chapter 6. The effectiveness of DARS is compared with level I design procedures and level II reliability methods like FORM. To compute a component reliability where few variables are involved, FORM is undoubtedly the best in efficiency. For cases with a high number of random variables it is concluded that DARS and FORM are equally efficient on component level. The DARS method is performing best when computing a systems reliability where many random variables are involved.

The DARS procedure is of course less efficient in checking the structural reliability than code type level I procedures. It should however be pointed out that the case studies performed in chapter 5 show that the reliability of structures designed by a code type level I procedure is either higher or lower than required. The code type level I procedures can only be used to give an impression of the goodness of an average structure with respect to its reliability requirements.

In a full level I procedure, much more combinations of partial safety factors are used than in code type level I methods. Consequently it is expected that a full level I procedure makes it more likely that the structure meets its reliability requirements. The cases in this thesis show that the effect of random fields should be taken into account for the computation of the reliability. This should therefore be present in the level I procedures as well. If done so, the number of random variables within the structure will increase considerably. The number of limit state function evaluations within the full level I procedure is equal to approximately three times the number of random variables. Consequently, taking the random fields into account, the level I calculations become more lengthy than usual in structural engineering practise.

The DARS method approximately uses seven times the number of variables to compute the structural reliability. At approximately two times the computational effort of a full level I procedure, the DARS procedure computes an accurate structural systems reliability automatically.

Samenvatting

Het constructieve gedrag van bouwconstructies wordt vaak berekend met de eindige elementen methode. Gegeven de (deterministische) parameters zoals belasting, geometrie en materiaalgedrag kunnen spanningen en vervormingen van de constructie worden berekend.

De constructieve betrouwbaarheid (kans op falen) van bouwwerken wordt in normen voorgeschreven. Deze betrouwbaarheidseis wordt in bouwnormen vertaald naar partiële veiligheidsfactoren waarmee de belastingen op de constructie worden vermenigvuldigd (belastingsfactoren) en waardoor de parameters die de sterkte van de constructie bepalen worden gedeeld. De zodoende verkregen rekenwaarden van parameters worden gebruikt als invoer voor een eindige elementen methode berekening. Het bouwwerk wordt geacht voldoende betrouwbaar te zijn als uit de resultaten van de eindige elementen methode berekening blijkt dat de grenstoestanden (bijvoorbeeld bezwijken of maximale doorbuiging) niet worden overschreden. Voor kleine bouwwerken of componenten van bouwwerken met bekend constructief systeem en bekend materiaal gedrag is een dergelijke aanpak waarschijnlijk voldoende. Voor andere typen bouwwerken leidt een dergelijke methode wellicht tot een substantiële onder- of overschatting van de constructieve betrouwbaarheid.

Doel van het onderzoek is de ontwikkeling van een methode voor de berekening van de werkelijke constructieve betrouwbaarheid van grote en complexe bouwconstructies met behulp van de eindige elementen methode. Deze berekening dient zo snel mogelijk en met voldoende nauwkeurigheid uitgevoerd te kunnen worden. De methode wordt geacht geen gedetailleerde kennis van probabilistiek of systeemgedrag van de gebruiker te vereisen.

Eerst zijn standaard betrouwbaarheidsanalyse methoden onderzocht op hun mogelijkheden. Bekende methoden voor betrouwbaarheidsanalyse zoals de Monte Carlo simulatie (MC), Monte Carlo Importance sampling (MCI), richtingsgewijs bemonsteren (Directional Sampling, DS), Numerieke Integratie (NI) en FORM/SORM (First and Second Order Reliability Method) worden beschreven in hoofdstuk 2. Het blijkt dat het herhaaldelijk evalueren van de grenstoestandsfunctie met behulp van de eindige elementen methode het grootste deel van de berekeningstijd vergt. Het onderzoek heeft zich daarom gericht op het minimaliseren van het aantal malen dat de grenstoestandsfunctie wordt geëvalueerd.

Grote en complexe bouwconstructies kenmerken zich, met betrekking tot de betrouwbaarheidsanalyse, door een groot aantal stochastische variabelen en vele (combinaties van) mogelijkheden waardoor de constructie kan falen. In hoofdstuk 2 wordt geconcludeerd dat Monte Carlo Importance sampling (MCI), richtingsgewijsbemonsteren (DS) en FORM hiervoor de meest efficiënte methoden voor betrouwbaarheidsanalyse zijn. De methoden vergen echter nog zoveel berekeningstijd dat deze vrijwel geen mogelijkheden bieden in combinatie met de eindige elementen methode.

Hoofdstuk 3 gaat in op mogelijkheden om de efficiëntie van de betrouwbaarheidsanalyse te vergroten. Voor FORM en Directional Sampling zijn nieuwe meer efficiënte varianten bedacht die gebruik maken van een responsie-oppervlak (Response Surface): FORM-ARS (Adaptive Response Surface) en DARS (Directional Adaptive Response surface Sampling). Beide methoden leiden tot een substantiële vermindering van het aantal evaluaties van de werkelijke grenstoestandsfunctie terwijl zij toch voldoende nauwkeurig zijn.

De FORM-ARS methode evalueert het responsie-oppervlak in plaats van de werkelijke grenstoestandsfunctie. Het responsie-oppervlak wordt telkens aangepast als FORM een nieuw ontwerppunt heeft gevonden. De FORM-ARS methode biedt voordelen bij niet gladde grenstoestandsfuncties en als vele grenstoestandsfuncties in één keer worden onderzocht.

De DARS methode maakt gebruik van de werkelijke grenstoestandsfunctie (gebaseerd op de eindige elementen methode) voor de interessante richtingen (richtingen met conditioneel hoge faalkans) en van een responsie-oppervlak voor de niet-interessante richtingen. Het gebruik van een responsie-oppervlak in plaats van de werkelijke grenstoestandsfunctie leidt tot een grote besparing in rekentijd. Overigens wordt elke keer als gebruik is gemaakt van de eindige elementen methode, onderzocht of bij de voorgaande richtingen niet ten onrechte alleen van het responsie-oppervlak gebruik is gemaakt.

In hoofdstuk 4 worden de nieuwe methoden onderzocht op hun efficiëntie en nauwkeurigheid. Zij worden vergeleken met de verschillende bestaande methoden voor betrouwbaarheidsanalyse. De vergelijking is uitgevoerd op basis van fictieve, niet constructieve grenstoestandsfuncties. Het blijkt dat de FORM-ARS methode het meest efficiënt is op componentniveau. Bij onbekend systeemgedrag is de FORM procedure niet altijd betrouwbaar. De Monte Carlo en Directional Sampling methoden leiden altijd tot een goede schatting van het antwoord maar gebruiken veel meer evaluaties van de grenstoestandsfunctie. Daar een goed antwoord nuttiger is dan een onbetrouwbaar snel antwoord en DARS het meest efficiënt is, is gekozen om deze methode verder te onderzoeken in combinatie met de eindige elementen methode.

De DARS methode is geïmplementeerd in een pilot versie van het eindige elementen computerprogramma DIANA. In hoofdstuk 5 is een aantal cases weergegeven die representatief worden geacht voor de civiele techniek. Gekozen is om constructies te onderzoeken met een uitgesproken systeemgedrag zoals staalconstructies en constructies waarbij gebruik wordt gemaakt van een in hoge mate onzeker materiaalgedrag zoals grond- en wegconstructies. Daarnaast zijn grote en kleine constructies onderzocht en constructies met een hoge mate van (geometrische en fysisch) niet-lineair gedrag. Uit de cases kan worden geconcludeerd dat de DARS methode een voldoende nauwkeurige methode is om de faalkans van complexe constructies te berekenen.

In hoofdstuk 6 vindt een evaluatie plaats van de gebruikte procedures. Daarnaast wordt gekeken naar de consequentie voor andere applicaties. De efficiëntie van DARS wordt vergeleken met de standaard niveau I ontwerp-methoden en niveau II methoden (FORM). Voor problemen met een relatief hoog aantal stochastische variabelen kan worden geconcludeerd dat FORM en DARS ongeveer even efficiënt zijn voor de berekening van een component betrouwbaarheid. FORM is het meest efficiënt voor problemen met weinig stochastische variabelen en waar systeemgedrag ontbreekt. Bij veel variabelen en systeemwerking is de DARS methode de beste keus qua efficiëntie.

De DARS methode is in het algemeen veel minder efficiënt in het controleren van de betrouwbaarheid dan een niveau I ontwerpmethode met partiële veiligheidsfactoren volgens de bouwnormen. Deze niveau I ontwerpmethode is echter ook veel onnauwkeuriger. De voorbeelden in hoofdstuk 5 laten zien dat de betrouwbaarheid van constructies, die zijn ontworpen met partiële veiligheidsfactoren uit de bouwnormen, groter of kleiner is dan wordt geëist. Geconcludeerd wordt dat het ontwerpen met behulp van deze partiële veiligheidsfactoren het alleen maar aannemelijk maken dat een gemiddelde constructie aan de betrouwbaarheidseis kan voldoen.

Bij een volledige niveau I procedure worden veel meer combinaties van veiligheidsfactoren gebruikt dan voorgeschreven door de bouwnormen. Hierdoor zal een volledige niveau I procedure waarschijnlijk meer zekerheid bieden dat aan de betrouwbaarheidseis voldaan wordt. Gezien de resultaten in dit proefschrift zal dan binnen deze niveau I procedure ook rekening gehouden moeten worden met de ruimtelijk fluctuaties van de stochastische parameters. Het aantal parameters in de niveau I procedure wordt hierdoor veel groter dan hetgeen tot nu in de praktijk gebruikelijk is. Het aantal evaluaties van de grenstoestandsfunctie bij een volledige niveau I procedure is gelijk aan ongeveer drie maal het aantal variabelen. Het gevolg is dat de het aannemelijk maken van het voldoen aan de betrouwbaarheidseis een behoorlijk aantal eindige elementen methode berekeningen vergt.

Het aantal grenstoestandsfunctie-evaluaties bij de DARS methode is ongeveer gelijk aan zeven maal het aantal variabelen. Dus met slechts ongeveer twee maal de reken-inspanning ten opzichte van een volledige niveau I procedure kan de DARS methode een goede schatting van de werkelijke betrouwbaarheid geven.

Curriculum vitae

Paul Hendrik Waarts

1961	Born in The Hague, The Netherlands.

Education

1973-1977	MAVO, Noordwijk.
1977-1979	HAVO, Leiden.
1979-1983	BSc, Institute of Technology (HTS), Civil Engineering, The Hague, with honours.
1983-1988	MSc, Delft University of Technology, faculty of Civil Engineering.

Experience

1986-1988	Research assistant at the Delft University of Technology, faculty of Civil Engineering.
1995-1999	Assistant researcher at the Delft University of Technology, faculty of Civil Engineering.
1988-present	Scientific researcher at TNO Building and Construction Research.